A Multiple Input-Output Theorem leading to A New Equalizer Structure

by

Chung-Yin Cheung, B.A.Sc.(Elect.Eng.)

A thesis submitted to the
School of Graduate Studies and Research
in partial fulfillment of the requirements
for the degree of
Master of Applied Sciences
in Electrical Engineering

Ottawa-Carleton Institute for Electrical Engineering,
Faculty of Engineering,
Department of Electrical Engineering,
University of Ottawa,
Ottawa, Ontario, Canada

August 10, 1993

ISBN 0-315-95900-2

Canada

UNIVERSITÉ D'OTTAWA
UNIVERSITY OF OTTAWA

Abstract

The study of the multiple-input/output inverse theorem(MINT) to realize exact inverse filtering has led to the proposal of new solution types. Digital processing functions of MINT other than the exact inverse filtering are explored. One such realization of MINT is the selective reception, filtering and distribution of signals in a multichannel system. This is demonstrated with the design of equalizers for a speakerphone system. Practical implementation problems associated with common zeros or close zeros in the channels are discussed and different solutions are proposed to address these issues. One of them is the use of the Minimum Norm Solution with system delay. Finally a novel equalizer structure, based on MINT, is proposed for realizing inverse filtering of a single analog transmission channel. Simulations show that its performance is comparable to that of the conventional equalizer based on the Least Square Error criterion.

Acknowledgments

The author wishes to express his sincere gratitude to his academic supervisor Professor Willem Steenaart, for his guidance, inspiration and continuous encouragement throughout the course of this research study. Additionally, the author is grateful to his friend and colleague, Tze-Wo Leung, for borrowing his computer resources which have helped tremendously to expedite the completion of this thesis.

The author also wishes to thank all professors, colleagues and friends at the Department of Electrical Engineering, University of Ottawa and the Department of System and Computer Engineering, Carleton University for the good academic atmosphere, the advice and the encouragement during the periods of his studies.

Table of Contents

Abstract iv
Acknowledgments v
List of Figures viii
List of Acronyms xi
List of Symbols xii

1 Introduction 1
1.1 Background 1
1.2 Thesis organization 3

2 Multiple-input/output Theorem 5
2.1 Introduction 5
2.2 Computation of the inverse FIR filters in the discrete time domain 8
2.3 Generalization of the MINT 9
2.4 Existence of exact solutions in a dual channel system 11
2.4.1 Requirement for the existence of exact solutions 11
2.4.2 Existence of exact solutions: a study 12
2.5 Minimum norm solution 18
2.5.1 Case 3: rectangular matrix solution 18
2.5.2 Characteristics of the minimum norm solution 19
2.6 Filter banks allowing perfect reconstruction 20
2.7 Conclusion 22

3 MINT: Applications 23
3.1 Introduction 23
3.2 Pre-channel and post-channel filtering 23
3.3 MINT in multi-channel system 25
3.3.1 Introduction 25
3.3.2 Restrictions on a multi-channel system 29
3.3.3 MINT for M-input-1-output system 29
3.3.4 Example of MINT in multi-channel system: speakerphone 33
3.3.4.1 Pre-channel filtering approach 34
3.3.4.2 Post-channel filtering approach 40
3.4 Conclusion 43

4 Solutions to common and close zeros on a dual-channel system 44
4.1 Introduction 44
4.2 Common zeros 44
4.2.1 Use of IIR in MINT filters 45
4.3 Close zeros 49
4.3.1 Minimum Norm solution with delay 51
4.4 Conclusion 57

5 Single channel MINT equalizer 59
5.1 Introduction 59
5.2 Background 60
5.3 A single channel equalizer structure 63
5.3.1 Deriving subchannels from a single channel 63
5.3.2 Design considerations on deriving subchannels 72
5.3.3 Components of the new equalizer structure 74
5.4 MINT equalizer with 3 virtual channels 76
5.5 Performance of the MINT equalizers 76
5.5.1 Measurement of equalizer performance 78
5.5.2 Effect of the filter length on performance 80
5.5.3 Aliasing of the derived channels 94
5.6 Application: Cancellation of reverberation 98
5.7 Conclusion 101

6 Conclusions 102
6.1 Summary 102
6.2 Suggestions for Future Research 104

References 105

Appendix A LSE Equalizer 108

Appendix B Simulation Data 116

List of Figures

Figure 1.1 An acoustic system consisting of a loudspeaker and a microphone.....1

Figure 2.1 The acoustic system of a room.....6

Figure 2.2 Discrete model of the acoustic system of a room.....6

Figure 2.3 Block diagram of a subsampled filter bank.....21

Figure 3.1: Pre-channel filtering.....24

Figure 3.2: Post-channel filtering.....24

Figure 3.3: Acoustic room with multiple speakers and microphones.....25

Figure 3.4: Discrete model of MINT in multi-channel system (pre-channel filtering).....26

Figure 3.5: The acoustic of a speakerphone system in a room.....33

Figure 3.6: Speakerphone system: Pre-channel approach.....34

Figure 3.7: Discrete model of the speakerphone system: Pre-channel approach. 35

Figure 3.8: Speakerphone system: Post-channel approach.....40

Figure 3.9: Discrete model of the speakerphone system: Post-channel approach.....41

Figure 4.1: IIR in MINT filter: Approach 1.....45

Figure 4.2: IIR in MINT filter: Approach 2.....46

Figure 4.3: Change of Filter Norm with no close zeros on 1) minimum phase, 2)maximum phase, 3) mixed phase channels. 53

Figure 4.4: Change of Filter Norm with 4)one close zero, 5)two close zeros on minimum phase channels; 6)one close zero, 7)two close zeros on maximum phase channels 54

Figure 4.5: Change of Filter norm with 8)one close zero inside the unit circle, 9)one close zero outside the unit circle, 10)two close zeros, both inside and outside the unit circle, on mixed phase channels.....55

Figure 5.1: Inverse filtering with a single channel. 61

Figure 5.2: Discrete linear shift-invariant channel-filter system. 62
Figure 5.3: MINT equalizer system with dual virtual channels. 64
Figure 5.4: The frequency spectrum of the input signal x(t), the channel G(jw), the receiving low-pass filter L(jw)....65
Figure 5.5: The discrete frequency spectrum of the distorted signal y(t) sampled at $2f_s$....65
Figure 5.6: Discrete frequency spectrums depicting how y(n) can be computed.... 67
Figure 5.7: Discrete frequency spectrums depicting how $\mathbf{y'}_1(n)$ is formed. 69
Figure 5.8: Discrete frequency spectrums depicting how $\mathbf{y'}_2(n)$ is formed. 70
Figure 5.9: Discrete frequency spectrums depicting how $\mathbf{y}_1(n)$ is formed....71
Figure 5.10: MINT equalizer with three channels....77
Figure 5.11: Discrete frequency (power) spectrum of the input signal x(n) and the low-pass channel GL(jw), oversampled by a factor of 6. 82
Figure 5.12: The input signal x(t) sampled at the system clock rate. 84
Figure 5.13: Comparison of error signals and restored signals in the time domain. 85
Figure 5.14: Comparison of the frequency spectrums of the input and error signals. 86
Figure 5.15: Comparison of the Signal -to-Error Ratio. 88
Figure 5.16: Comparison of the Filter Norm 89
Figure 5.17: Comparison of the Noise Enhancement ratio....90
Figure 5.18: System delay introduced by the equalizers. 92
Figure 5.19: Comparison of Signal-to-Error Ratio against the dimension of the equivalent channel matrix to be inverted....93
Figure 5.20: Frequency (power) spectrum of the error signals....96
Figure 5.21: Enhanced Noise Power Spectrum for different aliasing. 97
Figure 5.22: Frequency spectrum of the low-pass channel and input signal....99

Figure 5.23: Characteristic of the error signals of the three equalizers. 100

Figure A.1: Discrete model on inverse filtering with one channel. 108

Figure A.2: The FN and SERU of a LSE equalizer with different system delay. 112

Figure A.3: Change of SER with increasing filter length. 114

Figure A.4: Change of FN with increasing filter length. 115

List of Acronyms

CFN	Channel-Filter Norm
DECM	Dimension of the Equivalent Channel Matrix defined in section 5.5.1 (page 78).
DFT	Discrete Fourier transform
FN	Filter norm defined in equation (4.2) (page 50)
IIR	Infinite Impulse Response filter
LSE	Least Square Errors
MINT	Multiple-input/output theorem
2MINT equalizer	New equaliser, based on MINT, with two virtual channels.
3MINT equalizer	New equaliser, based on MINT, with three virtual channels.
NER	Noise Enhancement Ratio defined in section 5.5.1 (page 78).
SER	Signal-to-Error Ratio defined in section 5.5.1 (page 78).
SERU	SER when the input signal is a unit impulse;i.e. x(n) = 1.
TFL	Total filter length defined in section 5.5.1 (page 78).

List of Symbols

$[\mathbf{G_1 G_2}]$	Channel matrix of a dual channel-filter system.
$\mathbf{G}^T$	The transpose of the channel matrix $\mathbf{G}$.
$\mathbf{G}^{-1}$	The inverse of the channel matrix $\mathbf{G}$.
$\mathbf{h}_i(n)$	The time -domain representation of a filter vector (sequence) containing the coefficients of the *i*th filter in a multi-channel-filter system.
$\mathbf{H}_i(k)$	The discrete Fourier transform of a filter vector (sequence) containing the coefficients of the *i*th filter in a multi-channel-filter system.
$\mathbf{H}_i(z)$	The *z*-transform of a filter vector (sequence) of the *i*th filter in a multi-channel-filter system.
$\mathbf{H}^T\mathbf{H}$	The norm of the filter vector $\mathbf{H}$.
max(a,b)	The maximum of a or b.

Chapter 1

Introduction

1.1 Background

The multiple-input/output inverse theorem(MINT) was described in [1] [2] in the exact inverse filtering of room acoustics (see also the introduction of chapter 2). Since a room impulse response, modelled as **G**(z) in Figure 1.1, has non-minimum phase [3] in general, the infinite impulse response (IIR) digital filter **H**(z) constructed from the inverse of the room impulse response can become unstable.

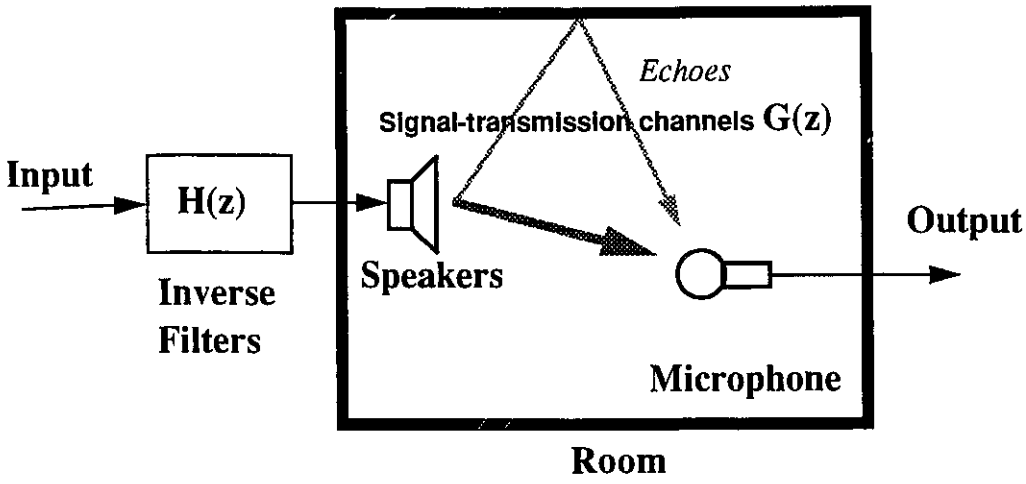

Figure 1.1 An acoustic system consisting of a loudspeaker and a microphone.

A number of inverse filtering methods [4] [5] with the finite impulse response (FIR) filter have been reported and they are based on the least square error (LSE) method [6] (see also the Appendix A). However, they cannot realize the exact inverse of an acoustic system that has non-minimum phases [7] [8]. The drawback is the use of a single signal-transmission channel. The use of additional signal-transmission channels depicted in Figure 2.1, according to the MINT, realizes the exact inverse of a set of static FIR room impulse responses with a set of FIR filters. The coefficients of these filters can be computed via matrix operations [9]- [13] on condition that these signal-transmission channels do not have common zeros.

In [1] [2], experiments on inverse filtering was conducted in a simulated sound field. It shown that:

1) The performance of the LSE method is deeply influenced by the nature of the acoustics signal-transmission channel in use.

2) The performance of the MINT method with two signal-transmission channels is superior to the LSE method.

The concept of the MINT in using multiple signal-transmission channels and the exact nature of its solution captured the attention of the author and motivated him to start the research work to identity the potential applications of this concept in a linear, shift-invariant, deterministic, FIR system.

The objectives of this thesis are:

- to understand the principle
- to extend its application to areas other than inverse filtering
- to resolve issues related to practical implementation
- to extend this concept to a single channel application

Results obtained are:†

- the study of other solution types; one of them is the Minimum Norm solution
- the application of MINT to selectively receive, filter, distribute signals in a multichannel system
- the different approaches that resolve problems associated with common or/and close zeros in the channels
- the derivation of new equalizer structures that support inverse filtering on a single channel

1.2 Thesis organization

The thesis is organized into four main chapters and a conclusion. In Chapter 2, the *m*ultiple-*i*nput/output *i*nverse *t*heorem(MINT) implemented with a square matrix solution, as proposed in [2], is described. This approach provides the exact inverse filtering. The properties and attributes of this solution are studied. Four general properties of the MINT are given. The dimensional requirement on the channels and filters as well as different solution types are demonstrated. This leads to new solution types. One of them is the Minimum Norm Solution. This chapter is concluded with a section describing the difference between MINT and the concept of a filter bank system.

Chapter 3 begins with describing the concept of pre-channel filtering and post-channel filtering. MINT in a multiple channels system is then examined. The dimensional requirement on the channels and the filters as well as the comparison with MINT in a dual

†. Some publications on other areas of the MINT were reported during the work of this thesis. In one application, the digital cancellation of engine noise by some fast adaptive IIR algorithms was proposed in [14]. The deconvolution of the, in general, non-minimum phase radiation path is conducted with additional filter. In another application, a sub-band MINT was proposed in the recovering of a broad band reverberant speech [15]. Dividing a full band speech signal into 512 sub-bands and processing each sub-band by the MINT method reduces the computational effort in removing the effect of the reverberation from the speech.

channel system are given. The application of MINT in areas other than the exact inverse filtering is explored. Examples on the design of a speakerphone system illustrates the capabilities of selective reception and distribution of signals by MINT.

Solutions to the problem of common and close zeros are presented in Chapter 4. This chapter begins with examining the possibility of having common zeros in the channels, thus an exact solution does not exist by conventional methods. Two solutions are suggested. One solution is the use of additional channel. The other is the use of an infinite impulse response (IIR) filter. This extends the application of MINT to those systems having minimum phase common zeros.

The issue of high filter gain in equalization is then reviewed. For MINT, it is associated with close zeros in the channels. In additional to the solution applied in solving the problem associated with common zeros, the use of the Minimum Norm solution is proposed. Simulations show this approach is valid.

After discussing in chapter 4 the technique to resolve the practical problem on the implementation of MINT, chapter 5 focuses on the application of MINT in exact inverse filtering. The conventional approach of MINT requires the existence of multiple channels. In this chapter, the approach of MINT is extended with application to a single channel; namely, the equalization of a single channel. The concept of derived channels is explained. New equalization structures (2-subchannel system and 3-subchannel system) are presented. Simulations are conducted to compare the performance of the new equalizer structures with those based on the least squares error (LSE) criterion.

Chapter 6 concludes the findings of this research and suggests possible areas of future research.

Chapter 2

Multiple-input/output Theorem

2.1 Introduction

The multiple-input/output theorem (MINT) was proposed by Masato Miyoshi and Yutaka Kaneda [1]. Application to inverse filtering of room acoustics was suggested [2].

Acoustic signals radiated inside a room are linearly distorted by wall reflections which lead to reverberations and echoes which reduce speech intelligibility. These undesirable effects can be reduced by applying inverse filtering. As opposed to the conventional LSE method of inverse filtering [4] [5] which is based on a single channel-filter model, two or more channels each with complementary filter are used to achieve an exact overall inverse. A simple system with two speakers and one listener (microphone) is shown in Figure 2.1. It can be modelled using FIR discrete filters as shown in Figure 2.2.

Two parallel filter-channel subsystems form a 2-input-1-output system of FIR filters. $\mathbf{x}(n)$ is the input signal to the two digital filters $\mathbf{H}_1(z)$ and $\mathbf{H}_2(z)$ which equalize the room acoustics channels represented by $\mathbf{G}_1(z)$ and $\mathbf{G}_2(z)$. The resulting signals are entered into the room via two speakers after digital-to-analog conversion and amplification. The different locations of the speakers result in different echo paths to the listener(microphone) and can be modeled as two discrete channels.

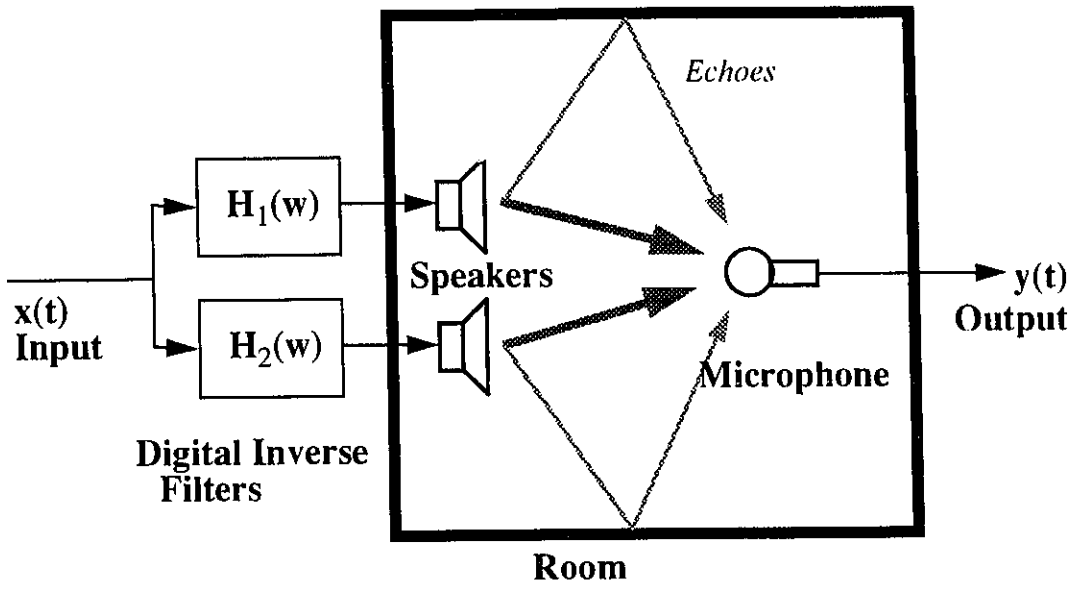

Figure 2.1 The acoustic system of a room

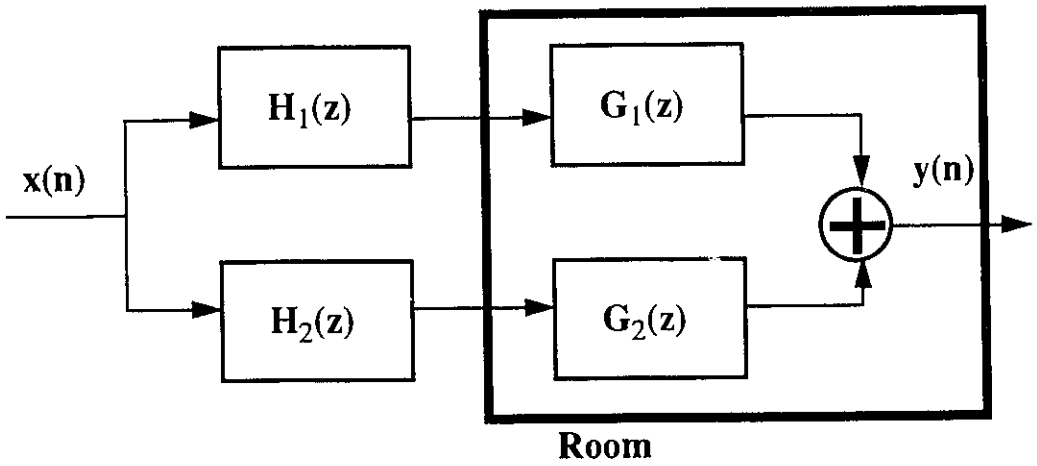

Figure 2.2 Discrete model of the acoustic system of a room.

The objective is to design the FIR filter pairs such that the input signal **x**(n) is perfectly reconstructed at the output. The following convolution equation must be satisfied.

$$\mathbf{h}_1(n) * \mathbf{g}_1(n) + \mathbf{h}_2(n) * \mathbf{g}_2(n) = \mathbf{d}(n)$$
$$\mathbf{d}(n) = \begin{cases} 1, & n = k \\ 0, & n \neq k \end{cases} \tag{2.1}$$

where k is the allowable delay; k=0,1,2,...K-1 and K is the length of the desired overall response **d**(n).

As such, **d**(n) is a unit impulse response with time delay. In other words, the output signal differs from the input signal by a time delay only. The equivalent multiplication equation in the **z**-domain is

$$\mathbf{H}_1(z)\,\mathbf{G}_1(z) + \mathbf{H}_2(z)\,\mathbf{G}_2(z) = \mathbf{D}(z)$$
$$\mathbf{D}(z) = z^{-n} \tag{2.2}$$

Equations (2.1) and (2.2) can be used for perfect cancellation of room echoes, and MINT is applied to provide an exact inverse filtering function for parallel channels (channel-filter subsystems).

Computation of FIR filters to obtain an exact inverse in the discrete time domain was proposed in [2] for a special case in which the channel matrix, defined on Section 2.2, is a square matrix. We shall describe this method in Section 2.2 of this chapter. In Section 2.3 the MINT is extended with four generalizations. Section 2.4 shows the existence of an exact solution in a dual-channel system with square channel matrix as well as with a rectangular channel matrix that has more columns than rows. This leads to the concept of minimum

norm solution shown in Section 2.5. This chapter is concluded with a comparison between the filter bank concept and MINT in Section 2.6.

2.2 Computation of the inverse FIR filters in the discrete time domain

Consider the dual-channel system depicted in Figure 2.2 and let the length of the sequences $\mathbf{g}_1(n)$, $\mathbf{g}_2(n)$, $\mathbf{h}_1(n)$, $\mathbf{h}_2(n)$, $\mathbf{d}(n)$ be M, N, I, J, K respectively. As proposed [2], K is equal to M+I-1and N+J-1. Equation (2.1) can be expressed in a matrix form:

$$\begin{bmatrix} g_1(0) & 0 & \cdots & 0 & g_2(0) & 0 & \cdots & 0 \\ g_1(1) & g_1(0) & \cdots & \vdots & g_2(1) & g_2(0) & \cdots & \vdots \\ \vdots & \vdots & \cdots & \vdots & \vdots & \vdots & \cdots & \vdots \\ \vdots & \vdots & \cdots & \vdots & \vdots & \vdots & \cdots & \vdots \\ g_1(M-1) & \vdots & \cdots & \vdots & g_2(N-1) & \vdots & \cdots & \vdots \\ 0 & g_1(M-1) & \cdots & g_1(0) & 0 & \vdots & \cdots & g_2(0) \\ \vdots & 0 & \cdots & \vdots & \vdots & g_2(N-1) & \cdots & \vdots \\ \vdots & \cdots & \cdots & \vdots & \vdots & \cdots & \cdots & \vdots \\ 0 & \cdots & \cdots & \vdots & 0 & \cdots & \cdots & \vdots \\ 0 & \cdots & 0 & g_1(M-1) & 0 & \cdots & 0 & g_2(N-1) \end{bmatrix} \begin{bmatrix} h_1(0) \\ h_1(1) \\ \vdots \\ h_1(I-1) \\ h_2(0) \\ h_2(1) \\ \vdots \\ h_2(J-1) \end{bmatrix} = \begin{bmatrix} d(0) \\ d(1) \\ \vdots \\ \vdots \\ \vdots \\ \vdots \\ \vdots \\ d(K-1) \end{bmatrix} \quad (2.3)$$

or

$$[\mathbf{G}_1 \mathbf{G}_2] \begin{bmatrix} \mathbf{H}_1 \\ \mathbf{H}_2 \end{bmatrix} = [\mathbf{D}]$$

or

$$\mathbf{GH} = \mathbf{D}$$

G, **H** and **D** are the channel matrix, filter vector and desired response vector respectively.

The dimension of $\mathbf{G}$ is K by I+J. If K is equal to I+J, $\mathbf{G}$ is square matrix. An unique solution for $\mathbf{H}$ can be computed as:

$$\mathbf{H} = \mathbf{G}^{-1}\mathbf{D} \tag{2.4}$$

provided that $\mathbf{G}_1(z)$ and $\mathbf{G}_2(z)$ do not contain common zeros [2]; otherwise, the inverse the channel matrix $\mathbf{G}$ is undefined. The solution is termed "*Square Matrix Solution*".

2.3 Generalization of the MINT

There are four points to extend the application of the Multiple-input/output Theorem:

1) ***Length requirement of the filters***

The square matrix solution proposed in [2] required that the length of the channels and filters must be $I = N - 1$ and $J = M - 1$. The length requirement should in fact be

$$\mathbf{I \geq N - 1 \text{ and } J \geq M - 1}$$

As an extension of the square matrix solution, the "*Minimum Norm Solution*", which is also an exact solution, is proposed and covered in Section 2.5. This new approach extends the length requirement.

2) ***Filtering capability***

In the application proposed in [2] for perfect reconstruction of distorted signals, output vector $\mathbf{D}$ is a unit impulse response.

In general, vector $\mathbf{D}$ can be any finite length column vector with real coefficients. This

allows MINT to be used in applications where the overall system response can assume any desired frequency spectrum in a controllable manner. This additional filtering capability is found useful. For example, it enables the perfect reconstruction of distorted signals with delays. Some other useful applications on selective reception and distribution of signals are demonstrated in Section 3.3.4.1 (page 34) and Section 3.3.4.2 (page 40).

3) ***Uniqueness of the solution***

The uniqueness of the *square matrix solution* implies the uniqueness of filter-channel subsystems. For a given output vector $\mathbf{D}$, the responses of all filter-channel subsystems are determined only by the location of the zeros of the channels and the length of the filter-channel subsystem. It is independent of the gain of the channels.

We shall illustrate this property with a simple example. Given the channels $\mathbf{g}_1(n)$, $\mathbf{g}_2(n)$ and the desired output $\mathbf{d}(n)$, the following equation is satisfied:

$$\mathbf{H}_1(z)\,\mathbf{G}_1(z) + \mathbf{H}_2(z)\,\mathbf{G}_2(z) = \mathbf{D}(z)$$

and the filter-channel subsystems are $\mathbf{H}_1(z)\mathbf{G}_1(z)$ and $\mathbf{H}_2(z)\mathbf{G}_2(z)$.

The only possible allocation of gain k_1, k_2 among channels and filters is depicted as

$$\frac{1}{k_1}\mathbf{H}_1(z)\,k_1\mathbf{G}_1(z) + \frac{1}{k_2}\mathbf{H}_2(z)\,k_2\mathbf{G}_2(z) = \mathbf{D}(z) \qquad (2.5)$$

such that the filter-channel subsystems remain unique. In other words, any increase of gain on one channel will be compensated by the corresponding lost on the filter in the same channel-filter subsystem.

The *minimum norm solution* described in Section 2.5 extends the attribute of uniqueness even further. It is shown that if $I = N$ and $J = M$, the channels $\mathbf{g}_1(n)$ and $\mathbf{g}_2(n)$ themselves are also the minimum norm solution of the filters $\mathbf{h}_1(n)$, $\mathbf{h}_2(n)$. This property is useful in applications such as system identification.

4) *Existence of exact solutions*

If $\mathbf{G}_1(z)$ and $\mathbf{G}_2(z)$ contain common zeros, an exact solution does not exist for the overall responses $\mathbf{d}(n)$ which do not contain these common zeros. On the other hand, exact solutions do exist if those common zeros are permitted in the desired responses $\mathbf{d}(n)$.

2.4 Existence of exact solutions in a dual channel system

In this section, we shall show the existence of the solutions for the vector $\mathbf{H}$ in a dual-channel system and the restrictions. Sample calculations are given.

2.4.1 Requirement for the existence of exact solutions

Recall that $\mathbf{g}_1(n)$, $\mathbf{g}_2(n)$, $\mathbf{h}_1(n)$, $\mathbf{h}_2(n)$ are channel and filter responses respectively (Figure 2.2). Their lengths are M, N, I, J respectively. MINT indicates that if $\mathbf{G}_1(z)$ and $\mathbf{G}_2(z)$ do not contain common zeros and

$$\max(M+I-1, N+J-1) \leq I+J, \tag{2.6}$$

or in other words

$$I \geq N-1 \qquad \text{and} \qquad J \geq M-1,$$

$\mathbf{h}_1(n)$ and $\mathbf{h}_2(n)$ exist such that the convolution equation (2.1) is satisfied:

$$\mathbf{h}_1(n) * \mathbf{g}_1(n) + \mathbf{h}_2(n) * \mathbf{g}_2(n) = \mathbf{d}(n)$$

where $\mathbf{d}(n)$ is the output vector of length K = max(M+I-1, N+J-1) and $*$ is the convolution operator.

Or in matrix equation, similar to (2.3), but not constrained to be a square matrix

$$\begin{bmatrix} g_1(0) & 0 & \cdots & 0 & g_2(0) & 0 & \cdots & 0 \\ g_1(1) & g_1(0) & \cdots & \vdots & g_2(1) & g_2(0) & \cdots & \vdots \\ \vdots & \vdots & \cdots & \vdots & \vdots & \vdots & \cdots & \vdots \\ \vdots & \vdots & \cdots & \vdots & \vdots & \vdots & \cdots & \vdots \\ g_1(M-1) & \vdots & \cdots & \vdots & g_2(N-2) & \vdots & \cdots & \vdots \\ 0 & g_1(M-1) & \cdots & g_1(0) & g_2(N-1) & g_2(N-2) & \cdots & g_2(0) \\ \vdots & 0 & \cdots & \vdots & \vdots & g_2(N-1) & \cdots & \vdots \\ \vdots & \cdots & \cdots & \vdots & \vdots & \cdots & \cdots & \vdots \\ \vdots & \cdots & \cdots & \vdots & \vdots & \cdots & \cdots & \vdots \\ 0 & \cdots & \cdots & g_1(M-1) & 0 & \cdots & \cdots & g_2(N-2) \\ 0 & \cdots & \cdots & 0 & 0 & \cdots & \cdots & g_2(N-1) \end{bmatrix} \begin{bmatrix} h_1(0) \\ h_1(1) \\ \vdots \\ \vdots \\ h_1(I-1) \\ h_2(0) \\ h_2(1) \\ \vdots \\ \vdots \\ h_2(J-1) \end{bmatrix} = \begin{bmatrix} d(0) \\ d(1) \\ \vdots \\ \vdots \\ \vdots \\ \vdots \\ \vdots \\ d(K-1) \end{bmatrix} \qquad (2.7)$$

(2.6) permits the occurrence of the zero values below $\mathbf{g}_1$(M-1) of the channel matrix in (2.7), since $M+I-1$ can be smaller than, equal to or bigger than $N+J-1$.

2.4.2 Existence of exact solutions: a study

The existence of exact solutions can be demonstrated in three cases.

Case 1 : $I+J = M+I-1 = N+J-1$
Case 2 : $I+J = \max(M+I-1, N+J-1)$
Case 3 : $I+J \geq \max(M+I-1, N+J-1)$

The channels $\mathbf{G}_1(z)$ and $\mathbf{G}_2(z)$ in each case do not contain common zeros.

Case 1 and 2 are described with sample calculation in this section. Case 3 will be covered in Section 2.5.

Case 1:

The channel matrix $[\mathbf{G_1G_2}]$ depicted in equation (2.3) is an I+J by I+J square matrix with M+I-1=N+J-1. There are at least two non-zero value coefficients present on each row of the channel matrix. For this case, we have to use Theorem 2.1 on page 30 of [10].

Theorem: *The polynomials* $\mathbf{g}_1(n)$, $\mathbf{g}_2(n)$ *with real coefficients have a common zero (of degree greater than zero) if and only if the M+N-2 order Sylvester determinant* $\mathbf{R}(\mathbf{g}_1(n), \mathbf{g}_2(n))$ *is zero, provided* $\mathbf{g}_1(0)$, $\mathbf{g}_2(0)$ *are not both zero.*

$$\mathbf{R}(\mathbf{g}_1(n), \mathbf{g}_2(n)) = \begin{vmatrix} g_1(0) & g_1(1) & g_1(2) & \cdots & g_1(M-1) & \cdots & \cdots & \cdots & 0 \\ 0 & g_1(0) & g_1(1) & \cdots & g_1(M-2) & g_1(M-1) & \cdots & \cdots & 0 \\ 0 & 0 & g_1(0) & \cdots & g_1(M-3) & g_1(M-2) & g_1(M-1) & \cdots & 0 \\ \vdots & \vdots & \vdots & \vdots & \vdots & \vdots & \vdots & \vdots & \vdots \\ \vdots & \vdots & \vdots & \vdots & g_1(0) & g_1(1) & g_1(2) & \cdots & g_1(M-1) \\ \vdots & \vdots & \vdots & g_2(0) & g_2(1) & g_2(2) & \cdots & \cdots & g_2(N-1) \\ \vdots & \vdots & \vdots & \vdots & \vdots & \vdots & \vdots & \vdots & \vdots \\ 0 & g_2(0) & g_2(1) & \cdots & \cdots & g_2(N-2) & g_2(N-1) & \cdots & 0 \\ g_2(0) & g_2(1) & g_2(2) & \cdots & \cdots & g_2(N-1) & \cdots & \cdots & 0 \end{vmatrix}$$

We see that the relationship between the channel matrix $[\mathbf{G_1G_2}]$ and the Sylvester determinant is:

$$\mathbf{R}(\mathbf{g}_1(n), \mathbf{g}_2(n)) = (-1)^L \det([\mathbf{G_1G_2}]^T)$$

$$L = \begin{cases} \dfrac{M-1}{2}, & M \text{ is odd} \\ \dfrac{M-2}{2}, & M \text{ is even} \end{cases} \tag{2.8}$$

thus

$$\det([\mathbf{G_1G_2}]) = (-1)^L \mathbf{R}(\mathbf{g}_1(n), \mathbf{g}_2(n))$$

Since:

1) the determinant of the square matrix is equal to the determinant of its transpose.

2) interchanging any two rows (or any two columns) of the square matrix changes the sign of its determinant,

the magnitude of the determinant of the channel matrix and the Sylvester determinant are identical. The conclusion is that common zeros in $\mathbf{G}_1(z)$, $\mathbf{G}_2(z)$ exist if the determinant of the channel matrix $[\mathbf{G}_1\mathbf{G}_2]$ is zero.

In other words, if $\mathbf{G}_1(z)$ and $\mathbf{G}_2(z)$ are relatively prime (having no common zeros), the determinant of the channel matrix $[\mathbf{G}_1\mathbf{G}_2]$ has a non-zero value. Hence solutions exist for $\mathbf{h}_1(n)$ and $\mathbf{h}_2(n)$, which can be computed by applying Cramer's Formula [6](also page 156 of [12]).

Example for case 1: Given the channels

$$\begin{aligned}\mathbf{G}_1(z) &= (1-(0.5-0.5i)z^{-1})(1-(0.5+0.5i)z^{-1})(1-(1-2i)z^{-1})(1-(1+2i)z^{-1}) \\ &= 1-3z^{-1}+7.5z^{-2}-6z^{-3}+2.5z^{-4} \\ \mathbf{G}_2(z) &= (1-(0.9i)z^{-1})(1+(0.9i)z^{-1}) \\ &= 1+0.81z^{-2}\end{aligned}$$

and M, N are 5, 3 respectively. Design the filters $\mathbf{h}_1(n)$, $\mathbf{h}_2(n)$ with length 2, 4 respectively:

The matrix equation is:

$$\begin{bmatrix} 1 & 0 & 1 & 0 & 0 & 0 \\ -3 & 1 & 0 & 1 & 0 & 0 \\ 7.5 & -3 & 0.81 & 0 & 1 & 0 \\ -6 & 7.5 & 0 & 0.81 & 0 & 1 \\ 2.5 & -6 & 0 & 0 & 0.81 & 0 \\ 0 & 2.5 & 0 & 0 & 0 & 0.81 \end{bmatrix} \begin{bmatrix} h_1(0) \\ h_1(1) \\ h_2(0) \\ h_2(1) \\ h_2(2) \\ h_2(3) \end{bmatrix} = \begin{bmatrix} 1 \\ 0 \\ 0 \\ 0 \\ 0 \\ 0 \end{bmatrix}$$

$$\Rightarrow \begin{bmatrix} h_1(0) \\ h_1(1) \\ h_2(0) \\ h_2(1) \\ h_2(2) \\ h_2(3) \end{bmatrix} = \begin{bmatrix} -0.10163217661329 \\ -0.10068510915504 \\ 1.10163217661329 \\ -0.20421142068482 \\ -0.43213606592223 \\ 0.31075650973777 \end{bmatrix}$$

Hence the filters are:

$$\mathbf{H}_1(z) = -0.10163217661329 - 0.10068510915504z^{-1}$$

$$\mathbf{H}_2(z) = 1.10163217661329 - 0.20421142068482z^{-1} - 0.43213606592223z^{-2} + 0.31075650973777z^{-3}$$

Case 2:

The channel matrix $[\mathbf{G_1}\mathbf{G_2}]$ depicted in (2.7) can also be a I+J by I+J square matrix but the lengths M+I-1, N+J-1 for the vectors $\mathbf{h}_1(n) * \mathbf{g}_1(n)$, $\mathbf{h}_2(n) * \mathbf{g}_2(n)$ need not be equal. There is at least one non-zero value coefficient present on each row of the channel matrix.

This case can also be proved by referring to the Theorem in case 1 on page 13 since the channel matrix is square. Besides requiring that $\mathbf{g}_1(0)$, $\mathbf{g}_2(0)$ not be both zero, the theorem also implies that $\mathbf{g}_1(M-1)$, $\mathbf{g}_2(N-1)$ are not both zero and that the rest of the coefficients can be zero. However, it does allow one of the polynomials to contain just one non-zero value coefficient if the first and the last coefficient of the other polynomial are not zero. With the same argument of case 1, this leads to the conclusion that there always exists a solution for the filter vectors $\mathbf{h}_1(n)$ and $\mathbf{h}_2(n)$ for a pair of channels with no common zeros such that

$$I + J = \max(M + I - 1, N + J - 1)$$

Example for case 2: Given the channels

$$\begin{aligned}\mathbf{G_1}(z) &= z^{-1}(1 - (0.5 - 0.5i)z^{-1})(1 - (0.5 + 0.5i)z^{-1}) \\ &= z^{-1} - z^{-2} + 0.5z^{-3} \\ \mathbf{G_2}(z) &= (1 - (0.9i)z^{-1})(1 + (0.9i)z^{-1}) \\ &= 1 + 0.81z^{-2}\end{aligned}$$

and M, N are 4, 3 respectively. Design the filters $\mathbf{h}_1(n)$, $\mathbf{h}_2(n)$ with lengths 2, 4 respectively such that the overall delay of the desired response $\mathbf{d}(n)$ shown in (2.1) is 5; i.e., $\mathbf{d}(5) = 1$.

The matrix equation is:

$$\begin{bmatrix} 0 & 0 & 1 & 0 & 0 & 0 \\ 1 & 0 & 0 & 1 & 0 & 0 \\ -1 & 1 & 0.81 & 0 & 1 & 0 \\ 0.5 & -1 & 0 & 0.81 & 0 & 1 \\ 0 & 0.5 & 0 & 0 & 0.81 & 0 \\ 0 & 0 & 0 & 0 & 0 & 0.81 \end{bmatrix} \begin{bmatrix} h_1(0) \\ h_1(1) \\ h_2(0) \\ h_2(1) \\ h_2(2) \\ h_2(3) \end{bmatrix} = \begin{bmatrix} 0 \\ 0 \\ 0 \\ 0 \\ 0 \\ 1 \end{bmatrix}$$

$$\Rightarrow \begin{bmatrix} h_1(0) \\ h_1(1) \\ h_2(0) \\ h_2(1) \\ h_2(2) \\ h_2(3) \end{bmatrix} = \begin{bmatrix} 0.42237727555757 \\ 1.10363094581172 \\ 0 \\ -0.42237727555757 \\ -0.68125367025415 \\ 1.23456790123457 \end{bmatrix}$$

Hence the filters are:

$$\mathbf{H}_1(z) = 0.42237727555757 - 1.10363094581172 z^{-1}$$

$$\mathbf{H}_2(z) = -0.42237727555757 z^{-1} - 0.68125367025415 z^{-2} + 1.23456790123457 z^{-3}$$

2.5 Minimum norm solution

In this section, the length requirement for exact solutions described in case 3 in Section 2.4.1 is discussed. The discussion results in a new approach for the exact solution; namely, the *minimum norm solution*.

2.5.1 Case 3: rectangular matrix solution

The channel matrix $[\mathbf{G}_1\mathbf{G}_2]$ is a rectangular matrix with more columns than rows (long matrix), i.e.

$$I + J \geq \max(M + I - 1, N + J - 1)$$

With the same $\mathbf{g}_1(n)$, $\mathbf{g}_2(n)$, $\mathbf{h}_1(n)$, $\mathbf{h}_2(n)$, $\mathbf{d}(n)$ from case 1 or 2, one can always form $\mathbf{h'}_1(n)$, $\mathbf{h'}_2(n)$, $\mathbf{d'}(n)$ with length I', J', max(M-I'-1, N-J'-1) by appending zero coefficients to the end of $\mathbf{h}_1(n)$, $\mathbf{h}_2(n)$, $\mathbf{d}(n)$ respectively so that the following equations is satisfied.

$$\mathbf{h'}_1(n) * \mathbf{g}_1(n) + \mathbf{h'}_2(n) * \mathbf{g}_2(n) = \mathbf{d'}(n) \tag{2.9}$$

In fact, there exists an infinite set of exact solution vectors $\mathbf{h'}_1(n)$, $\mathbf{h'}_2(n)$. The channel matrix represents a system with max(M+I'-1, N+J'-1) linear independent equations (rows) and I'+J' unknown variables (columns). Since the number of unknown variables is greater than the number of equations and there is no common zero, an infinite number of solutions, termed *long matrix solutions*, are obtained.

The approach with the *long matrix solution* provides extra degrees of freedom in tailoring the frequency spectrum of the filters.

Among the infinite set of long matrix solutions, one of them can be computed as

$$\begin{bmatrix} \mathbf{H}_1 \\ \mathbf{H}_2 \end{bmatrix} = [\mathbf{G}_1 \mathbf{G}_2]^T ([\mathbf{G}_1 \mathbf{G}_2] [\mathbf{G}_1 \mathbf{G}_2]^T)^{-1} [\mathbf{D}]$$

or

$$\mathbf{H} = \mathbf{G}^T (\mathbf{G}\mathbf{G}^T)^{-1} \mathbf{D} \tag{2.10}$$

such that the norm $\mathbf{H}^T\mathbf{H}$ is the smallest. This is the *Minimum Norm Solution* (page 86 of [6]). The use of the minimum norm solution in minimizing the impact of having close zeros in a dual-channels system is discussed in Section 4.3 (page 49)

2.5.2 Characteristics of the minimum norm solution

1) *Uniqueness of the minimum norm solution*

For given channels $\mathbf{g}_1(n)$, $\mathbf{g}_2(n)$ and fixed length filter vectors, there is only one solution among the infinite set of *long matrix solutions* with minimum norm.

If I = N and J = M, the channels $\mathbf{g}_1(n)$ and $\mathbf{g}_2(n)$ themselves are also the minimum norm solution of the filters $\mathbf{h}_1(n)$, $\mathbf{h}_2(n)$.

For the existence of an exact solution, it was stated in [2] that $\mathbf{G}_1(z)$ and $\mathbf{G}_2(z)$ must not contain a common zero. The uniqueness of minimum norm solution further implies that the channel-filter subsystems $\mathbf{G}_1(z)\mathbf{H}_1(z)$, $\mathbf{G}_2(z)\mathbf{H}_2(z)$ must not contain a common zero.

2) *Square matrix solution: a special case of the minimum norm solution*

When $I+J = \max(M+I-1, N+J-1)$, the same solution is obtained with the approach of the *square matrix solution* depicted in (2.4) and those of the minimum norm solution depicted in (2.10).

In fact, there exists only one solution because the number of linear independent equations (rows of the channel matrix) is equal to the number of unknowns (columns of the channel matrix). Therefore, this is also the solution with the minimum norm.

2.6 Filter banks allowing perfect reconstruction

This section describes the difference between the MINT concept and the concept of filter banks.

A related problem exists in publications on subsampled filter banks [16] [17] such as the N-path Channel Bank.

Figure 2.3 shows the block diagram of a subsampled filter bank. The idea is to design a pair of filter banks $\mathbf{G}_i(z)$ and $\mathbf{H}_i(z)$, i = 1,2, ..., N to obtain a perfectly reconstructed signal at the output. With this technique, the signal is split into several components for coding or other processing at reduced rate and is restored at the output by the receiving filter bank.

Applications such as a sub-band coder incorporating linear prediction, a scrambling scheme for analog signals, non-critically subsampled filter banks and filter banks on finite fields are described in [18].

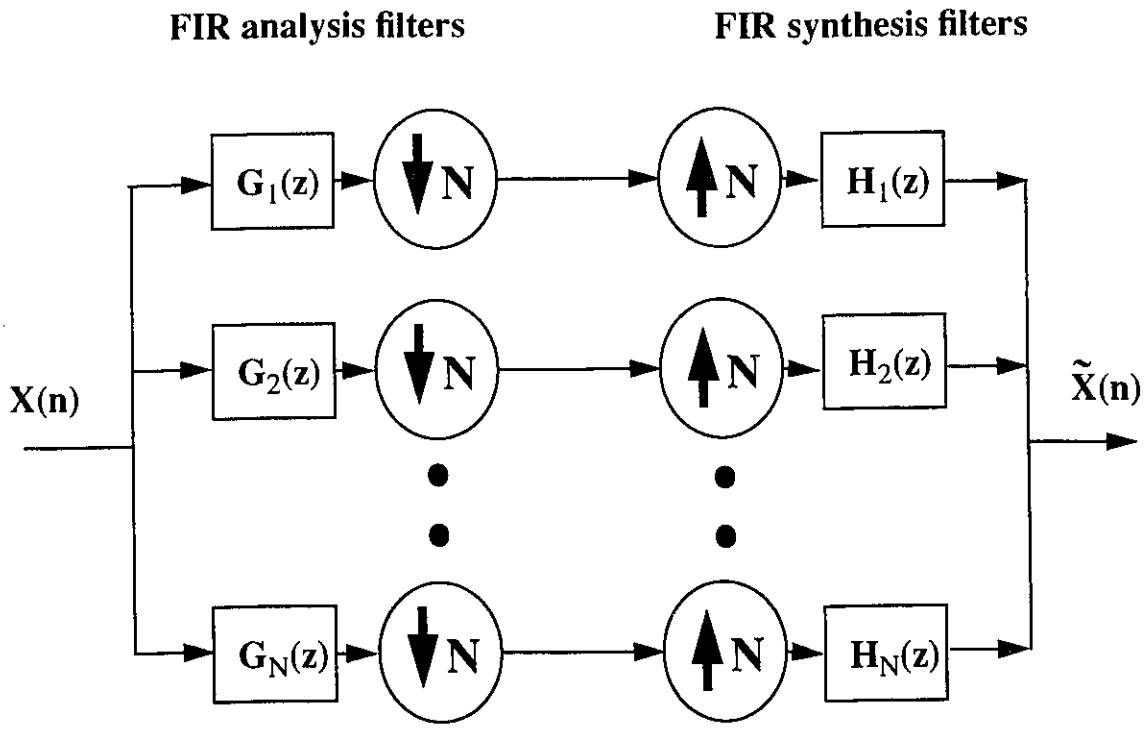

Figure 2.3 Block diagram of a subsampled filter bank

The difference between this filter bank concept and MINT is that they are formulated for different problems; therefore, different design parameters are used.

In the filter bank concept, both the analysis and synthesis filters, $\mathbf{G}_i(z)$ and $\mathbf{H}_i(z)$, can be designed to have the desired response (frequency spectrum) in order to meet the system objective. The technique of sampling rate reduction is employed in the filter bank concept, as the analysis and synthesis filters are strictly band limited.

For MINT, the channels $\mathbf{G}_i(z)$ are given and they overlap in frequency spectrum. Hence decimation cannot be applied. Only the filters $\mathbf{H}_i(z)$ are designed to compensate the distortion caused by the channels $\mathbf{G}_i(z)$ so as to meet the overall system response.

As in MINT (see chapter 4), large coefficients in $\mathbf{H}_i(z)$ can be caused by the presence of close zeros among channels. This property might not be important in the filter bank concept because the full control of both analysis and synthesis filter banks allows the designer to avoid this problem.

2.7 Conclusion

The *m*ultiple-*i*nput/output *i*nverse *t*heorem(MINT) implemented with a square matrix solution, as proposed in [2], was described. This approach provides the exact inverse filtering even on channels with non-minimum phase zeros. Solution do not exist for those channels with common zeros. The properties and attributes of this solution were studied. Four general properties of the MINT were given. The dimensional requirement on the channels and filters as well as different solution types were demonstrated. This leads to new solution types. One of them is the Minimum Norm Solution. The difference between MINT and the concept of a filter bank system was discussed.

Chapter 3

MINT: Applications

3.1 Introduction

This chapter extends the study of MINT by exploring its properties with some potential applications.

In Section 3.2. the concept of pre-channel filtering and post-channel filtering is described. The MINT in a multi-channel system is examined in the remaining chapter. Restriction on its configuration as well as comparison with a dual-channel system are given. Application to speakerphone (hands-free telephone) system are designed to illustrate the capabilities of selective signal reception and distribution of this system.

3.2 Pre-channel and post-channel filtering

With MINT, a signal distorted by a given pair of channels $\mathbf{g}_1(n)$, $\mathbf{g}_2(n)$ can be restored completely by a pair of filters. Figures 3.1 and 3.2 depict two scenarios: pre-channel

filtering and post-channel filtering.

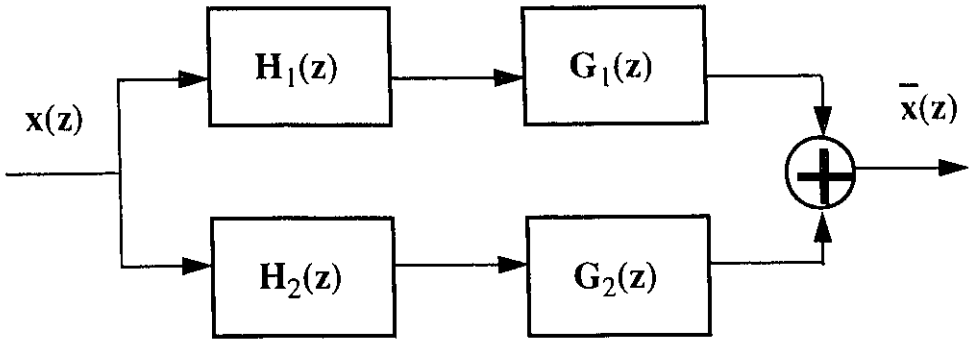

Figure 3.1: Pre-channel filtering.

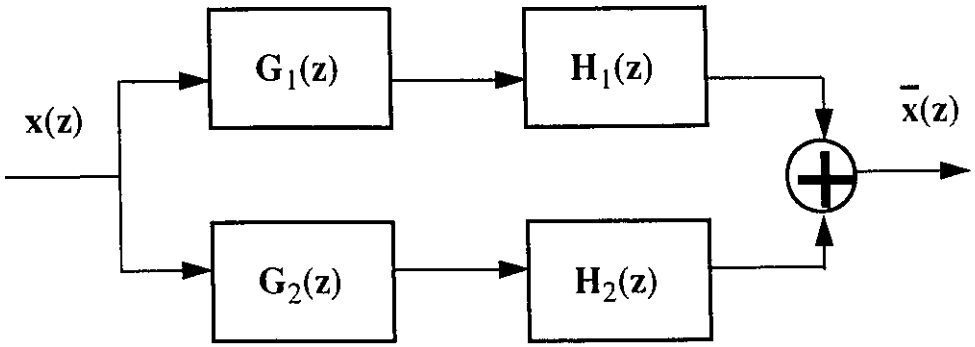

Figure 3.2: Post-channel filtering.

In each case, compensation for the signal distortion is provided by a pair of filters before or after the channels respectively. Given that the same set of channels $\mathbf{g}_1(n)$, $\mathbf{g}_2(n)$ is encountered in both scenarios, exact inverse filtering can be supported by the same set of filters $\mathbf{h}_1(n)$, $\mathbf{h}_2(n)$. Therefore the same amount of computational and filtering efforts are required in both scenarios. Sections 3.3.4.1 and 3.3.4.2 give the design examples.

3.3 MINT in multi-channel system

In this section MINT in a multi-channel system is discussed. Comparison with the dual-channel system and the usefulness of removing common zeros are examined. Examples that deploys the property of selective signal reception, filtering and distribution are presented.

3.3.1 Introduction

In the previous discussions, we mainly considered dual-channel systems. There are other situations with multiple channels where MINT can be applied to. Figure 3.3 shows a room

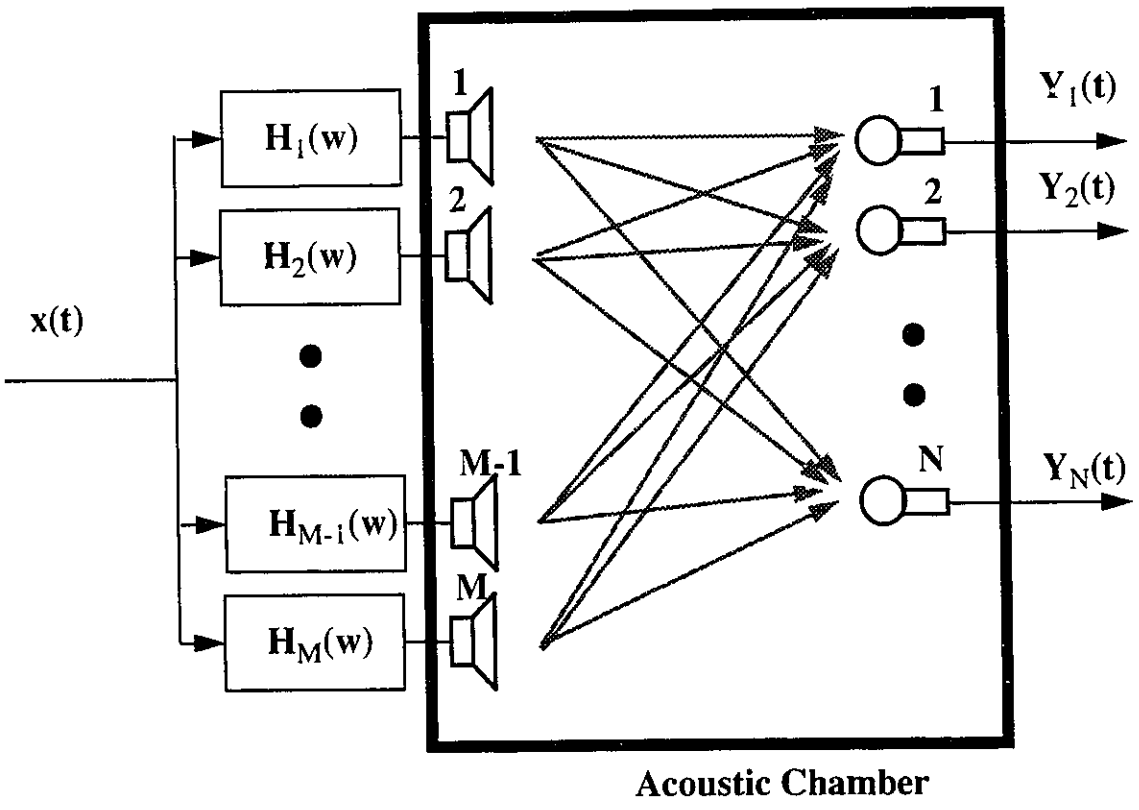

Figure 3.3: Acoustic room with multiple speakers and microphones.

with multiple speakers and microphones. There are M speakers and N microphones in the room. Effectively MN acoustic channels are formed. Filters, which can be implemented as digital FIR filters, are applied in front of speakers (in front of the D/A converters and power amplifiers); this is an example of MINT in pre-channel filtering (see Section 3.2).

The system can be modelled as a discrete system shown in Figure 3.4.

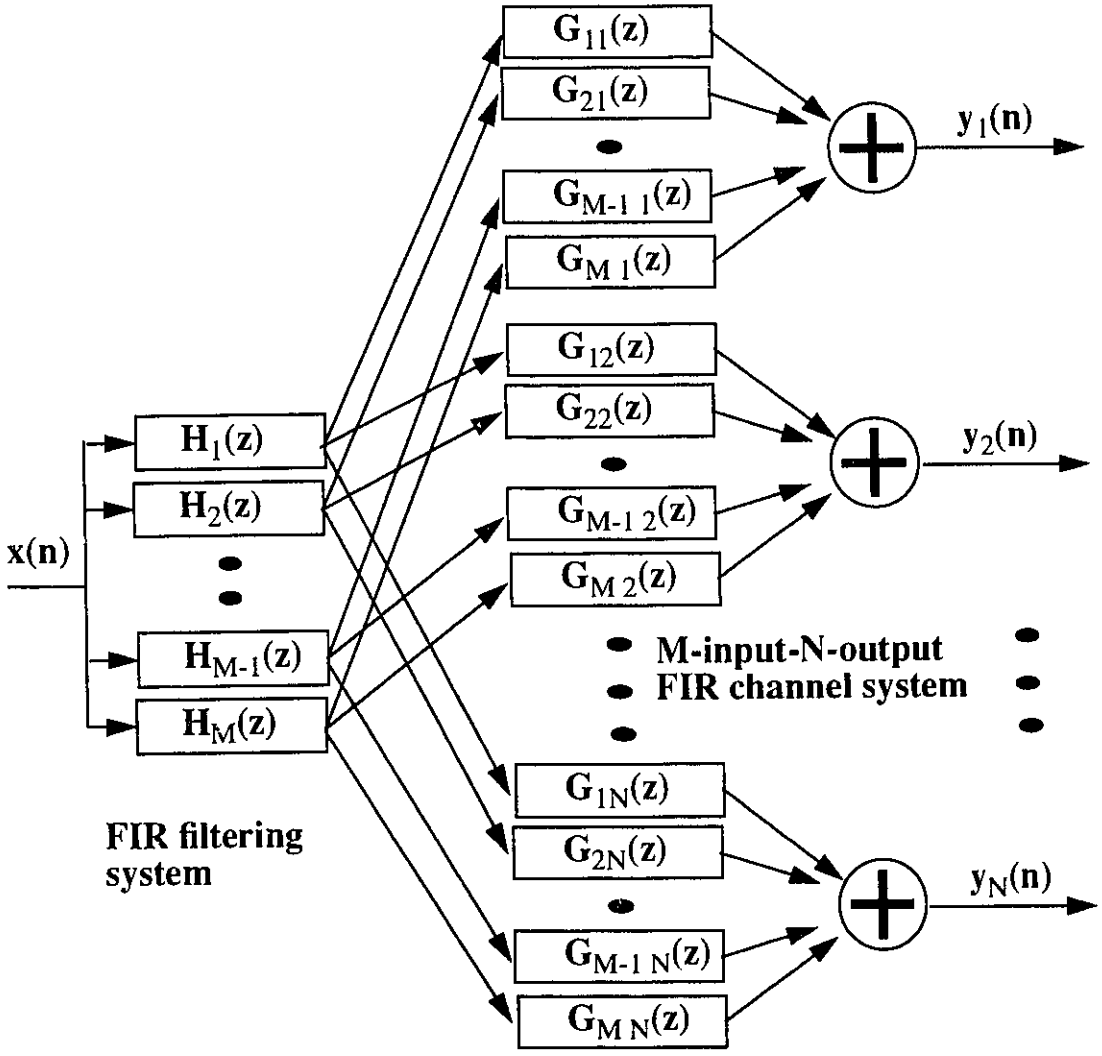

Figure 3.4: Discrete model of MINT in multi-channel system (pre-channel filtering).

The speakers are the signal entry points to the echo paths and the microphones represent the end points. Hence there are M entry points and N end points for the channel system which are modelled as a M-input N-output FIR system.

Filters $\mathbf{h}_1(n)$, $\mathbf{h}_2(n)$,..., $\mathbf{h}_M(n)$ are designed to meet the overall system output responses $\mathbf{d}_1(n)$, $\mathbf{d}_2(n)$,..., $\mathbf{d}_N(n)$ for each microphone. The following sets of convolution equations must be satisfied simultaneously:

$$\begin{aligned}
\mathbf{g}_{11}(n) * \mathbf{h}_1(n) + \mathbf{g}_{21}(n) * \mathbf{h}_2(n) + \ldots + \mathbf{g}_{M1}(n) * \mathbf{h}_M(n) &= \mathbf{d}_1(n) \\
\mathbf{g}_{12}(n) * \mathbf{h}_1(n) + \mathbf{g}_{22}(n) * \mathbf{h}_2(n) + \ldots + \mathbf{g}_{M2}(n) * \mathbf{h}_M(n) &= \mathbf{d}_2(n) \\
\vdots \qquad\qquad & \qquad \vdots \\
\mathbf{g}_{1N}(n) * \mathbf{h}_1(n) + \mathbf{g}_{2N}(n) * \mathbf{h}_2(n) + \ldots + \mathbf{g}_{MN}(n) * \mathbf{h}_M(n) &= \mathbf{d}_N(n)
\end{aligned} \tag{3.1}$$

We assume that all channels and filters have the same length L and J respectively. The set of equations can be expressed by a matrix equation shown below:

$$\begin{bmatrix} \mathbf{g}_{11} & \mathbf{g}_{21} & \cdots & \mathbf{g}_{M1} \\ \mathbf{g}_{12} & \mathbf{g}_{22} & \cdots & \mathbf{g}_{M2} \\ \vdots & \vdots & \ldots & \vdots \\ \mathbf{g}_{1N} & \mathbf{g}_{2N} & \cdots & \mathbf{g}_{MN} \end{bmatrix} \begin{bmatrix} \mathbf{h}_1 \\ \mathbf{h}_2 \\ \vdots \\ \mathbf{h}_M \end{bmatrix} = \begin{bmatrix} \mathbf{d}_1 \\ \mathbf{d}_2 \\ \vdots \\ \mathbf{d}_N \end{bmatrix} \tag{3.2}$$

or

$$\mathbf{GH} = \mathbf{D}$$

where

$$\mathbf{g}_{mn} = \begin{bmatrix} g_{mn}(0) & 0 & \cdots & \cdots & 0 \\ g_{mn}(1) & g_{mn}(0) & \cdots & \cdots & \vdots \\ \vdots & \vdots & \cdots & \cdots & g_{mn}(0) \\ g_{mn}(L-1) & g_{mn}(L-2) & \cdots & \cdots & g_{mn}(1) \\ \vdots & g_{mn}(L-1) & \cdots & \cdots & \vdots \\ \vdots & \cdots & \cdots & \cdots & g_{mn}(L-1) \end{bmatrix}$$

$$\mathbf{h}_m = \begin{bmatrix} h_m(0) \\ h_m(1) \\ \vdots \\ h_m(J-1) \end{bmatrix}$$

$$\mathbf{d}_n = \begin{bmatrix} d_n(0) \\ d_n(1) \\ \vdots \\ d_n(L+J-1) \end{bmatrix}$$

The expressions above form a set of N(L+J-1) linear independent equations with MJ variables if they do not include common zeros. When the number of variables (columns) is equal to or more than the number of equations (rows),i.e. $MJ \geq N(L+J-1)$, a solution for filters $\mathbf{h_m}(n)$ can be obtained by computing the inverse of the matrix as depicted in equation (2.4) (page 9) or (2.10) (page 19):

$$\mathbf{H} = \mathbf{G}^{-1}\mathbf{D}$$

or

$$\mathbf{H} = \mathbf{G}^{T}(\mathbf{G}\mathbf{G}^{T})^{-1}\mathbf{D}$$

3.3.2 Restrictions on a multi-channel system

The proof for the existence of a solution was pointed out in [2].This implies that no two rows or columns of the channel matrix $\mathbf{G}$ be the linear combination of other rows or columns. Furthermore, equation (3.2) assumes that all channels and filters have the same length L and J respectively; the channel matrix $\mathbf{G}$ has N(L+J-1) rows and MJ columns. This implies that M, the number of the input points of a multi-channel system with pre-channel filtering, must not be smaller than N, the number of the output points. It is because J, the length of filters, and L, the length of channels, are positive integer. Hence the existence of exact solutions imposes a restriction on how a M-input-N-output system with pre-channel filtering be configured; namely,

$$\begin{aligned} M \geq N, \quad & \text{when } L = 1 \\ M > N, \quad & \text{when } L > 1 \end{aligned} \tag{3.3}$$

In general, the channel L is bigger than 1 and if the channel matrix $\mathbf{G}$ is square, its dimension becomes K_r (rows) by K_c (columns) such that:

$$K_c = MJ = N(L+J-1) = K_r$$

This implies that:

$$K_r = \frac{MN}{M-N}(L-1) \tag{3.4}$$

and the dimension of the channel matrix $\mathbf{G}$ decreases to a lower bound, N(L-1)+1, as M increases to an upper bound, N[N(L-1)+1], if N and L are constant.

3.3.3 MINT for M-input-1-output system

The dual-channel system depicted in Figure 2.1 (page 6) is an example of MINT in a 2-

input-1-output system with pre-channel filtering. MINT in a M-input-1-output system with pre-channel filtering is discussed in this section.

Despite the need for more hardware, filtering in a M-input-1-output system has advantages over those in a 2-input-1-output system.

1) The existence of exact solutions for an M-input-1-output system requires that there is no common zeros in all M channels. In other word, it is permissible to have same zeros in some of the channels.

In general the chance of having common zeros is reduced as the number M of the independent channels increased. In most cases, the problem of having common zeros in the dual-channel system can be solved by introducing a third channel as demonstrated by an example to follow in this section.

2) The larger M is, the less computation efforts is required. In a M-input-1-output system, the existence of solution described in Section 3.3.1 requires $MJ = L + J - 1$ if we assume:

- all channels have the same length L,

- all filters have the same length J,

- the channel matrix is a square matrix.

In this case the channel matrix is K by K square matrix where K = L + J - 1 (an integer). This leads to the relation:

$$K = \frac{M}{M-1}(L-1) \tag{3.5}$$

The effort, in computing the inverse of the channel matrix, to determine the filter coefficients is related to the dimension of the channel matrix. K, the number of rows of the channel matrix, reduces to a lower bound L as M increases to an upper bound L. Furthermore the computational effort for the actual filtering is also smaller since the scale of the filters, which is related to MJ, the total number of filter coefficients, is proportional to K. For example, a 2-input-1-output pre-channel filtering system has K = 2(L-1); whereas a 3-input-1-output pre-channel filtering system has K = 1.5(L-1).

The following example demonstrates that the addition of one more analog hardware, which can be a transmitter (a speaker) or a receiver (a microphone), solves the problem of having common zeros in a dual-channel system and reduces computational requirement.

Example: In a acoustic system depicted in Figure 2.1 (page 6), given that two channels with a common zero at z = 1:

$$\begin{aligned}\mathbf{G}_1(z) &= (1-(1+2i)z^{-1})(1-(1-2i)z^{-1})(1-2z^{-1})(1-z^{-1}) \\ &= 1-5z^{-1}+13z^{-2}-19z^{-3}+10z^{-4} \\ \mathbf{G}_2(z) &= (1-(2+i)z^{-1})(1-(2-i)z^{-1})(1-3z^{-1})(1-z^{-1}) \\ &= 1-8z^{-1}+24z^{-2}-32z^{-3}+15z^{-4}\end{aligned}$$

A third channel is introduced:

$$\begin{aligned}\mathbf{G}_3(z) &= (1+(0.5+0.9i)z^{-1})(1+(0.5-0.9i)z^{-1})(1-2z^{-1})(1-3z^{-1}) \\ &= 1-4z^{-1}+2.06z^{-2}+0.7z^{-3}+6.36z^{-4}\end{aligned}$$

Note that the third channel $\mathbf{G}_3(z)$ has a common zero at z = 2 with $\mathbf{G}_1(z)$ and has another common zero at z = 3 with $\mathbf{G}_2(z)$; and yet there are no common zeros among all three channels.

The matrix equation is:

$$\begin{bmatrix} 1 & 0 & 1 & 0 & 1 & 0 \\ -5 & 1 & -8 & 1 & -4 & 1 \\ 13 & -5 & 24 & -8 & 2.06 & -4 \\ -19 & 13 & -32 & 24 & 0.7 & 2.06 \\ 10 & -19 & 15 & -32 & 6.36 & 0.7 \\ 0 & 10 & 0 & 15 & 0 & 6.36 \end{bmatrix} \begin{bmatrix} h_1(0) \\ h_1(1) \\ h_2(0) \\ h_2(1) \\ h_3(0) \\ h_3(1) \end{bmatrix} = \begin{bmatrix} 1 \\ 0 \\ 0 \\ 0 \\ 0 \\ 0 \end{bmatrix}$$

$$\Rightarrow \begin{bmatrix} h_1(0) \\ h_1(1) \\ h_2(0) \\ h_2(1) \\ h_3(0) \\ h_3(1) \end{bmatrix} = \begin{bmatrix} -24.43832839819552 \\ 88.50248519458674 \\ 10.33317677747934 \\ -52.66635355495914 \\ 15.10515162071619 \\ -14.94175292790572 \end{bmatrix}$$

Hence the desired filters are:

$$\mathbf{H}_1(z) = -24.43832839819552 + 88.50248519458674z^{-1}$$

$$\mathbf{H}_2(z) = 10.33317677747934 - 52.66635355495914z^{-1}$$

$$\mathbf{H}_3(z) = 15.10515162071619 - 14.94175292790572z^{-1}$$

The dimension of the channel matrix for this three channel system is 6 by 6; i.e. $K = 1.5 \times (L-1)$. It would be 8 by 8 for those of a two channel system because $K = 2 \times (L-1)$.

3.3.4 Example of MINT in multi-channel system: speakerphone

Other than the proposed application in [2] on exact inverse filtering, MINT in multiple channels system can have applications in the area of ***selective reception, filtering, and distribution of signals***. These properties will be illustrated with the design of a speakerphone (hands-free telephone) system†.

Two design approaches for the speakerphone system are visited. They are: pre-channel filtering and post-channel filtering (Section 3.2). In each design, different design objectives are applied.

In a room equipped with a speakerphone system as shown in Figure 3.5, there is a loudspeaker to produce the far-end speech signal **x**(t) and a microphone to pick up the near-end speech signal **y**(t).

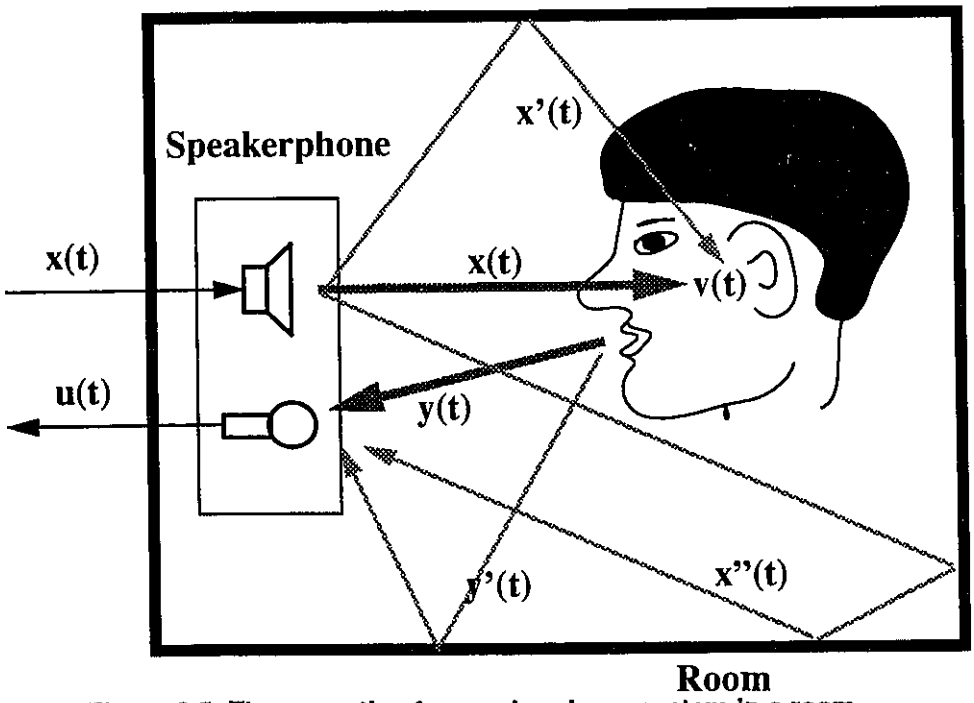

Figure 3.5: The acoustic of a speakerphone system in a room.

†. Not all design aspects of a speakerphone system are addressed here; this example serves only to demonstrate the filtering capabilities of MINT in a linear, shift-invariant, deterministic, noiseless, FIR system.

Because of the three system constraints:

1) the linear distortion on the near-end speech signal **y**(t) by wall reflections,

2) the linear distortion on the far-end speech signal **x**(t) by wall reflections,

3) the coupling of the far-end signal **x**(t) into the microphone,

the near-end speech signal **y**(t) is corrupted and transmitted onto the line as **u**(t); and the far-end speech signal is distorted before reaching the listener's ears as **v**(t).

3.3.4.1 Pre-channel filtering approach

The design goal is to dispatch the far-end speech signal **x**(t) free of distortion to the listener's ears; i.e. **v**(t) = **x**(t) and to cancel the coupling of far-end signal back into the microphone (**u**(t) = 0); thereby solving the system constraints 2 and 3. A speakerphone system with three speakers and filters, one microphone is shown in Figure 3.6.

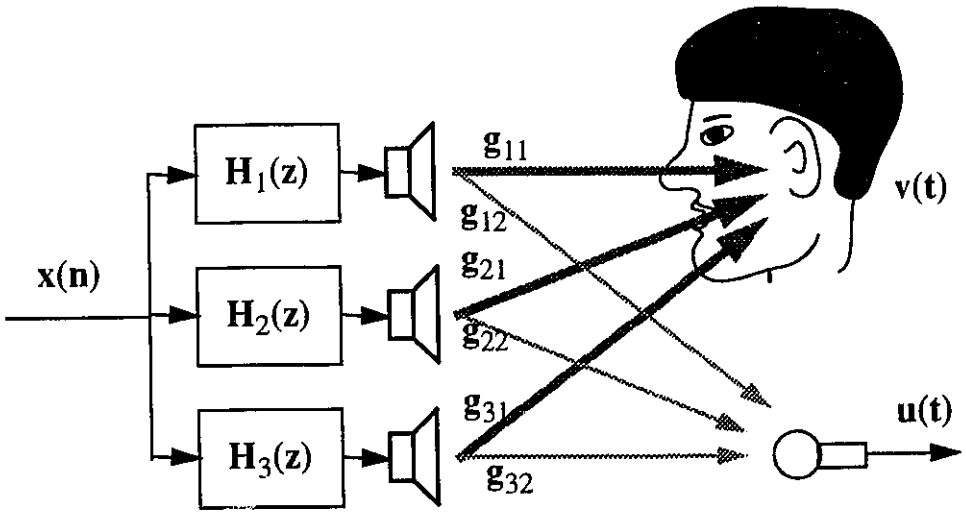

Figure 3.6: Speakerphone system: Pre-channel approach.

It can be modelled as a discrete system depicted in Figure 3.7.

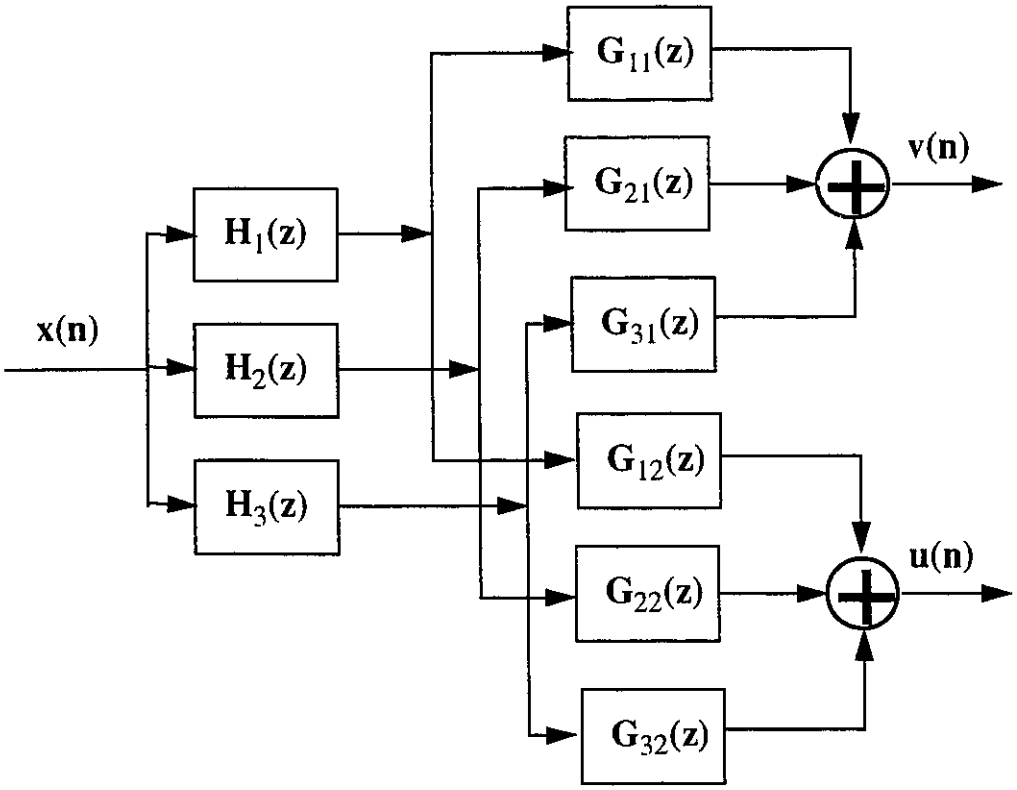

Figure 3.7: Discrete model of the speakerphone system: Pre-channel approach.

There are effectively six channels with three sources and two sinks (the ears and the microphone); thereby forming a 3-input-2-output channel system. We want the far-end signal **x**(n) to be transmitted to the ears and a null signal to the microphone. The following set of convolution equations must be satisfied:

$$\mathbf{g}_{11}(n) * \mathbf{h}_1(n) + \mathbf{g}_{21}(n) * \mathbf{h}_2(n) + \mathbf{g}_{31}(n) * \mathbf{h}_3(n) = \mathbf{d}_1(n)$$
$$\mathbf{g}_{12}(n) * \mathbf{h}_1(n) + \mathbf{g}_{22}(n) * \mathbf{h}_2(n) + \mathbf{g}_{32}(n) * \mathbf{h}_3(n) = \mathbf{d}_2(n)$$

$$\mathbf{d}_1(n) = \begin{cases} 1 & \text{when} \quad n = 0 \\ 0 & \text{when} \quad n = 1, 2, \ldots, L+J-1 \end{cases} \qquad (3.6)$$
$$\mathbf{d}_2(n) = 0 \quad \text{when} \quad n = 0.\ 1, 2, \ldots, L+J-1$$

where

L is the length of each channel,

J is the length of each filter,

L+J-1 is the length of each desired response.

As in Section 3.3.1, a matrix equation is formed and solution is found:

$$\begin{bmatrix} \mathbf{g}_{11} & \mathbf{g}_{21} & \mathbf{g}_{31} \\ \mathbf{g}_{12} & \mathbf{g}_{22} & \mathbf{g}_{32} \end{bmatrix} \begin{bmatrix} \mathbf{h}_1 \\ \mathbf{h}_2 \\ \mathbf{h}_3 \end{bmatrix} = \begin{bmatrix} \mathbf{d}_1 \\ \mathbf{d}_2 \end{bmatrix} \quad . \qquad (3.7)$$

with $2(L+J-1) \leq 3J$.

Example: Givens the sampled impulse response of the channels shown in Figure 3.6 are:

$$\mathbf{G}_{11}(z) = 2\,(1-(0.7+1.2i)\,z^{-1})\,(1-(0.7-1.2i)\,z^{-1})\,(1+0.4z^{-1})$$

$$\mathbf{G}_{21}(z) = (1-(-1+0.3i)\,z^{-1})\,(1-(-1-0.3i)\,z^{-1})\,(1-0.1z^{-1})$$

$$\mathbf{G}_{31}(z) = (1-(-0.2+0.7i)\,z^{-1})\,(1-(-0.2-0.7)\,z^{-1})\,(1-3.5z^{-1})$$

$$\mathbf{G}_{12}(z) = (1-(0.3+0.9i)\,z^{-1})\,(1-(0.3-0.9i)\,z^{-1})\,(1+1.1z^{-1})$$

$$\mathbf{G}_{22}(z) = (1-(1.3+1.4i)\,z^{-1})\,(1-(1.3-1.4i)\,z^{-1})\,(1+0.6z^{-1})$$

$$\mathbf{G}_{32}(z) = (1-(0.4+0.6)\,z^{-1})\,(1-(0.4-0.6i)\,z^{-1})\,(1+1.9z^{1})$$

or

$$\mathbf{G}_{11}(z) = 2-2z^{-1}+2.74z^{-2}+1.544z^{-3}$$

$$\mathbf{G}_{21}(z) = 1+1.9z^{-1}+0.89z^{-2}-0.109z^{-3}$$

$$\mathbf{G}_{31}(z) = 1-3.1z^{-1}-0.87z^{-2}-1.855z^{-3}$$

$$\mathbf{G}_{21}(z) = 1+0.5z^{-1}+0.24z^{-2}+0.99z^{-3}$$

$$\mathbf{G}_{22}(z) = 1-2z^{-1}+2.09z^{-2}+2.19z^{-3}$$

$$\mathbf{G}_{32}(z) = 1+1.1z^{-1}-1z^{-2}+0.988z^{-3}$$

The matrix equation is:

$$\begin{bmatrix}
2 & 0 & 0 & 0 & 0 & 0 & 1 & 0 & 0 & 0 & 0 & 0 & 1 & 0 & 0 & 0 & 0 & 0 \\
-2 & 2 & 0 & 0 & 0 & 0 & 1.9 & 1 & 0 & 0 & 0 & 0 & -3.1 & 1 & 0 & 0 & 0 & 0 \\
2.74 & -2 & 2 & 0 & 0 & 0 & 0.89 & 1.9 & 1 & 0 & 0 & 0 & -0.87 & -3.1 & 1 & 0 & 0 & 0 \\
1.544 & 2.74 & -2 & 2 & 0 & 0 & -0.109 & 0.89 & 1.9 & 1 & 0 & 0 & -1.855 & -0.87 & -3.1 & 1 & 0 & 0 \\
0 & 1.544 & 2.74 & -2 & 2 & 0 & 0 & -0.109 & 0.89 & 1.9 & 1 & 0 & 0 & -1.855 & -0.87 & -3.1 & 1 & 0 \\
0 & 0 & 1.544 & 2.74 & -2 & 2 & 0 & 0 & -0.109 & 0.89 & 1.9 & 1 & 0 & 0 & -1.855 & -0.87 & -3.1 & 1 \\
0 & 0 & 0 & 1.544 & 2.74 & -2 & 0 & 0 & 0 & -0.109 & 0.89 & 1.9 & 0 & 0 & 0 & -1.855 & -0.87 & -3.1 \\
0 & 0 & 0 & 0 & 1.544 & 2.74 & 0 & 0 & 0 & 0 & -0.109 & 0.89 & 0 & 0 & 0 & 0 & -1.855 & -0.87 \\
0 & 0 & 0 & 0 & 0 & 1.544 & 0 & 0 & 0 & 0 & 0 & -0.109 & 0 & 0 & 0 & 0 & 0 & -1.855 \\
1 & 0 & 0 & 0 & 0 & 0 & 1 & 0 & 0 & 0 & 0 & 0 & 1 & 0 & 0 & 0 & 0 & 0 \\
0.5 & 1 & 0 & 0 & 0 & 0 & -2 & 1 & 0 & 0 & 0 & 0 & 1.1 & 1 & 0 & 0 & 0 & 0 \\
0.24 & 0.5 & 1 & 0 & 0 & 0 & 2.09 & -2 & 1 & 0 & 0 & 0 & -1 & 1.1 & 1 & 0 & 0 & 0 \\
0.99 & 0.24 & 0.5 & 1 & 0 & 0 & 2.19 & 2.09 & -2 & 1 & 0 & 0 & 0.988 & -1 & 1.1 & 1 & 0 & 0 \\
0 & 0.99 & 0.24 & 0.5 & 1 & 0 & 0 & 2.19 & 2.09 & -2 & 1 & 0 & 0 & 0.988 & -1 & 1.1 & 1 & 0 \\
0 & 0 & 0.99 & 0.24 & 0.5 & 1 & 0 & 0 & 2.19 & 2.09 & -2 & 1 & 0 & 0 & 0.988 & -1 & 1.1 & 1 \\
0 & 0 & 0 & 0.99 & 0.24 & 0.5 & 0 & 0 & 0 & 2.19 & 2.09 & -2 & 0 & 0 & 0 & 0.988 & -1 & 1.1 \\
0 & 0 & 0 & 0 & 0.99 & 0.24 & 0 & 0 & 0 & 0 & 2.19 & 2.09 & 0 & 0 & 0 & 0 & 0.988 & -1 \\
0 & 0 & 0 & 0 & 0 & 0.99 & 0 & 0 & 0 & 0 & 0 & 2.19 & 0 & 0 & 0 & 0 & 0 & 0.988
\end{bmatrix}
\begin{bmatrix}
h_1(0) \\ h_1(1) \\ h_1(2) \\ h_1(3) \\ h_1(4) \\ h_1(5) \\ h_2(0) \\ h_2(1) \\ h_2(2) \\ h_2(3) \\ h_2(4) \\ h_2(5) \\ h_3(0) \\ h_3(1) \\ h_3(2) \\ h_3(3) \\ h_3(4) \\ h_3(5)
\end{bmatrix} =
\begin{bmatrix}
1 \\ 0 \\ 0 \\ 0 \\ 0 \\ 0 \\ 0 \\ 0 \\ 0 \\ 0 \\ 0 \\ 0 \\ 0 \\ 0 \\ 0 \\ 0 \\ 0 \\ 0
\end{bmatrix}$$

$$\Rightarrow \begin{bmatrix} h_1(0) \\ h_1(1) \\ h_1(2) \\ h_1(3) \\ h_1(4) \\ h_1(5) \\ h_2(0) \\ h_2(1) \\ h_2(2) \\ h_2(3) \\ h_2(4) \\ h_2(5) \\ h_3(0) \\ h_3(1) \\ h_3(2) \\ h_3(3) \\ h_3(4) \\ h_3(5) \end{bmatrix} = \begin{bmatrix} 1 \\ -0.84099538286947 \\ 0.24494952101691 \\ 0.67056414156225 \\ 0.83396886455283 \\ 0.55684486774203 \\ -0.10604995273216 \\ -0.02309557924017 \\ -1.23505631876450 \\ -0.14644331555302 \\ -0.24627040211082 \\ -0.47337131916770 \\ -0.89395004726784 \\ 1.13533610863993 \\ -0.79676203485956 \\ -0.72935318137655 \\ 1.07359179373970 \\ 0.49130239869702 \end{bmatrix}$$

Hence the desired filters are:

$$\mathbf{H}_1(z) = 1 - 0.84099538286947z^{-1} + 0.24494952101691z^{-2} + 0.67056414156225z^{-3} + 0.83396886455283z^{-4} + 0.55684486774203z^{-5}$$

$$\mathbf{H}_2(z) = -0.10604995273216 - 0.02309557924017z^{-1} - 1.23505631876450z^{-2} - 0.14644331555302z^{-3} - 0.24627040211082z^{-4} - 0.47337131916770z^{-5}$$

$$\mathbf{H}_3(z) = -0.89395004726784 + 1.13533610863993z^{-1} - 0.79676203485956z^{-2} - 0.72935318137655z^{-3} + 1.07359179373970z^{-4} + 0.49130239869702z^{-5}$$

Note that the structure has to be made adaptive, which is beyond the scope of this research, in order to cope with a moving user.

This example demonstrates that the structure sustains different filtering functions for each individual output paths. In fact, the filtering functions can be any responses other than those of the perfect channel or null channel. Hence, ***selective distribution and filtering of an input signal x(n) for multiple output ports (paths)*** is possible in a linear, shift-invariant, deterministic, noiseless, finite-impulse-response system.

3.3.4.2 Post-channel filtering approach

As pointed out in Section 3.2, the filtering function can be applied after the signal is distorted by the channels. A speakerphone system using additional circuitry of two microphones is shown in Figure 3.8.

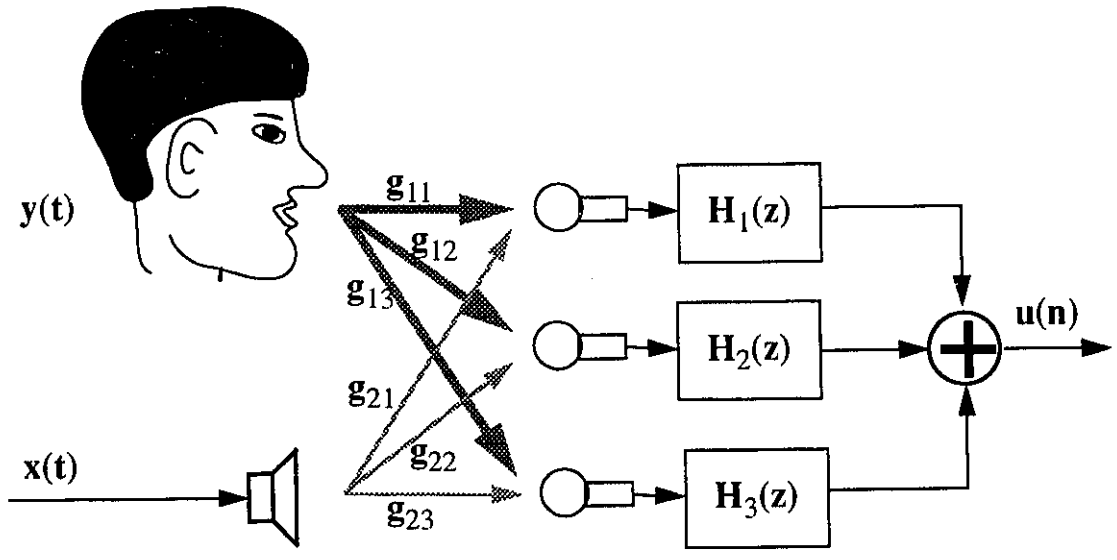

Figure 3.8: Speakerphone system: Post-channel approach.

There are two sources of signals coupling into the microphones. The design goal is to transmit perfectly recontructed near-end signal ($\mathbf{u}(n) = \mathbf{y}(n)$) and cancel (block) completely the coupled far-end signal $\mathbf{x}(n)$ from the telephone line; thereby solves the system constraints 1 and 3.

This can be modelled to a discrete system, which is a 2-input-3-output channel system, depicted in Figure 3.9.

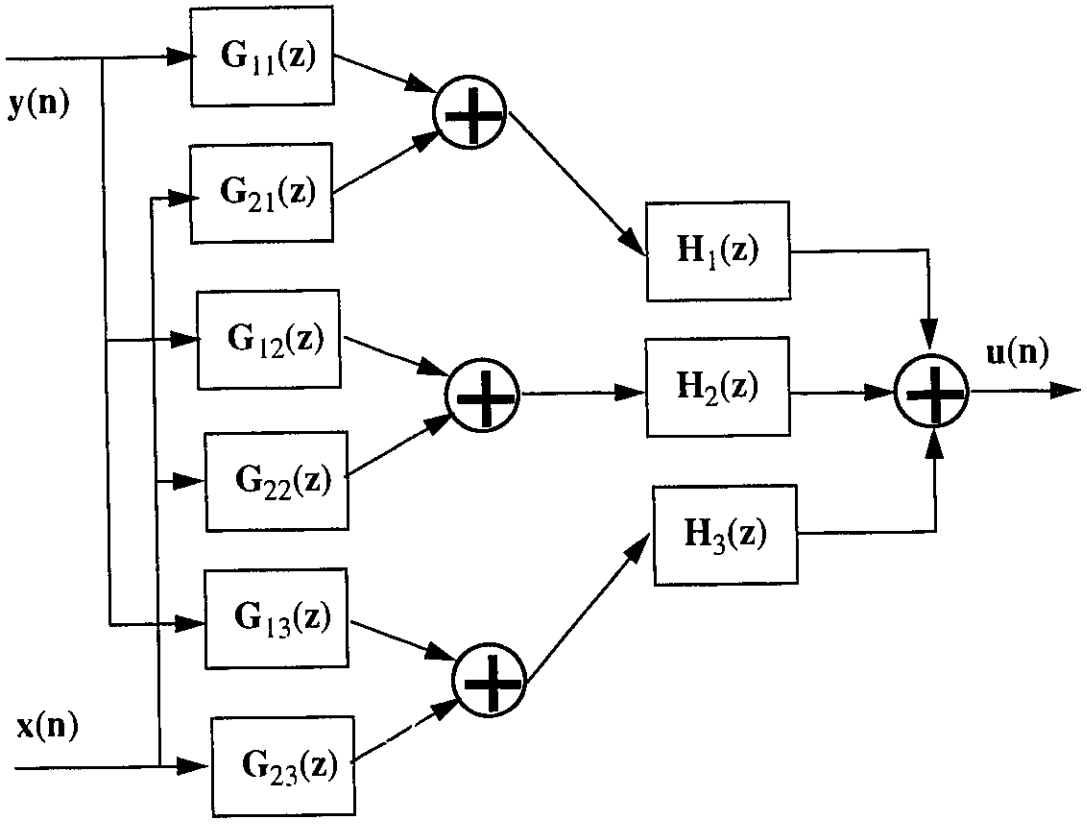

Figure 3.9: Discrete model of the speakerphone system: Post-channel approach.

The following set of convolution equations must be satisfied:

$$\mathbf{g}_{11}(n) * \mathbf{h}_1(n) + \mathbf{g}_{12}(n) * \mathbf{h}_2(n) + \mathbf{g}_{13}(n) * \mathbf{h}_3(n) = \mathbf{d}_1(n)$$
$$\mathbf{g}_{21}(n) * \mathbf{h}_1(n) + \mathbf{g}_{22}(n) * \mathbf{h}_2(n) + \mathbf{g}_{23}(n) * \mathbf{h}_3(n) = \mathbf{d}_2(n)$$

$$\mathbf{d}_1(n) = \begin{cases} 1 & \text{when} \quad n = 0 \\ 0 & \text{when} \quad n = 1, 2, \ldots, L+J-1 \end{cases} \qquad (3.8)$$

$$\mathbf{d}_2(n) = 0 \quad \text{when} \quad n = 0, 1, 2, \ldots, L+J-1$$

where

L is the length of each channel,

J is the length of each filter,

L+J-1 is the length of each desired response.

This can be expressed in a matrix equation:

$$\begin{bmatrix} \mathbf{g}_{11} & \mathbf{g}_{12} & \mathbf{g}_{13} \\ \mathbf{g}_{21} & \mathbf{g}_{22} & \mathbf{g}_{23} \end{bmatrix} \begin{bmatrix} \mathbf{h}_1 \\ \mathbf{h}_2 \\ \mathbf{h}_3 \end{bmatrix} = \begin{bmatrix} \mathbf{d}_1 \\ \mathbf{d}_2 \end{bmatrix} \qquad (3.9)$$

with $2(L+J-1) \leq 3J$

This design demonstrates the capability of this structure to ***selectively receive, filter signals from different input ports and route into a single output port*** in a linear, shift-invariant, deterministic, noiseless, finite-impulse-response system. In fact, this can be extended to the application of signal-mixing where signals from various sources are enhanced differently and then added up together accordingly at the output

3.4 Conclusion

The concept of pre-channel filtering and post-channel filtering was described. It follows with examining the MINT in a multiple channels system. The dimensional requirement on the channels and the filters as well as the comparison with MINT in a dual channel system were given. The equation (3.5) on page 30 for a M-input-1-output system with square channel matrix indicates that the total number of the filter coefficients and the computational effort for determining the filter coefficients reduce to a lower bound as M, the number of channels, increases to an upper bound L.

The application of MINT in areas other than the exact inverse filtering was explored. Examples on the design of a speakerphone system illustrated the capabilities of selective reception and distribution of signals by MINT in a linear, shift-invariant, deterministic, noiseless, finite-impulse-response system.

Chapter 4

Solutions to common and close zeros on a dual-channel system

4.1 Introduction

In this chapter, the problems related to finding a solution with common or close zeros in the channels are described. Approaches to minimize the impact of common or close zeros are suggested. The use of an infinite impulse response(IIR) filter, which is presented in Section 4.2.1, gives the exact solution, even if the channels contain minimum phase common zeros. The use of the minimum norm solution, which is presented in Section 4.3., resolves the problems associated with having close but not common zeros in the channels.

4.2 Common zeros

It is pointed out in [2] that no exact solution is available for a dual channel system if the two channels contain common zeros. As described in Section 2.4.2 (page 12), this leads to

a zero value for the determinant of the channel matrix $[\mathbf{G_1 G_2}]$.

When the problem of common zeros is encountered during the design of the filtering system with MINT, two approaches can be considered. These are:

1) the use of a third channel,

2) the use of an IIR filter.

The first approach has already been discussed in Section 3.3.3 (page 29) and an example was given.The second approach is discussed next.

4.2.1 Use of IIR in MINT filters

Consider the acoustic system of a room depicted in Figure 2.1 (page 6). When the channels have common zeros which can be identified and are within the unit circle on the complex z-plane, an IIR filter can be applied to remove these minimum phase common zeros. The use of IIR filter extends the inverse-filtering capacity of MINT to systems with minimum phase common zeros in their channels. Figures 4.1 and 4.2 depict two designs for the utilization of an IIR filter.

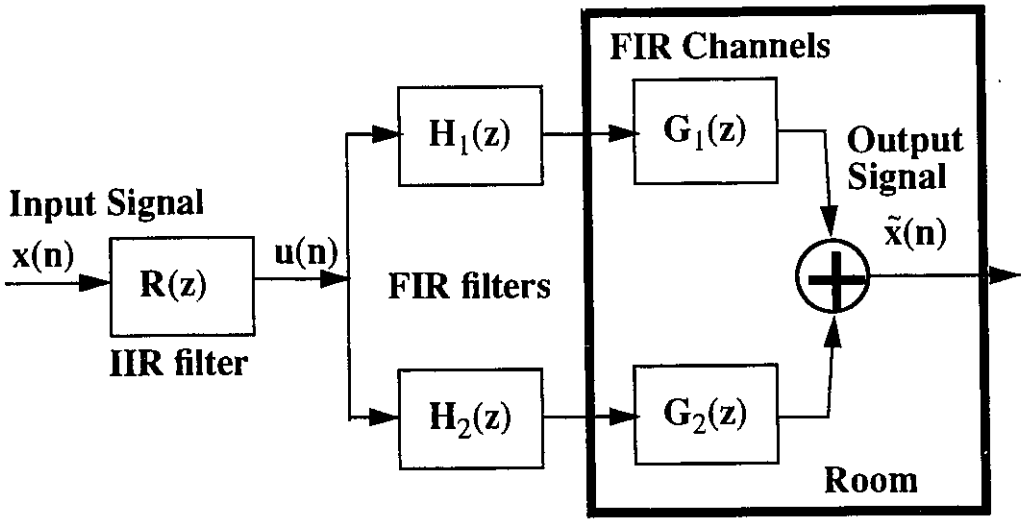

Figure 4.1: IIR in MINT filter: Approach 1.

The IIR filter of Figure 4.1 is applied before the FIR filters $\mathbf{H}_1(z)$, $\mathbf{H}_2(z)$. The design consists of two parts. First, the minimum phase common zeros of the two channels are identified. The IIR filter $\mathbf{R}(z)$ is designed to introduce corresponding poles to compensate these common zeros.

Second, the design of the FIR filters $\mathbf{H}_1(z)$, $\mathbf{H}_2(z)$ is based on the effective channels which are derived by removing the minimum phase common zeros from the channels $\mathbf{G}_1(z)$, $\mathbf{G}_2(z)$. The IIR filter $\mathbf{R}(z)$ first introduces the poles, which will compensate the common zeros of the channels, into the input signal $\mathbf{x}(n)$. The resultant signal $\mathbf{u}(n)$ is then shaped by the filters $\mathbf{H}_1(z)$, $\mathbf{H}_2(z)$ so that the distortion caused by the channels $\mathbf{G}_1(z)$, $\mathbf{G}_2(z)$ is equalized and the output signal is equal to $\mathbf{x}(n)$.

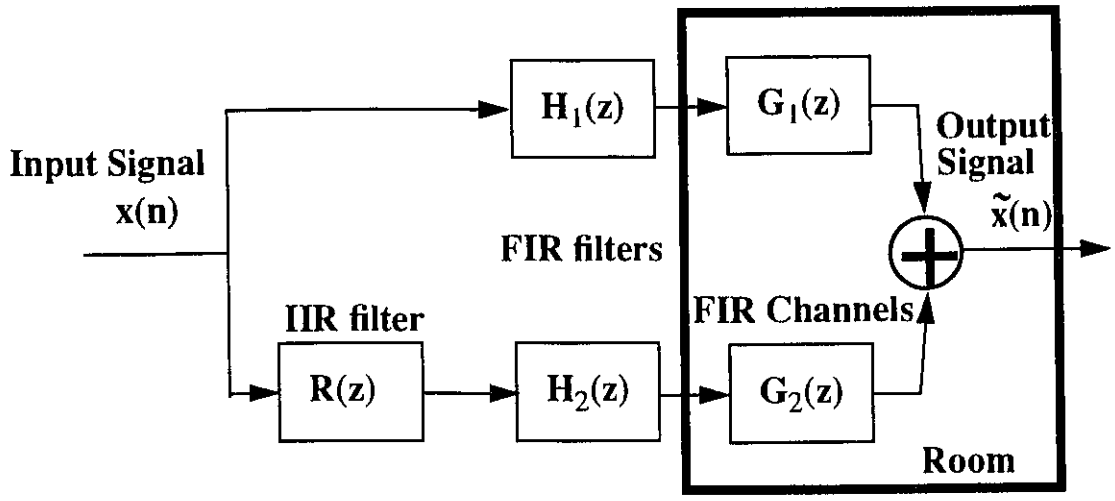

Figure 4.2: IIR in MINT filter: Approach 2.

In second design, of Figure 4.2, one IIR filter is applied before the FIR filter $\mathbf{H}_2(z)$. This design also consists of two parts. First, the minimum phase common zeros of the two channels are identified. The IIR filter $\mathbf{R}(z)$ is designed to introduce corresponding poles to compensate these common zeros.

Second, the design of the FIR filters $\mathbf{H}_1(z)$, $\mathbf{H}_2(z)$ is based on the channels $\mathbf{G}_1(z)$ and the effective channel $\mathbf{G'}_2(z)$ which is derived by removing the minimum phase common

zeros from $\mathbf{G}_2(z)$. After the cancelation, the effective channel $\mathbf{G'}_2(z)$ has fewer coefficients than $\mathbf{G}_1(z)$, the determination of the filters coefficients is similar to the example for case 1 in Section 2.4.2 (page 12).

The second design is better than the first one in terms of the length of the FIR filters. A smaller channel matrix is formed for the second design because the effective channel $\mathbf{G'}_2(z)$ has fewer coefficients than $\mathbf{G}_2(z)$. This leads to less computational effort in determining the FIR filters coefficient and less processing effort because of shorter length of FIR filter. Furthermore, the second design can be applied to solve the problem related to minimum phase close zeros which is discussed in next section. The design of the IIR filters is same for both approaches.

An example of the second approach is given below.

Example: Consider the example presented in Section 3.3.3 (page 29), the acoustic system depicted in Figure 2.2 (page 6) has a common zero at z = 1 in the channels:

$$\begin{aligned}\mathbf{G}_1(z) &= (1-(1+2i)z^{-1})(1-(1-2i)z^{-1})(1-2z^{-1})(1-0.5z^{-1}) \\ &= 1-4.5z^{-1}+11z^{-2}-14.5z^{-3}+5z^{-4} \\ \mathbf{G}_2(z) &= (1-(2+i)z^{-1})(1-(2-i)z^{-1})(1-3z^{-1})(1-0.5z^{-1}) \\ &= 1-7.5z^{-1}+20.5z^{-2}-23.5z^{-3}+7.5z^{-4}\end{aligned}$$

Hence a pole at z = 1 is required; the IIR filter $\mathbf{R}(z)$ depicted in Figure 4.2 is:

$$\mathbf{R}(z) = \frac{1}{1-0.5z^{-1}}$$

The effective channel $\mathbf{G'}_2(z)$ becomes:

$$\mathbf{G'}_2(z) = (1-(2+i)z^{-1})(1-(2-i)z^{-1})(1-3z^{-1})$$
$$= 1-7z^{-1}+17z^{-2}-15z^{-3}$$

The filters $\mathbf{H}_1(z)$, $\mathbf{H}_2(z)$ are designed such that the following convolution equation is satisfied:

$$\mathbf{H}_1(z)\mathbf{G}_1(z)+\mathbf{H}_2(z)\mathbf{G'}_2(z) = 1$$

and the matrix equation is:

$$\begin{bmatrix} 1 & 0 & 0 & 1 & 0 & 0 & 0 \\ -4.5 & 1 & 0 & -7 & 1 & 0 & 0 \\ 11 & -4.5 & 1 & 17 & -7 & 1 & 0 \\ -14.5 & 11 & -4.5 & -15 & 17 & -7 & 1 \\ 5 & -14.5 & 11 & 0 & -15 & 17 & -7 \\ 0 & 5 & -14.5 & 0 & 0 & -15 & 17 \\ 0 & 0 & 5 & 0 & 0 & 0 & -15 \end{bmatrix} \begin{bmatrix} h_1(0) \\ h_1(1) \\ h_1(2) \\ h_2(0) \\ h_2(1) \\ h_2(2) \\ h_2(3) \end{bmatrix} = \begin{bmatrix} 1 \\ 0 \\ 0 \\ 0 \\ 0 \\ 0 \\ 0 \end{bmatrix}$$

$$\Rightarrow \begin{bmatrix} h_1(0) \\ h_1(1) \\ h_1(2) \\ h_2(0) \\ h_2(1) \\ h_2(2) \\ h_2(3) \end{bmatrix} = \begin{bmatrix} 9.3403846154 \\ 34.9 \\ 57.086538462 \\ -8.3403846154 \\ 18.549038462 \\ -45.250961538 \\ 19.028846154 \end{bmatrix}$$

Hence the desired filters are:

$$\mathbf{H}_1(z) = 9.3403846154 - 34.9z^{-1} + 57.086538462z^{-2}$$

$$\mathbf{H}_2(z) = -8.3403846154 + 18.549038462z^{-1} - 45.250961538z^{-2} + 19.028846154z^{-3}$$

With the application of an IIR filter which removes the minimum phase common zeros from $\mathbf{G}_2(z)$, the FIR filters $\mathbf{H}_1(z)$, $\mathbf{H}_2(z)$ are designed for the exact inverse filtering. Less computational effort is required with the second approach as the total number of the FIR filter coefficients is 7 and the dimension of the channel matrix is 7 by 7. It would be 8 and 8 by 8 respectively if the first approach were adopted.

4.3 Close zeros

Sometimes close but not common zeros occur in the dual channel system. The determinant equation of case1 on Section 2.4.2 (page 12) is given in [10] as

$$\mathbf{R}(\mathbf{g}_1(n), \mathbf{g}_2(n)) = (-1)^{\frac{(M-1)(M-2)}{2}} \mathbf{g}_1(0)\,\mathbf{g}_2(0) \prod_{i=1}^{M-1} \prod_{j=1}^{N-1} (\alpha_i - \beta_j) \tag{4.1}$$

where α_i and β_j are the zeros of the channels $\mathbf{G}_1(z)$ and $\mathbf{G}_2(z)$ respectively. This indicates that the occurrence of a close zero pair will lead to a small value for the determinant and generally large values for the filter coefficients of $\mathbf{H}_1(z)$ and $\mathbf{H}_2(z)$. In general, the closer the zero pair is, or if there are more than one pair of close zeros, the larger the filter

coefficients will be. Filter coefficients of large value are also found to be a problem in the digital transversal equalizer[26] based on the LSE criterion[6]

There is no simple expression in estimating the magnitude of the filter coefficients, since this depends on:

1) the relative location of the channel zeros,

2) the gain of channels $\mathbf{G}_1(z)$ and $\mathbf{G}_2(z)$,

3) the desired response of the overall system $\mathbf{D}(z)$.

Large values of the filter coefficients of $\mathbf{H}_1(z)$, $\mathbf{H}_2(z)$ make the system sensitive to the quantization noise as well as the noise due to round-off of the multipliers which is amplified by the filters [21]- [24]. One measure of the gain of the filter coefficients is the filter norm $\mathbf{H}^T\mathbf{H}$, where $\mathbf{H}$ is the filter vector depicted in equation (2.10) (page 19). The filter norm (FN) for a dual-channel system is defined as:

$$\mathbf{FN} = \mathbf{H}^T\mathbf{H} = \sum_{i=1}^{2}\sum_{n=0}^{J_i-1} |h_i(n)|^2 \qquad (4.2)$$

where J_i is the filter length (number of coefficients) of $\mathbf{h}_i(n)$ and i is 1 and 2. It is equivalent to the sum of the signal energy of the impulse response of the filters.

Three approaches are considered here:

1) the use of a third channel,

2) the use of an IIR filter.

3) the use of Minimum Norm solution with delay.

The first approach has been discussed and an example given in Section 3.3.3 (page 29). The second approach is shown in Figure 4.2 and is described in Section 4.2.1. The third approach is discussed in the following section.

4.3.1 Minimum Norm solution with delay

The use of minimum norm solution to determine the filter coefficients for exact inverse filtering is suggested in Section 2.5 (page 18). The filter coefficients are computed such that the norm $\mathbf{H}^T\mathbf{H}$ is minimized.

When the length of the filters is increased, the additional degree of freedom should lead to a solution with a smaller norm if a minimum exists. There is no known analytical model to describe the nature of the solution. Instead, an experiment was conducted for some typical channels, to study how the filter length affects the norm of the solution. Moreover the experiment also showed that permitting system delays in the overall response $\mathbf{d}(n)$ of the equation (2.1) (page 7) leads to a further reduction in the filter norm (FN).

Consider the discrete model of an acoustic system shown in Figure 2.1 (page 6), the coefficients of the filters $\mathbf{H}_1(z)$, $\mathbf{H}_2(z)$ as well as the filter norm (FN) are computed for different filter length (from 4 to 120) for a set of channels $\mathbf{G}_1(z)$ and $\mathbf{G}_2(z)$. Ten sets of channels, representing ten different scenarios, are used and are summarized in table 4.1.

Each channel has 4 zeros (5 coefficients). They are normalized to have unity energy; i.e.:

$$\sum_{n=0}^{4} |g(n)|^2 = 1$$

The following table summarizes the different channel systems investigated:

Table 4.1:

Channel set	Channel characteristics and zeros of the channels	
1	Minimum phase channels, no close zeros.	
	0.7+0.7j, 0.7-0.7j, 0.2, -0.9	-0.7+0.7j, -0.7-0.7j, -0.2, 0.9
2	Maximum phase channels, no close zeros.	
	1.4+1.4j, 1.4-1.4j, 5, -1.1	-1.4+1.4j, -1.4-1.4j, -5, 1.1
3	Mixed phase channels, no close zeros.	
	1.4+1.4j, 1.4-1.4j, 0.2, -0.9	-1.4+1.4j, -1.4-1.4j, -5, 0.9
4	Minimum phase channels, one close zero pair.	
	0.7+0.7j, 0.7-0.7j, 0.2, -0.9	-0.7+0.7j, -0.7-0.7j, -0.2, -0.901
5	Minimum phase channels, two close zeros.	
	0.7+0.7j, 0.7-0.7j, 0.2, -0.9	-0.7+0.7j, -0.7-0.7j, 0.201, -0.901
6	Maximum phase channels, one close zero pair.	
	1.4+1.4j, 1.4-1.4j, 5, -1.1	-1.4+1.4j, -1.4-1.4j, -5, -1.099
7	Maximum phase channels, two close zeros.	
	1.4+1.4j, 1.4-1.4j, 5, -1.1	1.4+1.399j, 1.4-1.399j, -5, 1.1
8	Mixed phase channels, one close zero pair inside the unit circle.	
	1.4+1.4j, 1.4-1.4j, 0.2, -0.9	-1.4+1.4j, -1.4-1.4j, -5, -0.901
9	Mixed phase channels, one close zero pair outside the unit circle.	
	0.7+0.7j, 0.7-0.7j, 0.2, -1.1	-0.7+0.7j, -0.7-0.7j, -5, -1.099
10	Mixed phase channels, two close zeros, inside and outside the unit circle.	
	1.4+1.4j, 1.4-1.4j, 0.9, -1.1	-1.4+1.4j, -1.4-1.4j, 0.901, -1.099

Figures 4.3 to 4.5 show the change of the filter norm (FN in dB) with increasing filters length for each scenario. Please refer to appendix B for the data.

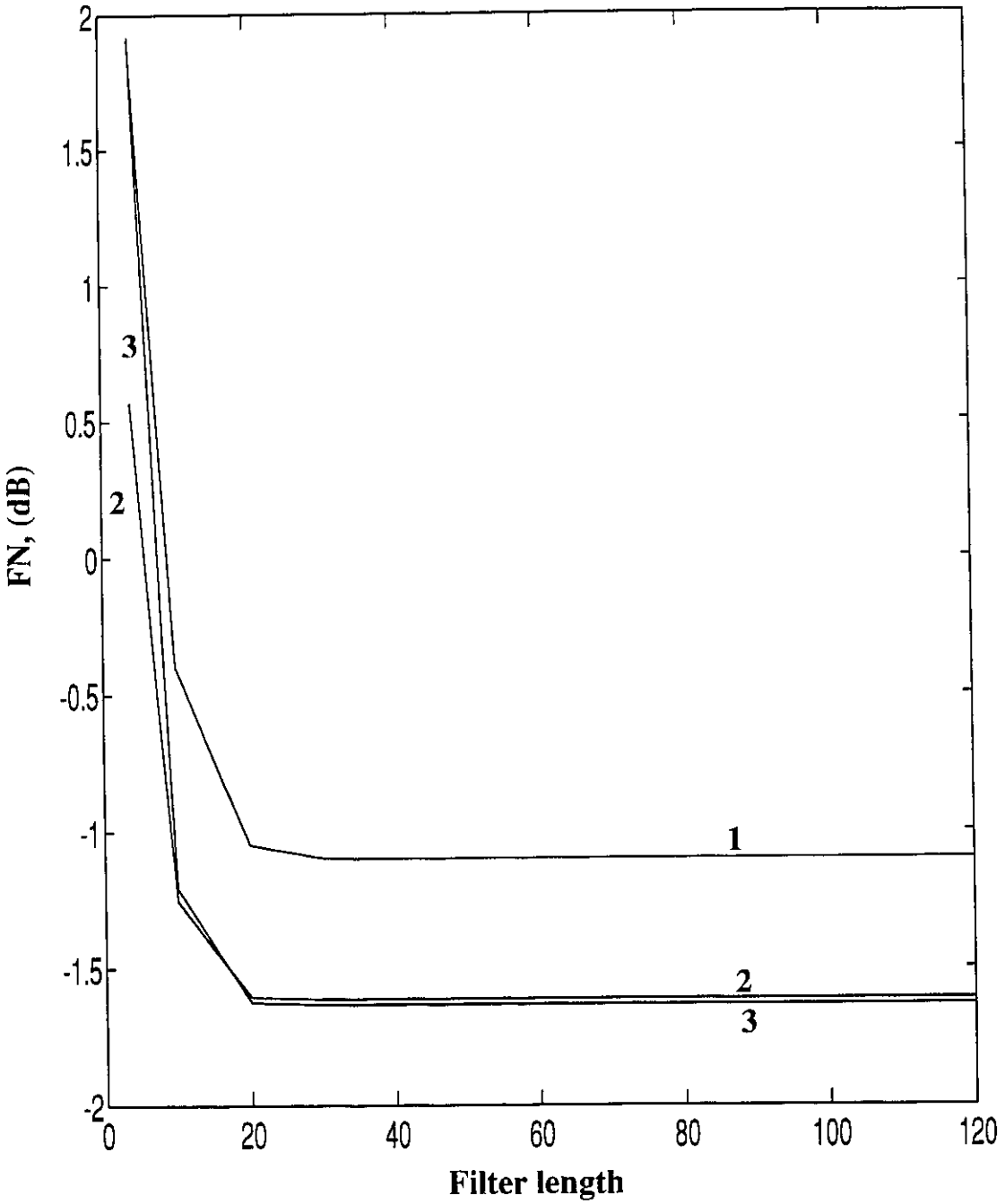

Figure 4.3: Change of Filter Norm with no close zeros on 1) minimum phase, 2)maximum phase, 3) mixed phase channels.

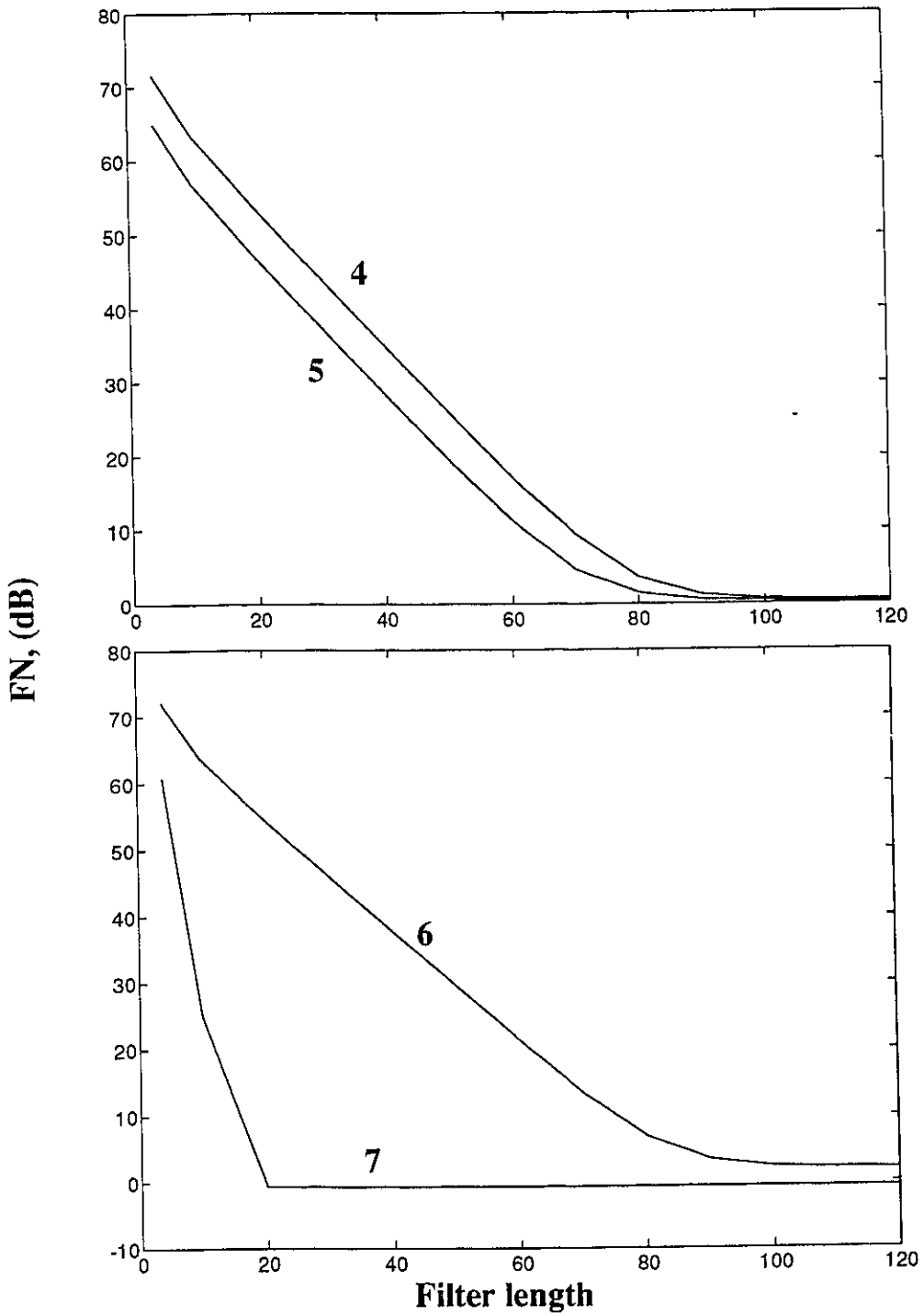

Figure 4.4: Change of Filter Norm with 4)one close zero, 5)two close zeros on minimum phase channels; 6)one close zero, 7)two close zeros on maximum phase channels

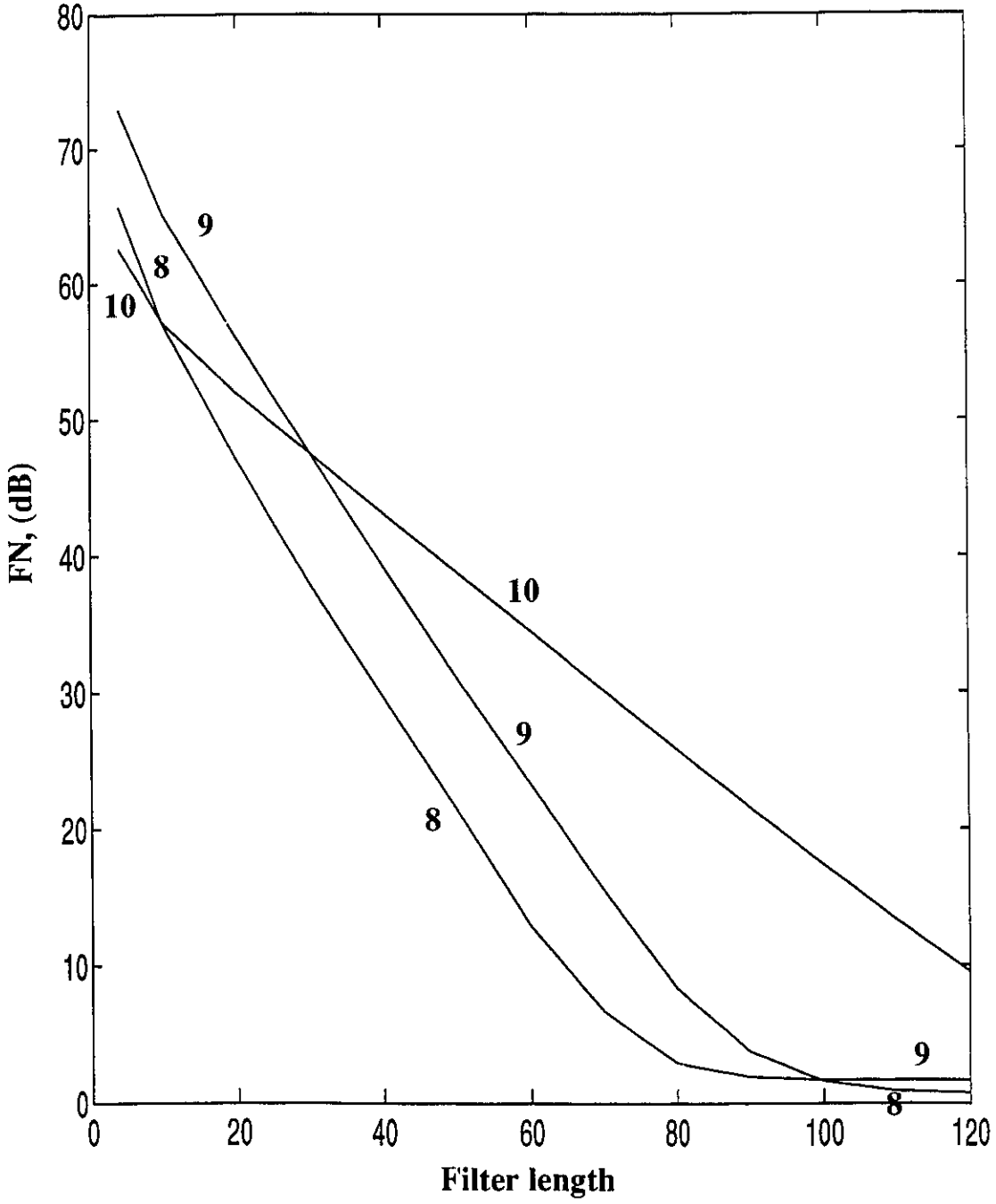

Figure 4.5: Change of Filter norm with 8)one close zero inside the unit circle, 9)one close zero outside the unit circle, 10)two close zeros, both inside and outside the unit circle, on mixed phase channels.

The following points are observed:

- Close zeros in the channels lead to higher filter norms (Compare Figure 4.3 with others.)
- The filter norm decreases with increasing filter length for all sets of channels.
- Each channel set has a different decline rate for the filter norm.
- The decline rate decreases as the filter length increases.
- As the filter length increases, the filter norm converts to a lower bound.(not shown in channel set 10 yet because the filter length is not large enough).
- Each channel set has a different lower bound.
- The lower bounds are all below 3dB with four of them (scenario 1, 2, 3, 7) below 0dB. This means that the average noise amplification over the filter spectrum is small or even negative; i.e., the noise input is attenuated. Therefore the MINT filtering systems are no longer sensitive to noise due to the present of close zeros in the channels.
- Channels with no close zeros have the lowest FN (below 0dB).
- Channels with no close zeros require the smallest filter length to reach their lower bound of FN.
- The phase of the channels do not lead to much difference in FN (scenario 4, 6, 9). However, the system delay introduced is affected by the phase of the channels as described in next paragraph.

Table 4.2 shows the system delay required to achieve the lowest filter norm. In general, close zeros outside the unit circle require a large system delay that is close to the length of the overall desired response **d**(n) of (2.1) (page 7). Close zeros inside the unit circle, on the other hand, lead to only a few delays. No analytical model is developed to explain this phenomenon as yet.

This simulation indicates that the filter norm (FN) is always reduced and converted to a lower bound, which is a small value, when the number of filter coefficient increases. Henceforth the average noise amplification over the filter spectrum is small or even negative; i.e., noise input is attenuated. Thus the system impact, such as amplification of noise, due to close zeros in the channels is reduced with increasing filter length.

Table 4.2:

length of $\mathbf{H}_1(n)$	4	10	20	30	40	50	60	70	80	90	100	110	120
Channel set	System delay introduced by the filter												
1	0	4	9	13	19	23	29	33	39	43	49	53	59
2	7	9	15	19	25	29	35	39	45	49	53	55	55
3	5	7	12	17	22	27	32	37	42	46	50	52	52
4	0	0	0	0	0	0	0	1	2	4	5	7	9
5	0	0	0	0	0	0	0	1	2	4	6	7	9
6	7	13	23	33	43	53	63	73	83	92	101	111	119
7	7	13	20	26	31	36	42	48	58	68	78	88	98
8	0	0	0	0	1	1	2	2	5	6	7	9	10
9	7	13	23	33	43	53	63	72	82	90	100	107	115
10	6	9	14	20	25	30	35	40	46	51	56	61	66

4.4 Conclusion

Common zeros or, more likely, close zeros may occur in the channels. The common zeros leads to the non-existence of the solution. The problem of having common zeros can be solved by introducing a third channel so that the three channels do not have the same zero in common. Another approach is the use of an IIR filter to remove one or two minimum phase common zeros.

Filter coefficients of large value, which render the filter impractical, are also found to be a problem in the equalizer based on the LSE criterion. They are associated with close

zeros for MINT. In addition to the two solutions for common zeros, the minimum norm solution with system delay can resolve the problem. Simulations show this approach is valid. However there is no known analytical model to describe the nature of the solution.

Chapter 5

Single channel MINT equalizer

5.1 Introduction

A detailed description of the application of MINT in equalization, in particular to a system with a single channel, is given in this chapter.

Section 5.2 describes the concept of the equalization of a single channel.

A single channel equalizer structure, shown in Figure 5.3, is presented in Section 5.3. Two virtual subchannels are derived from a single analog channel. Sections 5.3.1 to 5.3.3 explain the principle and mechanism of deriving parallel virtual subchannels from a single channel.

In Section 5.4, the concept of the single channel equalizer is further extended into the structure shown in Figure 5.10, which processes three virtual channels.

A comparison is given for the two equalizer structures of Sections 5.3 and 5.4 and a conventional equalizer, based on the LSE principle. This is discussed in Section 5.5. The performance with a simulated acoustic room is given in Section 5.6.

5.2 Background

A digital inverse filtering system is shown in Figure 5.1, which changes the linearly distorted signal **y**(t) back to **x**(t). The linear distortion on any input signals which are bandlimited to f_x Hz (i.e. the Fourier Transform of **x**(t) is zero[†] for all frequency components outside $\pm f_x$) can be restored by this digital inverse filtering system. In other word, the digital inverse filtering system is designed to restore any linearly distorted frequency components of an input signal **x**(t) over the spectrum from 0 to f_x Hz only; the output signal of the digital-to-analog converter can have bandwidth up to f_x Hz.

x(t) is an input signal, which has a bandwidth of f_x Hz, is distorted by the channel **G**(jw) which has a bandwidth f_g Hz. The receiving low-pass filter **L**(jw), which has a bandwidth f_l Hz, serves to limit the bandwidth of the channel and reduce the input noise. Hence the signal **x**(t) is linearly distorted by the effective channel **GL**(jw), which has bandwidth f_l Hz since $f_g \geq f_l$, to form **y**(t).

The distorted signal **y**(t) is fed into the analog-to-digital converter and is sampled at f_s samples per second to form **y**(n). Based on the Nyquist sampling theorem [22], the required sampling rate is $f_s \geq 2f_x$ and $f_l = f_x$ [‡]so that the restored signal can have a bandwidth f_x. **y**(n) is processed by the digital filter **H**(z) and is restored to the discrete signal **x**(n). The output signal from the digital-to-analog converter should be equal to or close to **x**(t) with minimum loss of signal fidelity.

[†]Zero value for frequency components over the stop-band [21] is only a concept to describe the theoretical model of Ideal filters [23], on which the Nyquist sampling theorem is based. Ideal filters, though desirable, are not physically realizable. In our discussion, the bandwidth f_x of a low-pass signal is chosen such that no significant aliasing errors occur when this signal is sampled at $2f_x$, the Nyquist sampling rate [23] [24]. Similarly, the bandwidth f_g of a low-pass (bandlimited) channel is chosen such that no significant aliasing errors incur when the impulse response **g**(t) of this low-pass channel is sampled at $2f_g$; thereby, the frequency components of the sampled sequence **g**(n) over the spectrum from 0 to f_g have nearly identical characteristics as those of **g**(t).

[‡]This condition can be extended as $f_l \geq f_x$ and $f_s \geq f_x + f_l$.

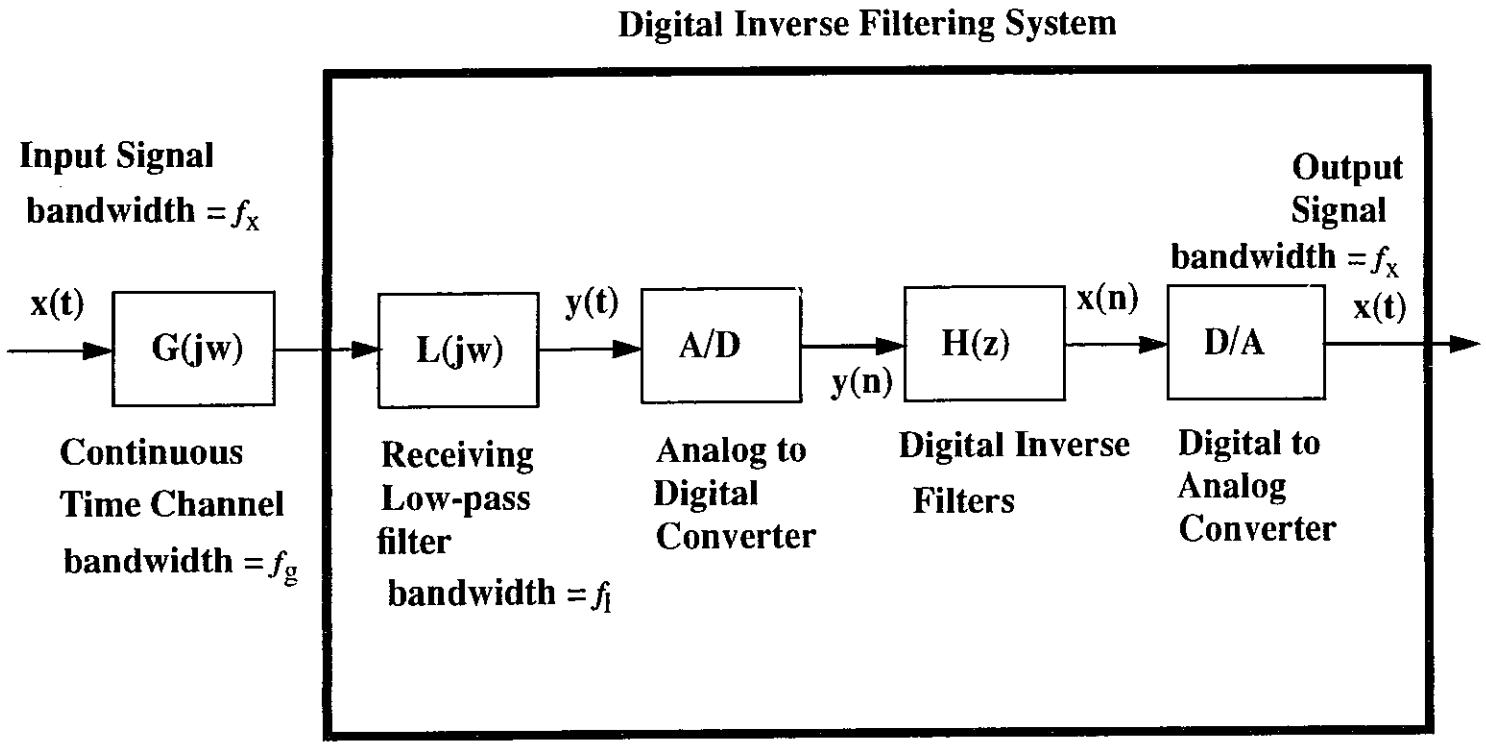

Figure 5.1: Inverse filtering with a single channel.

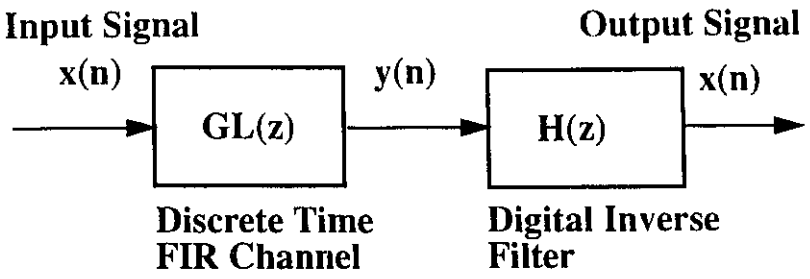

Figure 5.2: Discrete linear shift-invariant channel-filter system.

The system can be modelled as a discrete linear shift-invariant system depicted in Figure 5.2. The objective is to design a digital filter that restores the linearly distorted signal **x**(n). This digital filter is to be a discrete-time, causal, Finite Impulse Response (FIR) system.

The usual method for simple channel equalization is to design an FIR filter based on the Least-Square Error (LSE) criterion [4] [6]. Only a signal approximate to **x**(n) is restored. In general, the higher order the filter is, the more accurate the output. If the channel **GL**(z) is minimum phase, the error converges to zero. For non-minimum phase channels, the error remains of finite value [2]. Refer to appendix A for the implementation and properties of the LSE equalizer.

MINT can yield an exact inverse filter system for both the minimum phase and non-minimum phase channel; however, it requires the existence of multiple channels which do not contain common zeros [1]. Additional physical channels are required.

A new equalizer structure based on MINT is proposed here to work on a single channel. Basically multiple parallel subchannels are derived from a single channel with the technique of oversampling; thereby, MINT (post-channel filtering of Section 3.2 (page 23))

can be applied.

5.3 A single channel equalizer structure

Figure 5.3 depicts the proposed equalizer structure. Two subchannels are derived from a single channel and MINT is applied to restore the linearly distorted signal **x**(t).

The principle of deriving subchannels from a single channel is explained in Section 5.3.1. Design considerations on deriving subchannels is given in Section 5.3.2 The components of the new equalizer structure is described in Section 5.3.3.

5.3.1 Deriving subchannels from a single channel

In this section the principle of deriving subchannels from a single channel with the equalizer structure shown in Figure 5.3. is explained. Let the continuous frequency spectrum of the input signal **x**(t), the channel **G**(jw), the receiving low-pass filter **L**(jw) be as shown in Figure 5.4 and the discrete frequency spectrum of the distorted sequence **y**(n) as in Figure 5.5. With no loss of generality and for mathematical convenience, the ideal filter model [23](see footnote on page 60) is adopted here, for the channel spectrum.

The same conditions of a regular digital inverse filtering system described in Section 5.2 are assumed; i.e. $f_l = f_x$, $f_s \geq 2f_x$ and $f_g \geq f_l$.

The distorted signal **y**(t) is the convolution product of the input signal **x**(t) and the effective channel **GL**(jw) which has a bandwidth f_l. It is sampled at $2f_S$ to form **y**(n) which is then split into 2 signals $\mathbf{y}_1$(n), $\mathbf{y}_2$(n), each of data rate f_S.

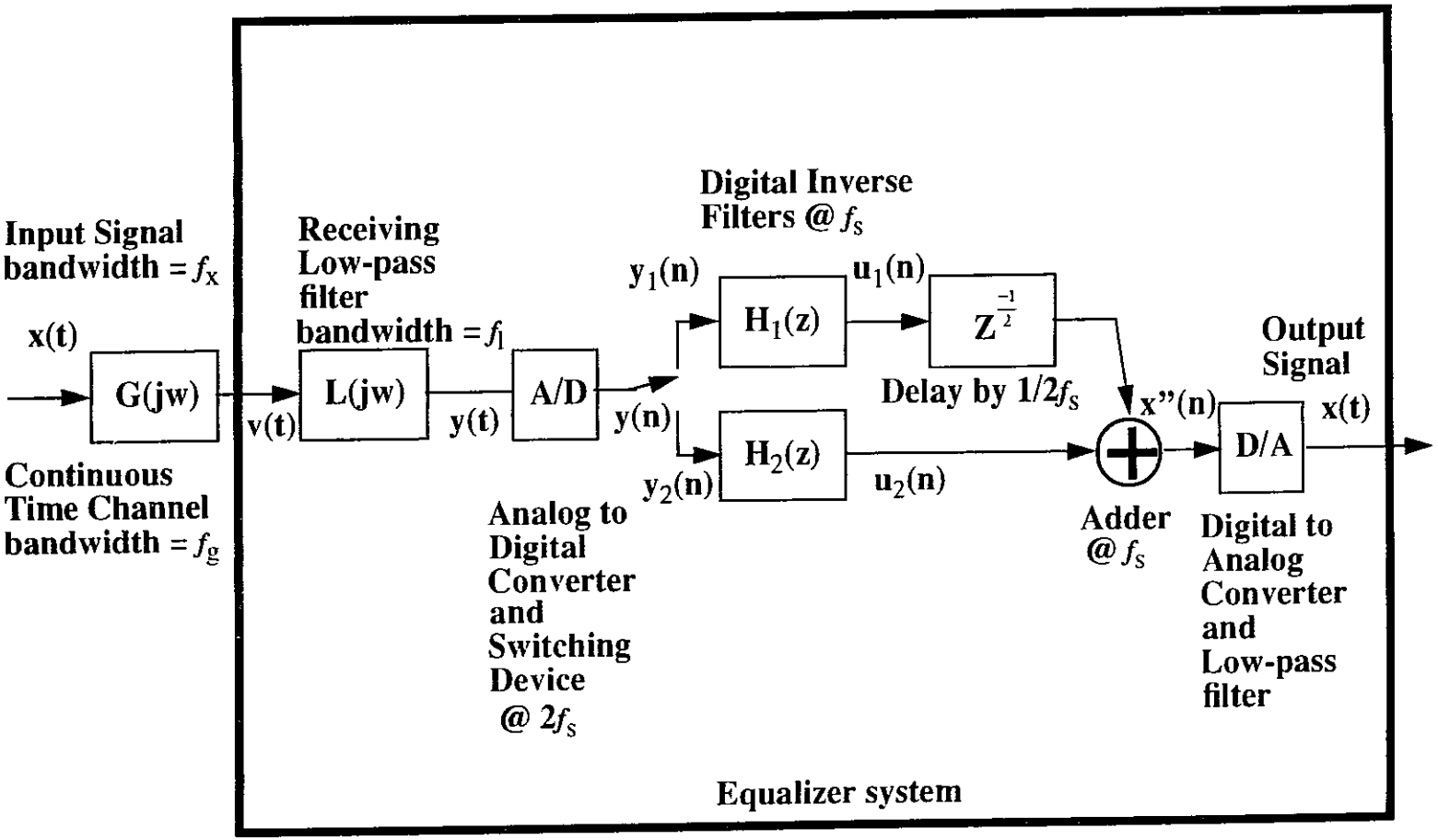

Figure 5.3: MINT equalizer system with dual virtual channels.

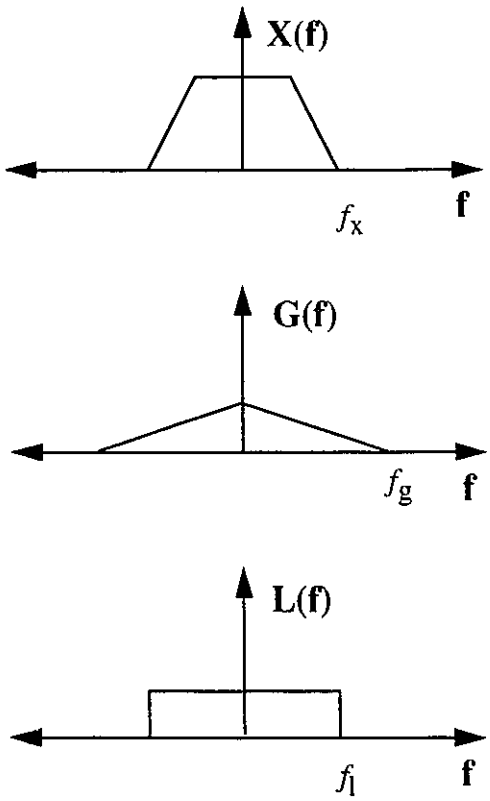

Figure 5.4: The frequency spectrum of the input signal x(t), the channel G(jw), the receiving low-pass filter L(jw).

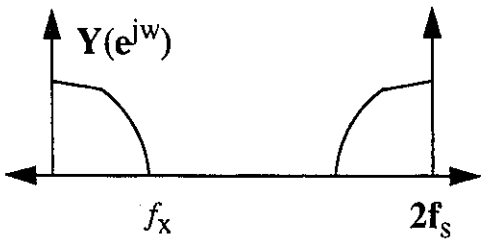

Figure 5.5: The discrete frequency spectrum of the distorted signal y(t) sampled at $2f_s$

Given $\frac{f_s}{2} \geq f_1 = f_x$, $\mathbf{y}(n)$ can be modelled as the convolution product of $\mathbf{x}(n)$ and $\mathbf{gl}(n)$ where $\mathbf{x}(n)$ is the discrete sequence of the input signal $\mathbf{x}(t)$ sampled at $2f_S$ and $\mathbf{gl}(n)$ is the discrete sequence of the impulse response of the effective channel $\mathbf{GL}(w)$ sampled at $2f_S$; i.e.

$$\mathbf{y}(n) = \{\mathbf{y}_0, \mathbf{y}_1, \mathbf{y}_2, \mathbf{y}_3, \mathbf{y}_4, \mathbf{y}_5, \cdots\}$$
$$\mathbf{gl}(n) = \{\mathbf{gl}_0, \mathbf{gl}_1, \mathbf{gl}_2, \mathbf{gl}_3, \mathbf{gl}_4, \mathbf{gl}_5, \cdots\}$$
$$\mathbf{x}(n) = \{\mathbf{x}_0, \mathbf{x}_1, \mathbf{x}_2, \mathbf{x}_3, \mathbf{x}_4, \mathbf{x}_5, \cdots\}$$

The discrete frequency spectrum $\mathbf{Y}(e^{jw})$, of Figure 5.6, is formed by multiplying of $\mathbf{X}(e^{jw})$ with $\mathbf{GL}(e^{jw})$. $\mathbf{X}(e^{jw})$ and $\mathbf{GL}(e^{jw})$ are the discrete frequency spectrum of $\mathbf{x}(n)$ and $\mathbf{gl}(n)$ respectively.

With the same condition that $\frac{f_s}{2} \geq f_1 = f_x$, however, $\mathbf{y}(n)$ can also be modelled as the convolution product of $\mathbf{x}'(n)$ and $\mathbf{gl}(n)$ where $\mathbf{x}'(n)$ is the discrete even sequence of the input signal $\mathbf{x}(t)$ sampled at $2f_S$;

$$\mathbf{x}'(n) = \{\mathbf{x}_0, 0, \mathbf{x}_2, 0, \mathbf{x}_4, 0, \cdots\}$$

Figure 5.6 shows that $\mathbf{Y}(e^{jw})$ can also be formed by multiplying of $\mathbf{X}'(e^{jw})$ with $\mathbf{GL}(e^{jw})$ where $\mathbf{X}'(e^{jw})$ is the discrete frequency spectrum of $\mathbf{x}'(n)$. Hence $\mathbf{x}'(n)$, ***other than*** $\mathbf{x}(n)$, ***is also a valid representation of the input sequence for this equalizer system***[†]. Note that $\mathbf{x}'(n)$ has a data rate of $2f_S$ and has interleaved zero value at its odd time slots.

[†] In order to suppress the frequency components of $\mathbf{X}'(e^{jw})$ from f_X to $2f_S - f_X$ (shown in Figure 5.6), the frequency components of $\mathbf{GL}(e^{jw})$ from f_1 to $2f_S - f_1$ must be close to zero; and $f_s \geq f_1 + f_x$ is required.

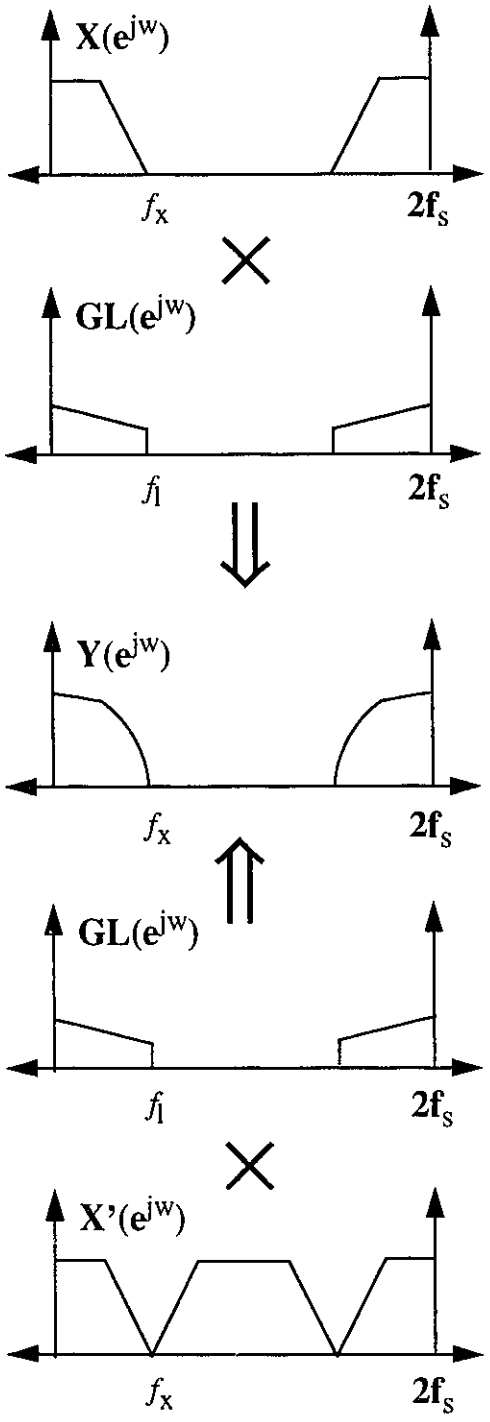

Figure 5.6: Discrete frequency spectrums depicting how y(n) can be computed.

Consider the discrete model of a dual channel filtering system depicted in Figure 3.2 (page 24). MINT can be applied only if the filtering system can be modelled as having a single source of input signal $\mathbf{x}(t)$ and two channels $\mathbf{G}_1(z)$, $\mathbf{G}_2(z)$ with two separate distorted signal outputs.

For the filtering system depicted in Figure 5.3, $\mathbf{gl}(n)$ can be represented as the sum of two subchannels $\mathbf{gl'}_1(n)$, $\mathbf{gl'}_2(n)$:

$$\mathbf{gl}(n) = \mathbf{gl'}_1(n) + \mathbf{gl'}_2(n)$$

where

$$\mathbf{gl'}_1(n) = \{\mathbf{gl}_0, 0, \mathbf{gl}_2, 0, \mathbf{gl}_4, 0, \ldots\}$$
$$\mathbf{gl'}_2(n) = \{0, \mathbf{gl}_1, 0, \mathbf{gl}_3, 0, \mathbf{gl}_5, \ldots\}$$

Similarly $\mathbf{y}(n)$ can also be considered as the sum of two signals $\mathbf{y'}_1(n)$, $\mathbf{y'}_2(n)$ with data rate of $2f_S$:

$$\mathbf{y}(n) = \mathbf{y'}_1(n) + \mathbf{y'}_2(n)$$

where:

$$\mathbf{y'}_1(n) = \{\mathbf{y}_0, 0, \mathbf{y}_2, 0, \mathbf{y}_4, 0, \ldots\}$$
$$\mathbf{y'}_2(n) = \{0, \mathbf{y}_1, 0, \mathbf{y}_3, 0, \mathbf{y}_5, \ldots\}$$

As a consequence of $\frac{f_s}{2} \geq f_1 = f_x$ [†], $\mathbf{y'}_1(n)$ can be formed by convolving $\mathbf{x'}(n)$ with $\mathbf{gl'}_1(n)$:

$$\mathbf{y'}_1(n) = \mathbf{x'}(n) * \mathbf{gl'}_1(n) \tag{5.1}$$

[†] This condition can be extended as $f_s \geq f_1 + f_x$ and $f_1 \geq f_x$ as depicted in (5.4).

Figure 5.7. shows that $\mathbf{Y'}_1(e^{jw})$ is formed by multiplying of $\mathbf{X'}(e^{jw})$ with $\mathbf{GL'}_1(e^{jw})$, where $\mathbf{X'}(e^{jw})$ and $\mathbf{GL'}_1(e^{jw})$ are the discrete frequency spectrum of $\mathbf{x'}(n)$ and $\mathbf{gl'}_1(n)$ respectively:

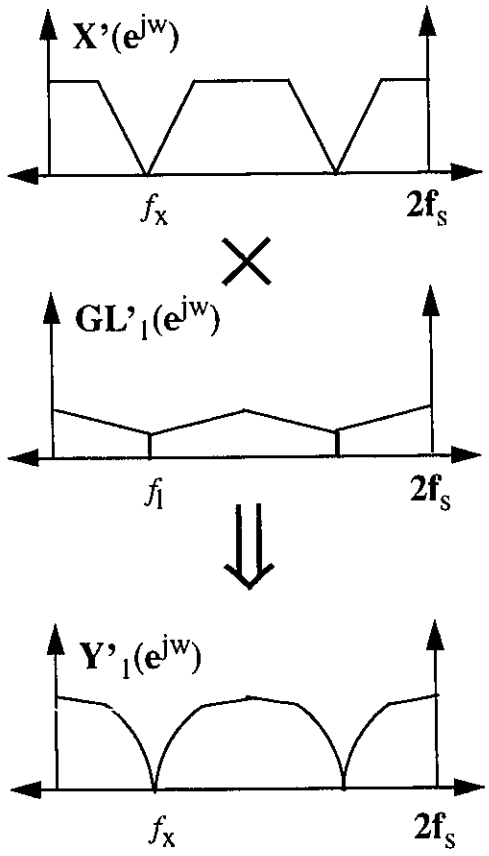

Figure 5.7: Discrete frequency spectrums depicting how $\mathbf{y'}_1(n)$ is formed.

This is also applicable to $\mathbf{y'}_2(n)$ as depicted Figure 5.8. $\mathbf{y'}_2(n)$ is formed by the convolution of $\mathbf{x'}(n)$ with $\mathbf{gl'}_2(n)$. The dotted line represents the phase difference between $\mathbf{Y'}_1(e^{jw})$ and $\mathbf{Y'}_2(e^{jw})$.

$$\mathbf{y'}_2(n) = \mathbf{x'}(n) * \mathbf{gl'}_2(n) \tag{5.2}$$

With (5.1) and (5.2), we have demonstrated that ***a single channel equalizer system, with the condition*** $\frac{f_s}{2} \geq f_1 = f_x$, ***can be modelled as having two channels*** $\mathbf{gl'}_1(n)$, $\mathbf{gl'}_2(n)$ ***and a single source of input signal x'(n) which is distorted by the two channels to form two separate signals*** $\mathbf{y'}_1(n)$, $\mathbf{y'}_2(n)$. Therefore, ***MINT can be applied to restore the distorted signals*** $\mathbf{y'}_1(n)$, $\mathbf{y'}_2(n)$ ***with two digital FIR filters to*** $\mathbf{x'}(n)$ as shown in Figure 3.2 (page 24). Note that the signal and channels are at a rate of $2f_S$.

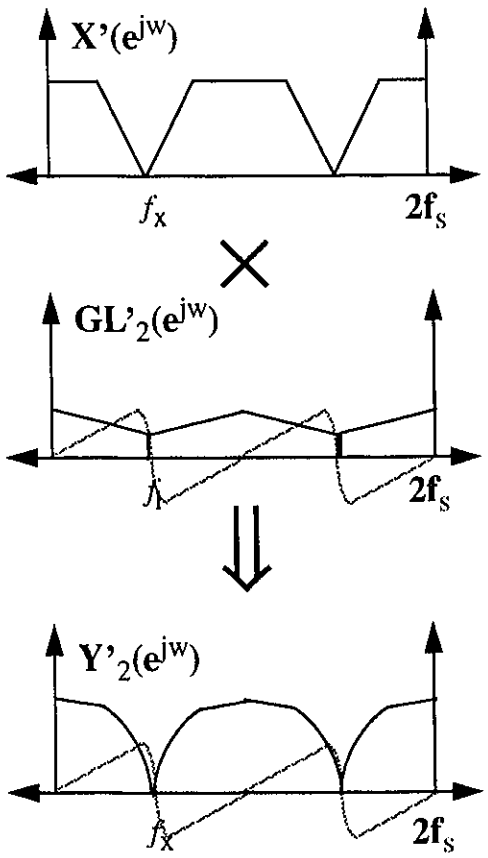

Figure 5.8: Discrete frequency spectrums depicting how $y'_2(n)$ is formed.

Furthermore, the condition, $\frac{f_s}{2} \geq f_1 = f_x$, also allows the downsampling of the signals and channels to f_S by removing all the interleaved zeros as depicted in Figure 5.9.

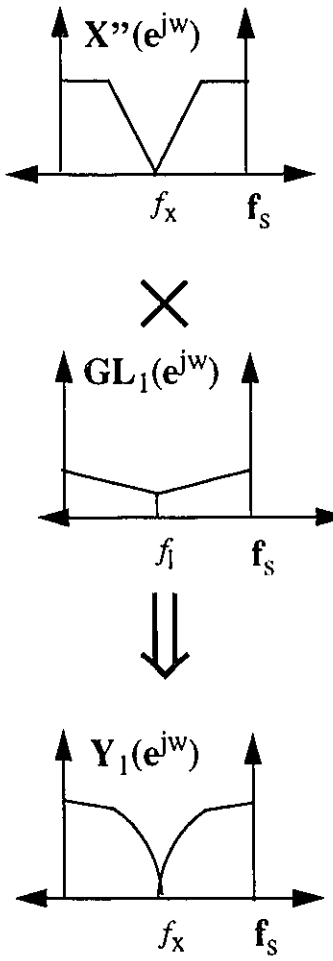

Figure 5.9: Discrete frequency spectrums depicting how $y_1(n)$ is formed.

The model described in (5.1) and (5.2) becomes:

$$\begin{aligned} \mathbf{y}_1(n) &= \{\mathbf{y}_0, \mathbf{y}_2, \mathbf{y}_4, \cdots\} \\ &= \mathbf{x}''(n) * \mathbf{gl}_1(n) \end{aligned}$$

$$\begin{aligned} \mathbf{y}_2(n) &= \{\mathbf{y}_1, \mathbf{y}_3, \mathbf{y}_5, \cdots\} \\ &= \mathbf{x}''(n) * \mathbf{gl}_2(n) \end{aligned} \qquad (5.3)$$

where

$$\mathbf{gl}_1(n) = \{\mathbf{gl}_0, \mathbf{gl}_2, \mathbf{gl}_4, \ldots\}$$
$$\mathbf{gl}_2(n) = \{\mathbf{gl}_1, \mathbf{gl}_3, \mathbf{gl}_5, \ldots\}$$
$$\mathbf{x}''(n) = \{\mathbf{x}_0, \mathbf{x}_2, \mathbf{x}_4, \ldots\}$$

and $\mathbf{X}''(e^{jw})$ is the discrete frequency spectrum of $\mathbf{x}''(n)$ which is obtained by sampling the input signal $\mathbf{x}(t)$ at f_S. Note that there is a delay of $\frac{1}{2f_s}$ on $\mathbf{y}_2(n)$ from $\mathbf{y}_1(n)$. It is because $\mathbf{gl'}_2(n)$ has interleaved zeros in its odd time slots and the first sampled coefficient $\mathbf{gl}_1$ is at the second time slot.

With (5.3), we have demonstrated that ***the single channel equalizer system depicted in Figure 5.3, with the condition*** $\frac{f_s}{2} \geq f_1 = f_x$ ***, can be modelled as having two channels*** $\mathbf{gl}_1(n)$, $\mathbf{gl}_2(n)$ ***and a single source of input signal x"(n) which is distorted by the two channels to form two signals*** $\mathbf{y}_1(n)$, $\mathbf{y}_2(n)$. Therefore, ***MINT can be applied to restore the distorted signals*** $\mathbf{y}_1(n)$, $\mathbf{y}_2(n)$ ***with two digital FIR filters back to*** $\mathbf{x}''(n)$ as shown in Figure 3.2 (page 24).

To summarize, deriving two subchannels from a single channel, which has a data rate of $2f_S$, is possible when the input signal can be modelled as $\mathbf{x'}(n)$. This requires the condition $\frac{f_s}{2} \geq f_1 = f_x$. In fact the condition can be extended as

$$f_s \geq f_1 + f_x \qquad \text{and} \qquad f_1 \geq f_x \tag{5.4}$$

such that the input signal can be modelled as $\mathbf{x'}(n)$ depicted in Figure 5.6.

5.3.2 Design considerations on deriving subchannels

There are two considerations on deriving subchannels. They govern the choice of sampling frequency $2f_S$ of the analog-to-digital converter and the bandwidth f_1 of the receiving low-pass filter $\mathbf{L}(jw)$.

1) Deriving different subchannels which have no common zeros.

The chance of having common zeros is reduced by making the derived subchannels $\mathbf{GL}_1(z)$, $\mathbf{GL}_2(z)$ different from each other. There is already a phase difference between the derived subchannels, which have same number of zeros, as shown in Figure 5.8. However an additional difference can be introduced by the condition:

$$\frac{f_s}{2} < f_1$$

Consider the process of splitting the distorted signal $\mathbf{y}(n)$ into 2 signals $\mathbf{y}_1(n)$, $\mathbf{y}_2(n)$ shown in Figure 5.3. It effectively reduces the clock rate from $2f_s$ to f_s. This leads to the aliasing of the frequency spectrum for the effective channel $\mathbf{GL}(jw)$. The result of overlapping frequency components at the region $f_s - f_1$ *to* f_1 of the subchannels are not the same because of the phase difference between the two subchannels $\mathbf{GL'}_1(e^{jw})$, $\mathbf{GL'}_2(e^{jw})$ depicted in Figures 5.7 and 5.8 respectively.

Since the characteristics of the frequency spectrum is determined by the location of the zeros in the complex z-plane, the difference between the frequency spectrums reduces the chance of having common zeros between the derived channels $\mathbf{GL}_1(z)$, $\mathbf{GL}_2(z)$. In general this also reduces the impact associated with close zeros (discussed in chapter 4) between the derived channels. This is confirmed by the results of the simulation described in Section 5.5.3.

Therefore, a partial aliasing in the frequency spectrum of the effective channel $\mathbf{GL}(jw)$ at sampling rate of f_s is recommended so that the two virtual channels have more difference. Note that no analytic model is yet found to predict the impact of close zeros with respect to the degree of aliasing in the frequency spectrum of the effective channel $\mathbf{GL}(jw)$.

2) Maximize the usable pass-band of the equalizer.

The usable pass-band of an equalizer limits (defines) the maximum bandwidth f_x that

the restored signal **x**(t) can have. Therefore the condition $2f_x \leq f_s$ is required for the single channel equalizer structure depicted in Figure 5.3 so that no significant aliasing error occurs in the sampled signal **x**(n).

The aliasing error of the subchannels can only occur outside the usable pass-band. This allows any frequency components, from 0 to f_x Hz, of an input signal, which is distorted by the analog channel **G**(jw), be compensated exactly by the digital filters $\mathbf{H}_1(z)$, $\mathbf{H}_2(z)$, which designs are based on the sampled subchannels $\mathbf{GL}_1(e^{jw})$, $\mathbf{GL}_2(e^{jw})$. Consequently, the condition:

$$f_x \leq f_s - f_l$$

is required. This agrees with (5.4).

These two considerations drive the design in opposite directions for a given f_s. A small value f_l[†] for the effective channel **GL**(jw) ensures little distortion within the usable pass-band f_x; and a larger usable pass-band is possible. However this makes the derived channels $\mathbf{GL}_1(z)$, $\mathbf{GL}_2(z)$ less different from each other.

In general this is not an issue since the design of the equalizer is always based on a specific usable pass-band f_x. One can always design in a higher f_s and f_l as long as f_l, the bandwidth of the receiving low-pass filter **L**(jw) which serves to limit the bandwidth of the channel, is greater than f_g. The only cost is the higher clock rate of the equalizer system.

5.3.3 Components of the new equalizer structure

The proposed equalizer structure is shown in Figure 5.3. The structure supports two functions:

[†] Per (5.4) the smallest value of f_l is f_x.

1) capturing of the distorted signal: low-pass filtering, analog-to-digital conversion, splitting of signal,

2) restoring the distorted signal: inverse filtering with phase synchronization, low-pass filtering, digital-to-analog conversion.

The front end of the equalizer system is a receiving low-pass filter **L**(jw). It limits the bandwidth of the channel **G**(jw) and the input signal **x**(t) as well as controls the noise input. The effective channel of this system becomes **GL**(jw) of bandwidth f_l.

In fact, **L**(jw) denotes a low-pass filter subsystem which has two sets of bandwidth to support two different operating modes of the equalizer. When the equalizer is operating at the "running" mode, in which the inverse filtering is being performed, the bandwidth of the low-pass filter **L**(jw) is set to f_x to bandlimited the input signal **x**(t) and remove any out-of-band noise components. When the equalizer is operating at the "setting" mode, in which the filter coefficients is being determined from the sampled impulse response of the effective channel **GL**(jw), the bandwidth of the low-pass filter **L**(jw) is set to f_l such that $f_g \geq f_l \geq f_x$ and $f_s \geq f_l + f_x$. This enables the determination of filter coefficients to meet the design considerations described in Section 5.3.2.

An analog signal **x**(t), which is bandlimited to f_x Hz, is distorted by an analog channel **G**(jw), which has a bandwidth f_g, which is greater than f_x, to form signal **v**(t). The distorted signal **v**(t) is filtered by the receiving low-pass filter **L**(jw) of bandwidth f_l. The analog-to-digital converter, working at a clock rate of $2f_s$ samples per second, samples the filtered signal **y**(t). The switching device splits the resultant sequence **y**(n), by separating the adjacent samples into two sequences $\mathbf{y}_1(n)$, $\mathbf{y}_2(n)$ each with f_s samples per second.

MINT is applied in the digital filters $\mathbf{H}_1(z)$, $\mathbf{H}_2(z)$ to restore, from $\mathbf{y}_1(n)$, $\mathbf{y}_2(n)$, the signal sequence **x**"(n) (derived from **x**'(n) which is an valid digital representation of the input signal **x**(t) as depicted in Section 5.3.1) completely within the usable bandwidth f_x. A delay of $\frac{1}{2f_s}$, implemented by a buffer, is introduced to $\mathbf{u}_1(n)$ to compensate the time

different between $\mathbf{u}_1(n)$ and $\mathbf{u}_2(n)$ incurred at the switching device. An optional low-pass filter (not shown) removes all noise outside the usable bandwidth f_x before the output signal $\mathbf{x}''(n)$ the adder is converted back to $\mathbf{x}(t)$ by the digital-to-analog converter.

5.4 MINT equalizer with 3 virtual channels

The single channel equalizer structure presented in Section 5.3 can be extended to employ multiple virtual channels. Figure 5.10 depicts an equalizer structure with three virtual channels.

It can be shown with the same explanation in Section 5.3.1 that the condition for the existence of the virtual channels is also:

$$f_s \geq f_1 + f_x \qquad \text{and} \qquad f_1 \geq f_x$$

where the sampling rate of the distorted signal $\mathbf{y}(t)$ is $3f_s$; i.e., three times the filter clock rate.

Comparisons of the new equalizer structures in next section show that the MINT equalizer with 3 subchannels has better performance than those with 2 subchannels. However this comes with the expense of higher oversampling rate.

5.5 Performance of the MINT equalizers

In this section, the performance of the MINT equalizers, proposed in Section 5.3 and 5.4, as well as their design considerations, are discussed. The comparison of their performances with the conventional equalizer which is based on the Least Square Error (LSE) criterion [6] is studied with simulations. These equalizer structures are termed as LSE, 2MINT, 3MINT equalizers respectively.

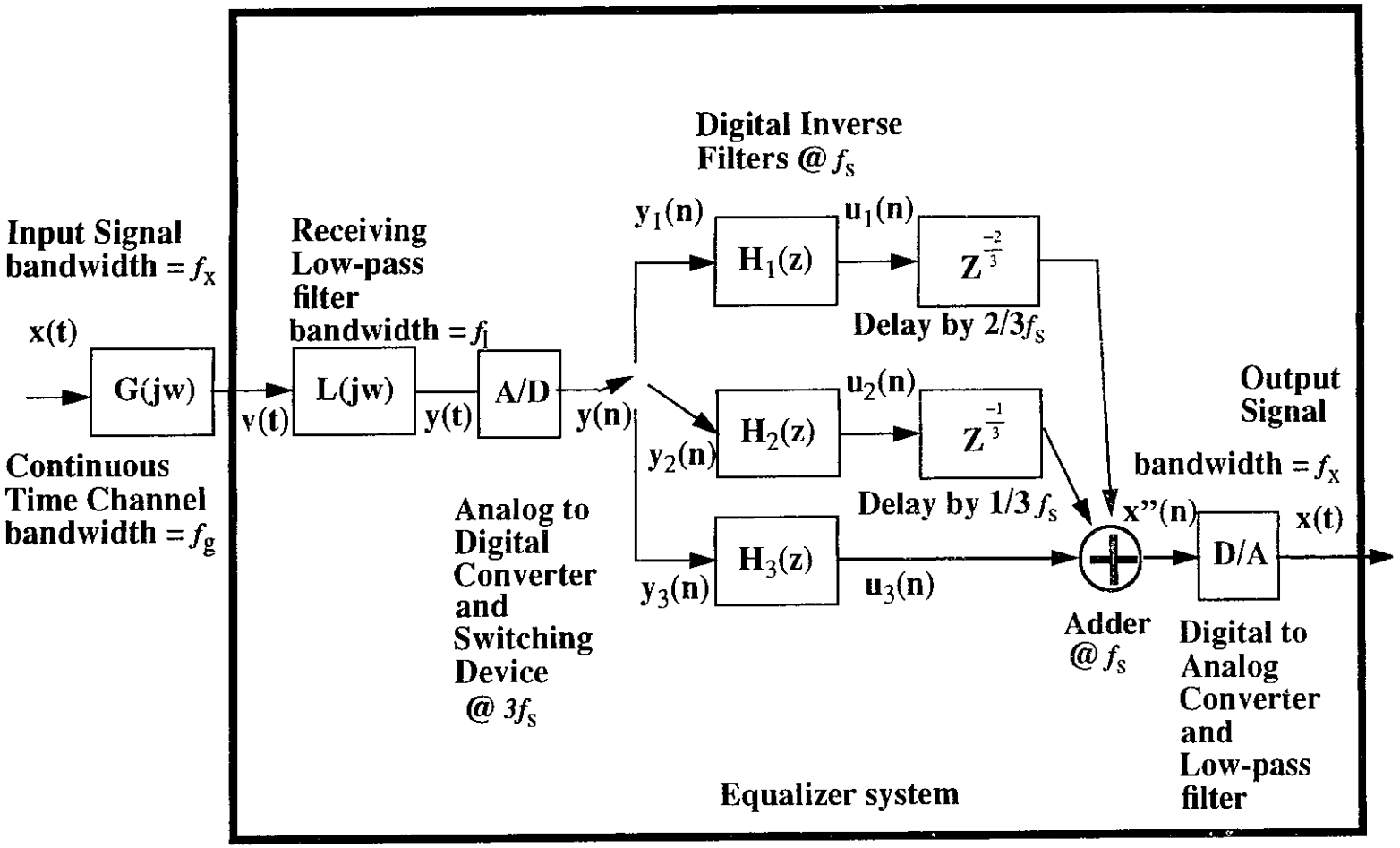

Figure 5.10: MINT equalizer with three channels

5.5.1 Measurement of equalizer performance

Consider the inverse filtering system depicted in Figure 5.1, the design objective is to realize the equalizer (inverse filtering system) restoring any linearly distorted frequency components of an input signal **x**(t) over the usable pass-band of the equalizer (i.e., the frequency spectrum from 0 to f_X Hz) with minimum implementation cost.

A high performance equalizer should produce a small, or even zero, error signal **e**(t), which is the difference between the restored signal and the original signal (bandlimited to the equalizer usable pass-band f_X) with system delay that is introduced by the filtering system. Hence, the inverse filtering capacity of an equalizer can be evaluated by reviewing the frequency (power) spectrum of the error signal **e**(t), or the discrete frequency spectrum of the error signal sequence **e**(n) which is obtained by sampling **e**(t) at $2f_X$ or higher. One other measure is the Signal-to-Error Ratio (SER), the energy ratio of a finite length signal sequence **x**(n) to its corresponding error signal **e**(n) sequence, both sampled at $2f_X$ or higher:

$$\mathbf{SER} = \frac{\sum_n |\mathbf{x}(n)|^2}{\sum_n |\mathbf{e}(n)|^2}$$

This finite length signal chosen should have a constant energy intensity over the usable pass-band of the equalizer. In general, the larger SER the equalizer has, the higher the performance on inverse filtering.

Another aspect of equalizer performance is the energy gain of an equalizer over the usable pass-band f_X. This is related to how noise presented at the input of an equalizer is amplified over the usable pass-band. The energy gain of an equalizer can be evaluated by reviewing the frequency (power) spectrum of the filtered noise. Alternatively, the frequency spectrum, from 0 to f_X, of the impulse response of an equalizer can be studied. One other measure is the Noise Enhancement Ratio (NER), the energy ratio of the output

$\mathbf{q}(n)$ of an equalizer to a finite length low-pass signal $\mathbf{p}(n)$ which bypasses the channel $\mathbf{G}(w)$ and is fed into the equalizer directly.

$$\mathbf{NER} = \frac{\sum_n |\mathbf{q}(n)|^2}{\sum_n |\mathbf{p}(n)|^2}$$

This finite length signal $\mathbf{p}(n)$ is bandlimited to f_x and has a constant energy intensity over the pass-band. In general, the smaller NER the equalizer has, the less amplification it has on the input noise.

The measurement of NER assumes a single noise source. For MINT equalizers, however, noises such as the quantization noise or the aliasing error of the channels[†], which are inputted into different filter branches, may not be the same. The amplification of multiple input noises of an equalizer can be measured by the Filter Norm(FN), described in Section 4.3 (page 49) In general, the larger FN the equalizer has, the more sensitive it is to

$$\mathbf{FN} = \mathbf{H}^T\mathbf{H} = \sum_i \sum_n |\mathrm{h}_i(n)|^2$$

multiple input noises.

The implementation cost of an equalizer depends largely on the technology used. For our purpose, two parameters are measured. The first one is the filtering effort. It represents the processing effort during the inverse filtering. One of the measurements for the filtering effort is the total number of filter coefficients, termed the Total Filter Length (TFL).

The second one is the computational effort in determining the filter coefficients. Once the characteristics of the channel is detected or identified, the corresponding filter coefficients are computed, usually via matrix algebra ((2.3) (page 8), (2.10) (page 19),

[†]·The aliasing error of the channels is due to the difference between the discrete frequency spectrum of the sampled channels and the continuous frequency spectrum of the actual channel.

(A.2) (page 110)). One of the measurements for the computational effort is the dimension of the channel matrix, or the equivalent square matrix, to be inverted. This is termed the Dimension of the Equivalent Channel Matrix (DECM). DECM is the number of row of the equivalent square matrix to be inverted.

5.5.2 Effect of the filter length on performance

It is shown in Section 5.3.1 that multiple subchannels can be derived from a single channel for the proposed equalizer structures depicted in Figure 5.3 and 5.10. These channels would tend to contain close zeros because of their similarity with each others. The impact of having close zeros is the high filter norm (FN) of the equalizer (Section 4.3 (page 49)). This makes the equalizer sensitive to multiple source noises such as the quantization noise or the aliasing error of the channels. Although applying MINT leads to exact solutions, the amplification of these noises by the equalizer impairs its performance in terms of the Signal-to-Noise Ratio. Introducing aliasing in the channels as described in Section 5.3.2 can reduce this impact.

The use of minimum norm solution with system delay in reducing the FN is demonstrated Section 4.3.1 (page 51). Therefore the performance of the MINT equalizer is expected to be improved by adopting a larger total filter length (TFL) with appropriate system delay. It is also demonstrated in Section A.2.2 (page 111) that the inverse filtering capability of a LSE equalizer can be improved with increasing TFL if system delays are allowed.

A simulation was conducted to study the effect of the total filter length on the

performance (SER, NER, FN) of the following equalizers:

1) the traditional equalizer based on LSE criterion described in appendix A,

2) the 2MINT equalizer depicted in Figure 5.3,

3) the 3MINT equalizer depicted in Figure 5.10.

Setup of the simulation:

In this simulation a bandlimited low-pass signal **X**(w), channel **G**(w) and receiving low-pass filter **L**(w) are assumed. Normalized frequency is displayed and the data rate of filter elements is 2, generally termed as the system clock rate. The discrete frequency spectrum of the input signal sequence **x**(n) and the effective channel **GL**(z) sampled at 12 (a oversampling factor of 6) in Figure 5.11. Note that the effective channel **GL**(z) has a gentle transition from the pass band to stop band. This leads to considerable aliasing error in the discrete channel when sampled at 2. This aliasing error on channel is expected to impair the performance of the equalizers when they have a high filter norm (FN).

To conveniently compare the restored signal sequences of these equalizers at the same data rate (at 2 units of normalized frequency or the system clock rate), the distorted signal **y**(t) is oversampled by a factor of 6 so that the sampled signal can be used, with appropriate decimation, by the three equalizers accordingly. The sampled, distorted signal sequence is decimated by a factor of 6, 3, 2 before it is fed to the LSE, 2MINT, 3MINT equalizers respectively, so that the effective oversampling factor of each equalizer structures relative to the system clock rate is 1, 2, 3 respectively.

Refer to the appendix B for the detail on the setup of this simulation.

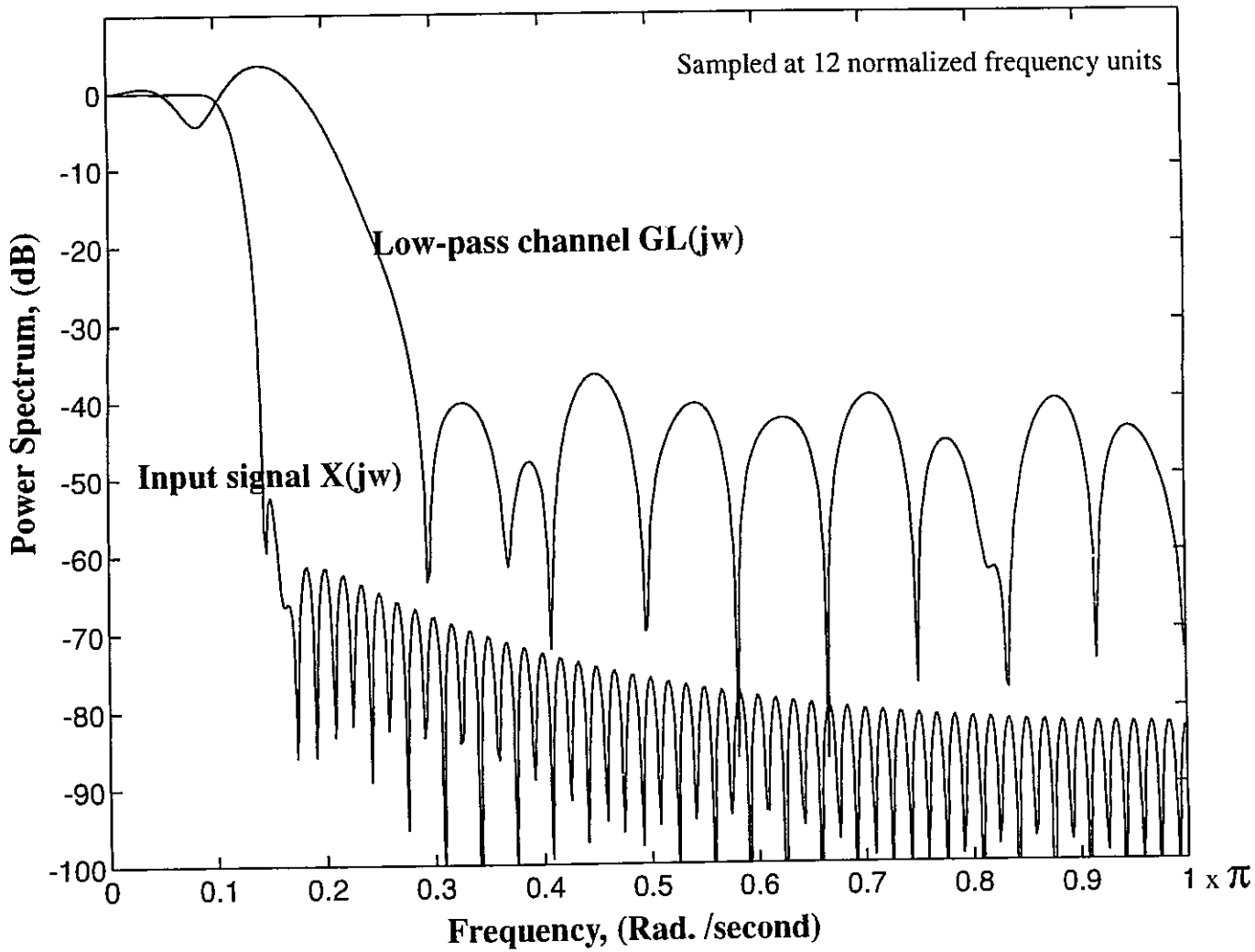

Figure 5.11: Discrete frequency (power) spectrum of the input signal x(n) and the low-pass channel GL(jw), oversampled by a factor of 6.

Results of the simulation:

The detail of the simulation result is tabulated in appendix B and presented graphically in this section.

Figures 5.13 and 5.14 depicted both the time domain representation and the frequency (power) spectrum of the error signals and the restored signals (before the digital-to-analog converter) of each equalizers. At TFH = 102, the 3MINT equalizer attains the smallest error sequence and the LSE equalizer the largest.

Figures 5.15 to 5.17 showed the comparison of the performances among different equalizers with the same total filter length TFL (number of filters coefficients), from 12 to 102. (12, 18, 30, 54, 102). Figure 5.15 showed that the MINT equalizers have a poor performance in terms of the Signal-to-Error Ratio (SER) when TFL is small. As TFL increases, their SER improves and eventually surpasses those of the LSE equalizer.

The ability of a digital equalizer in restoring a linearly distorted analog signal is affected by two factors (the impact of additive input noise is not considered yet). It depends on:

1) how well its filter components restore the digital signal,
2) how close the actual analog signal or channel are represented by the digital counterparts.

For factor one, LSE equalizer can only provide an approximate solution [4] [6] due to the nature of its channel matrix. On the other hand, MINT equalizer can provide the exact solutions with precision limited only by the computing device.

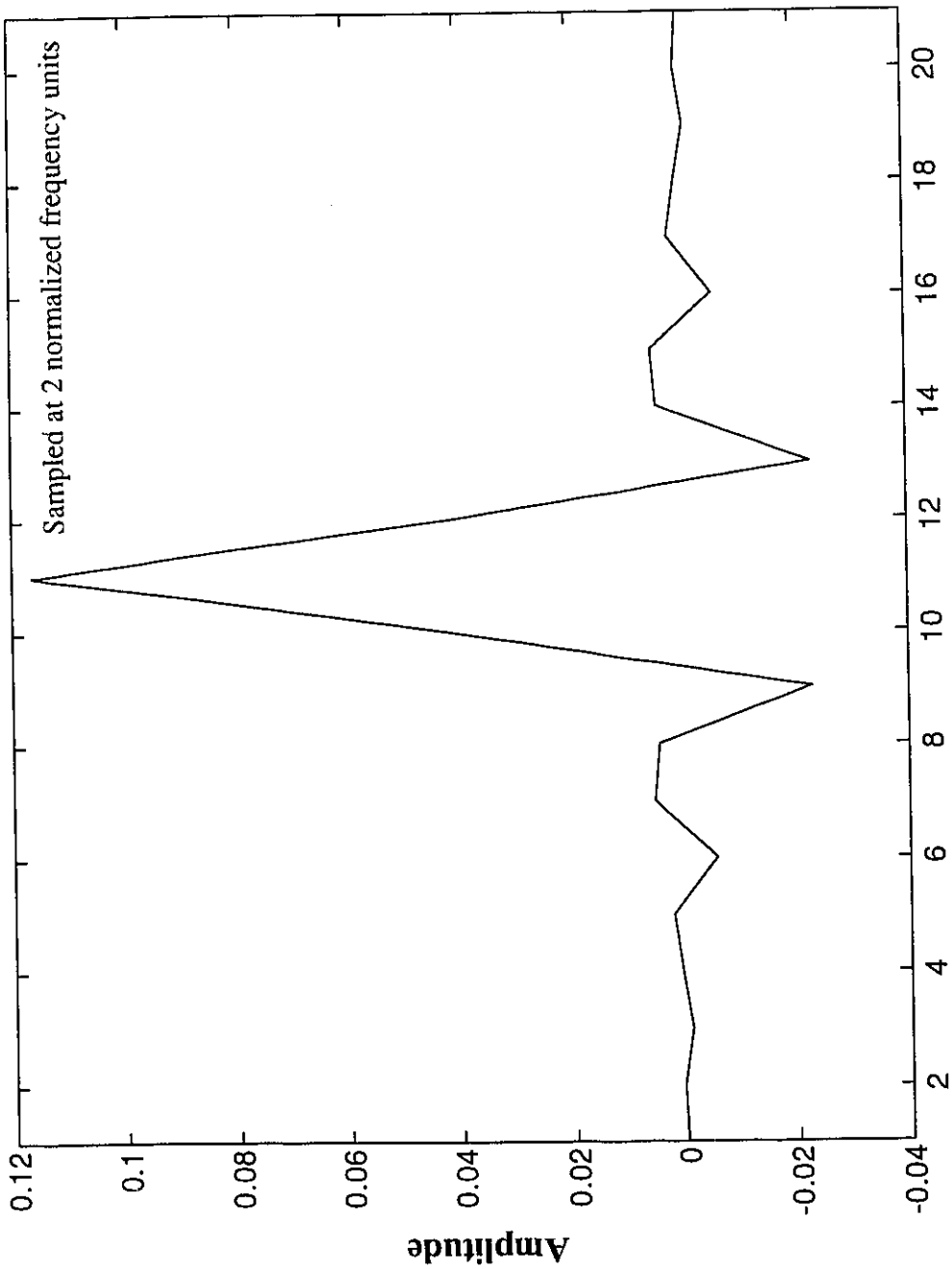

Figure 5.12: The input signal x(t) sampled at the system clock rate.

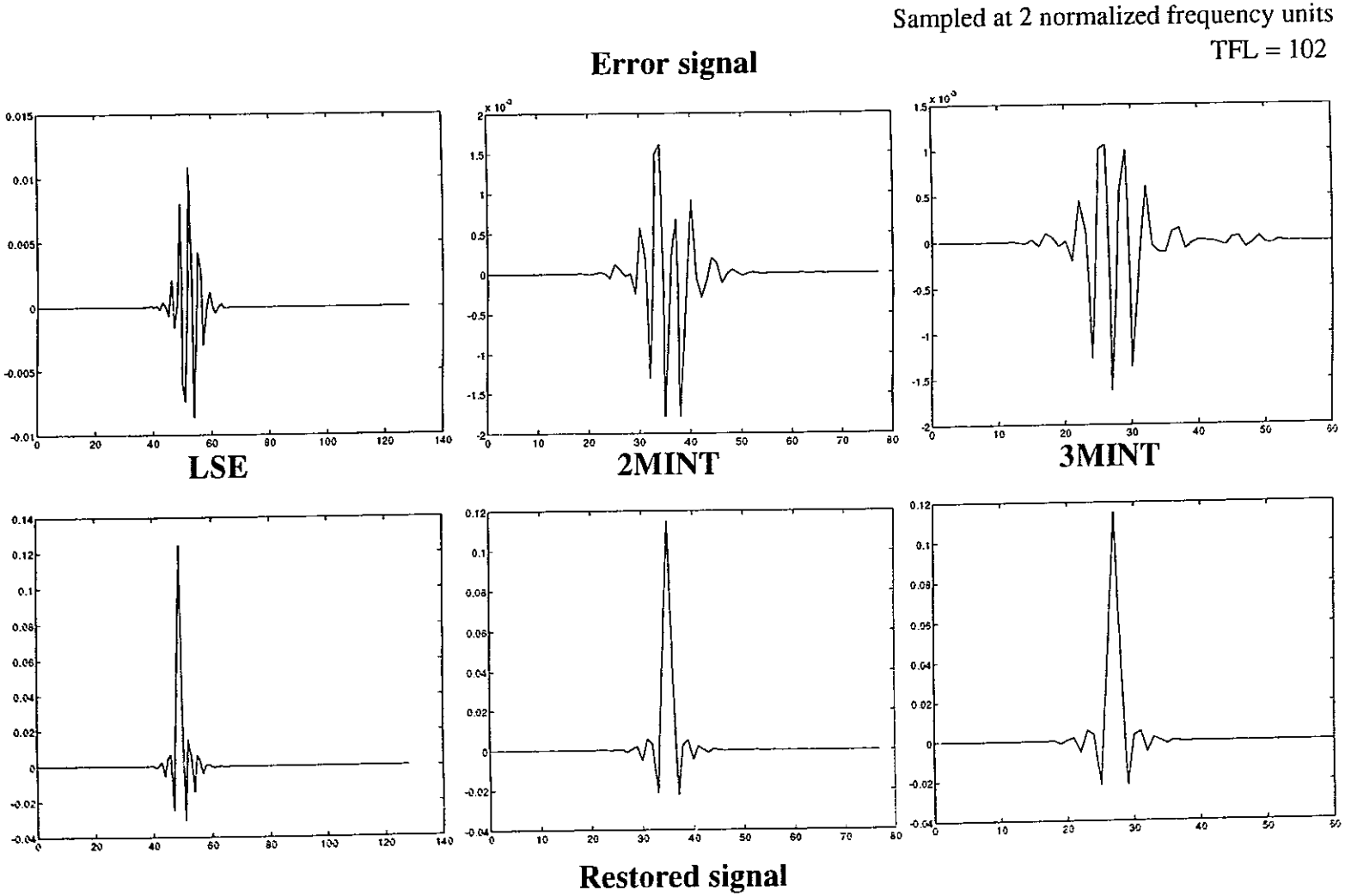

Figure 5.13: Comparison of error signals and restored signals in the time domain.

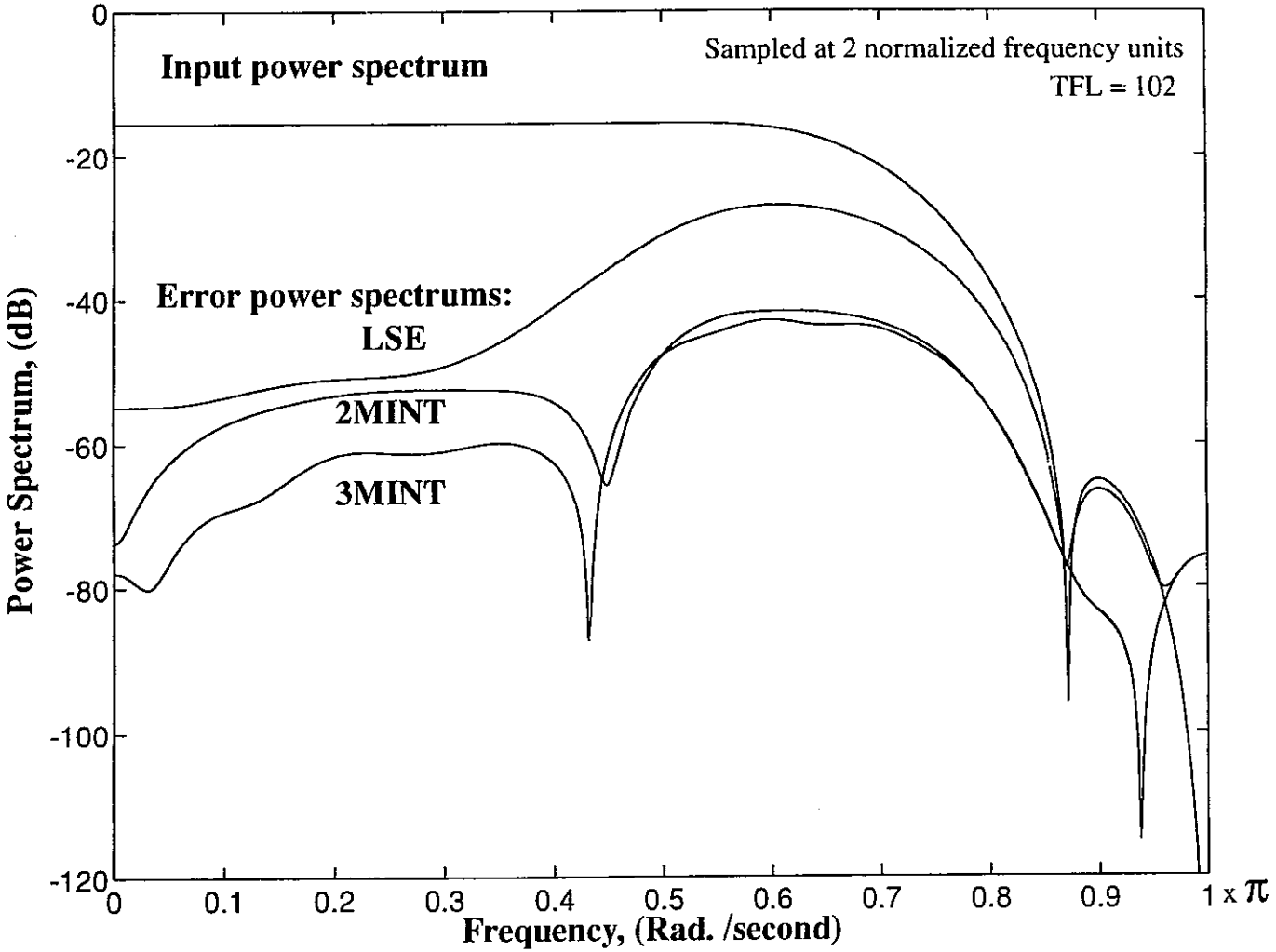

Figure 5.14: Comparison of the frequency spectrums of the input and error signals.

For factor two, the aliasing error, together with the quantization error, introduced during the sampling process leads to the differences between the digital channel[†] and its analog counterpart, even over the usable pass-band of the equalizer. The design of the filter component is based on the digital channel, and yet the input signal is distorted by the analog channel. This leads to a residue error in the restored signal which is amplified as the gain of the filter is bigger than unity. The amplification of the residue error also occurs in MINT equalizer since the residue error on one filter branch is not necessarily the same as, thereby compensated by, those on the other filter branches.

Comparing Figure 5.15 with Figure 5.16 which shows the change of the filter norm (FN) of each equalizers with respect to the total filter length (TFL), one could observe that SER and FN are inversely related. Factor 2 is shown to be the dominant factor that limits the performance of the equalizers when FN is high.

In general, the FN of the LSE equalizer is fairly constant (refer to appendix A). The MINT equalizers, on the other hand, has a large initial FN. However, the FNs of the MINT equalizers decrease as their total filters length (TFL) increase (refer to Section 4.3.1 (page 51)), eventually drop below those of the LSE equalizer. The 3MINT equalizer has the smallest FN. This trend affects the SER of the equalizers depicted in Figure 5.15.

Another aspect is the amplification on a single additive input noise by the equalizers. Figure 5.17 depicts the change of Noise Enhancement Ratio NER of the three equalizers. In general, NER of the 3MINT equalizer is the smallest and those of the LSE equalizer is the largest. Hence the 3MINT equalizer has the least noise amplification if a single source noise is assumed. Nonetheless, the 3MINT equalizer is also expected to have the least noise amplification with multiple input noise sources when the total filters length (TFL) is large enough since it has the smallest FN.

[†] The aliasing error and quantization error on the input signal are not amplified by the equalizer since the total gain on the original signal $x(t)$ by the channel-filter system is one in general.

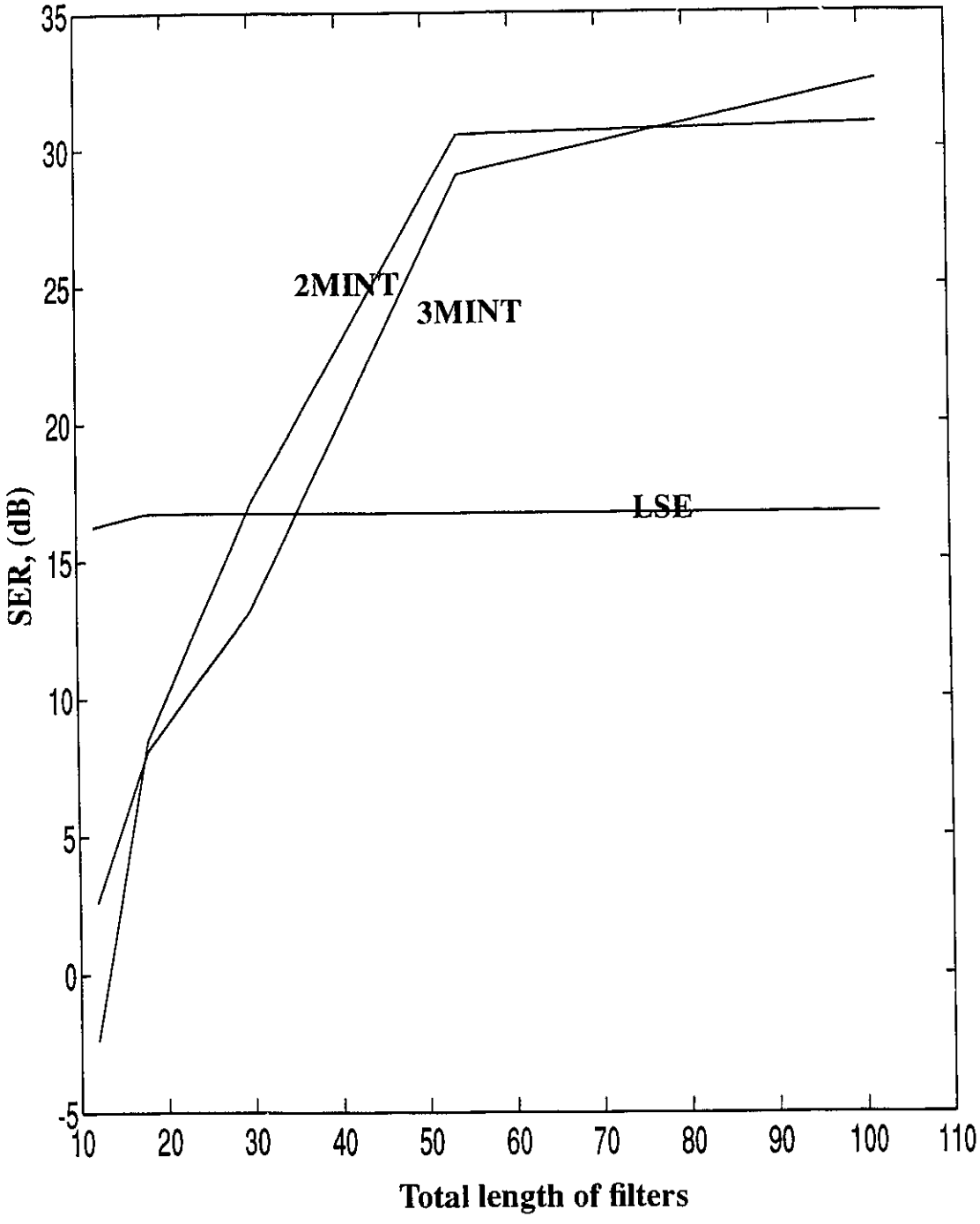

Figure 5.15: Comparison of the Signal -to-Error Ratio.

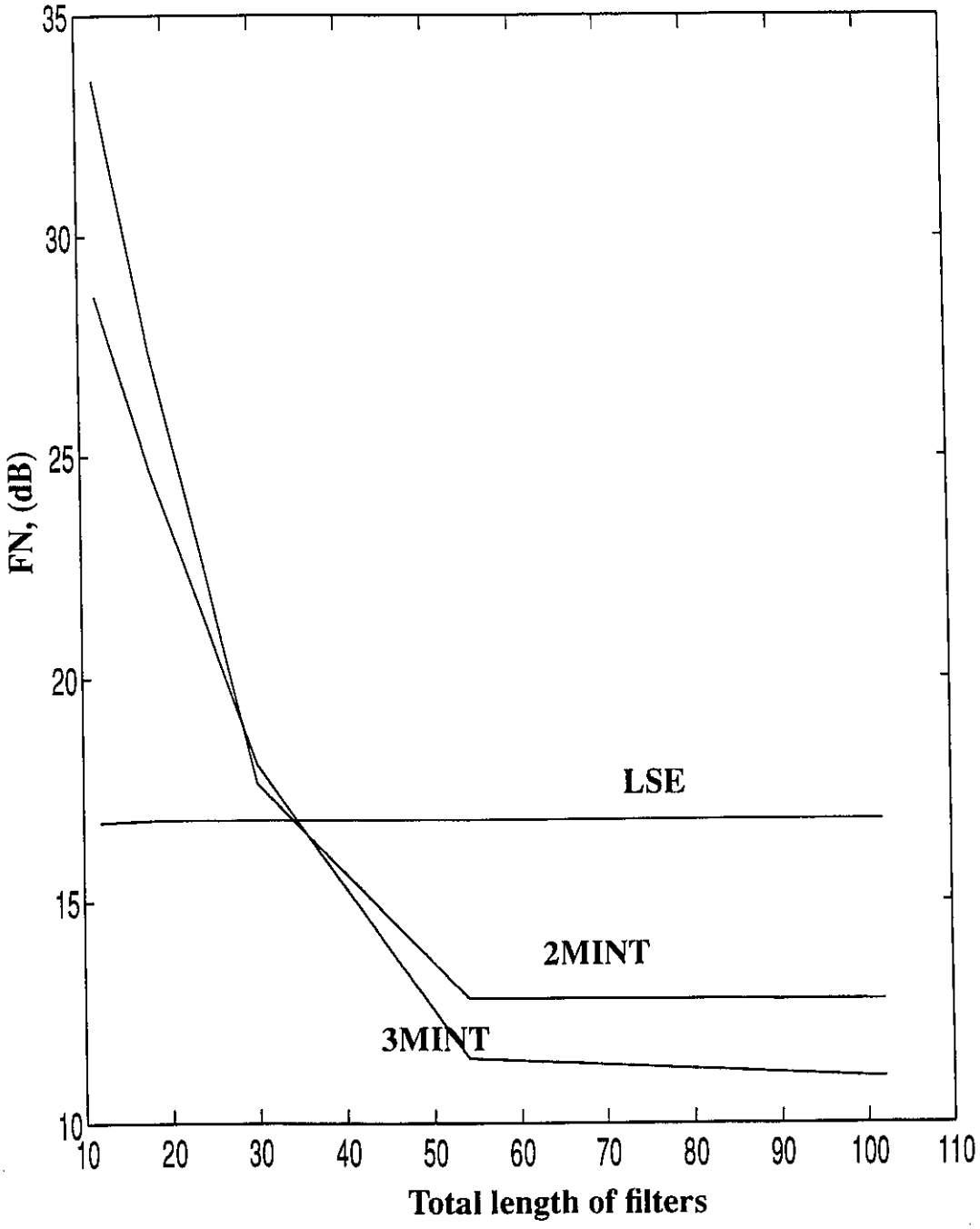

Figure 5.16: Comparison of the Filter Norm

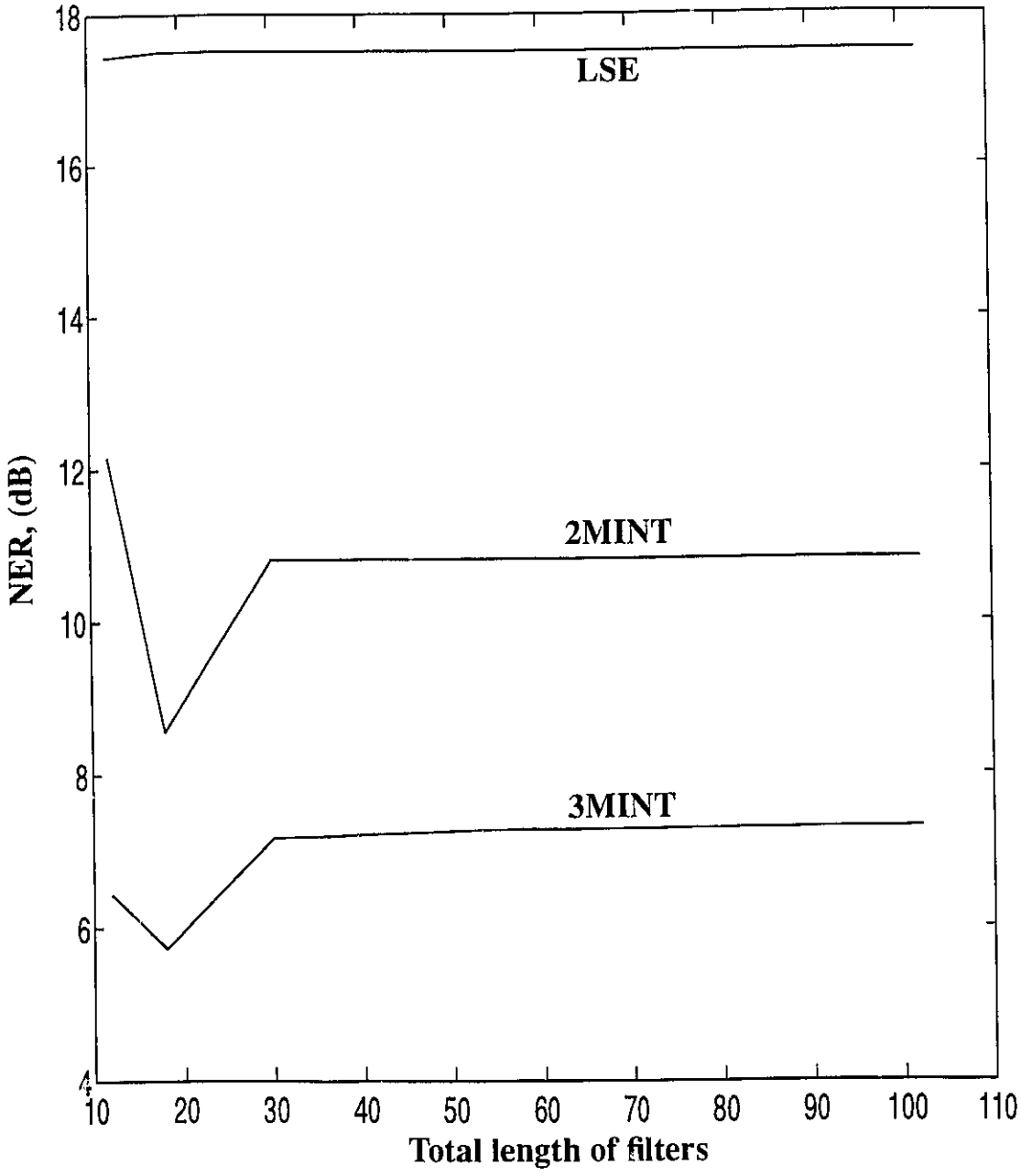

Figure 5.17: Comparison of the Noise Enhancement ratio.

System delays are introduced. This enables the LSE equalizer to restore the distorted at its maximum accuracy [4]. This also enables the lowest filter norm (FN) possible for the MINT equalizers. Figure 5.18 indicates the introduction of system delays by the equalizers.

We note from Figure 5.15 that the LSE equalizer reach its maximum performance with SER of about 16 dB at early stage. At this level of performance, the total filter length (TFL) are about 12, 28, 33 for the LSE, 2MINT, 3MINT equalizers respectively. Hence the dimension of the equivalent channel matrix to be inverted are 12 by 12, 26 by 26, 23 by 23 respectively.

Figure 5.19 depicts the change of SER of each equalizers with respect to the dimension of the equivalent channel matrix (DECM). This showed that the 3MINT equalizer requires less computational effort than the 2 MINT equalizer in determining the filter coefficients.

In general the LSE equalizer has a better performance than MINT equalizers when the TFL or DECM is small. But as the TFL increases, the SER of MINT equalizers increase whereas the SER of the LSE equalizer remains fairly constant. Thus MINT equalizers provide an opportunity to trade off performance with computational effort.

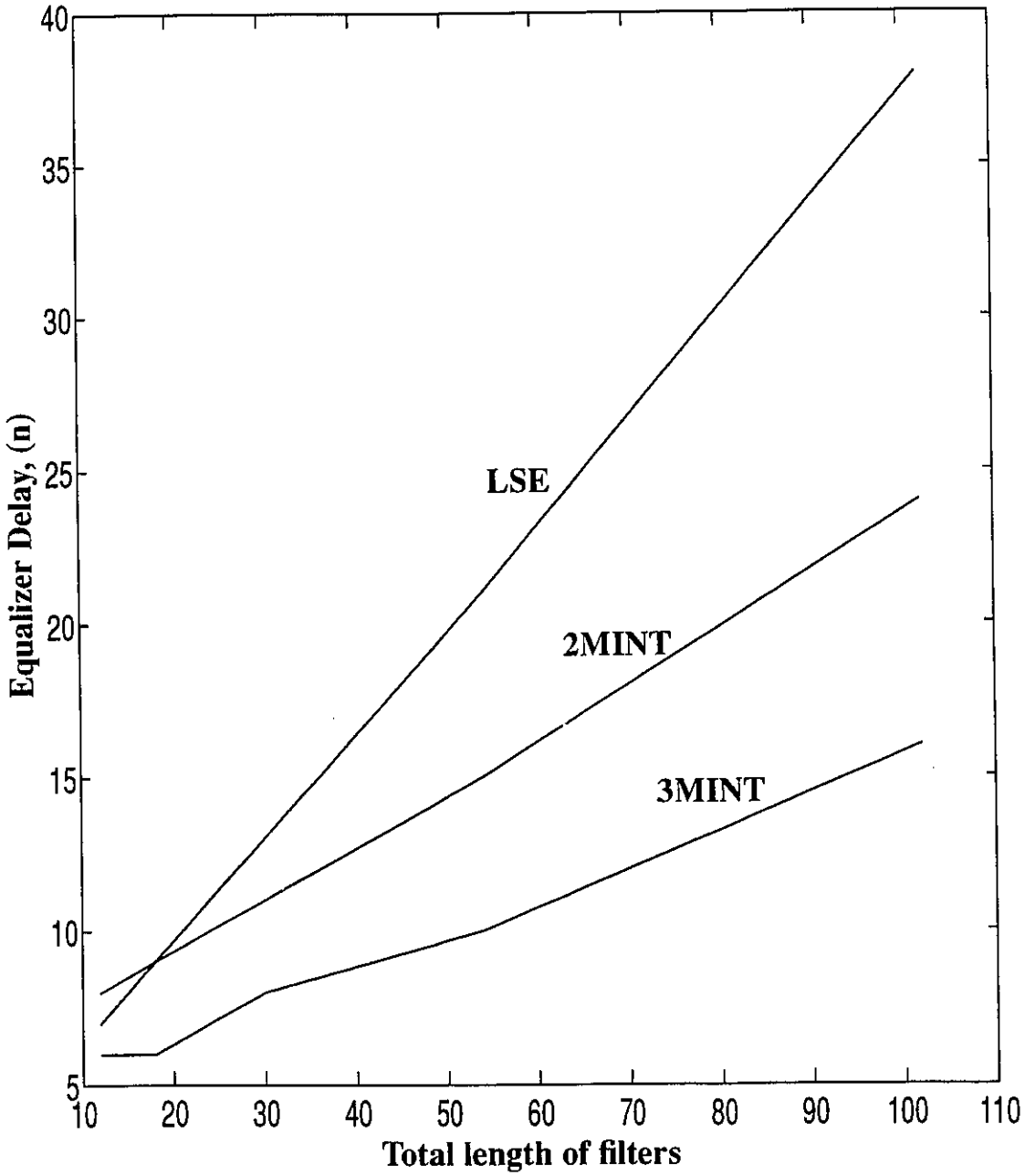

Figure 5.18: System delay introduced by the equalizers.

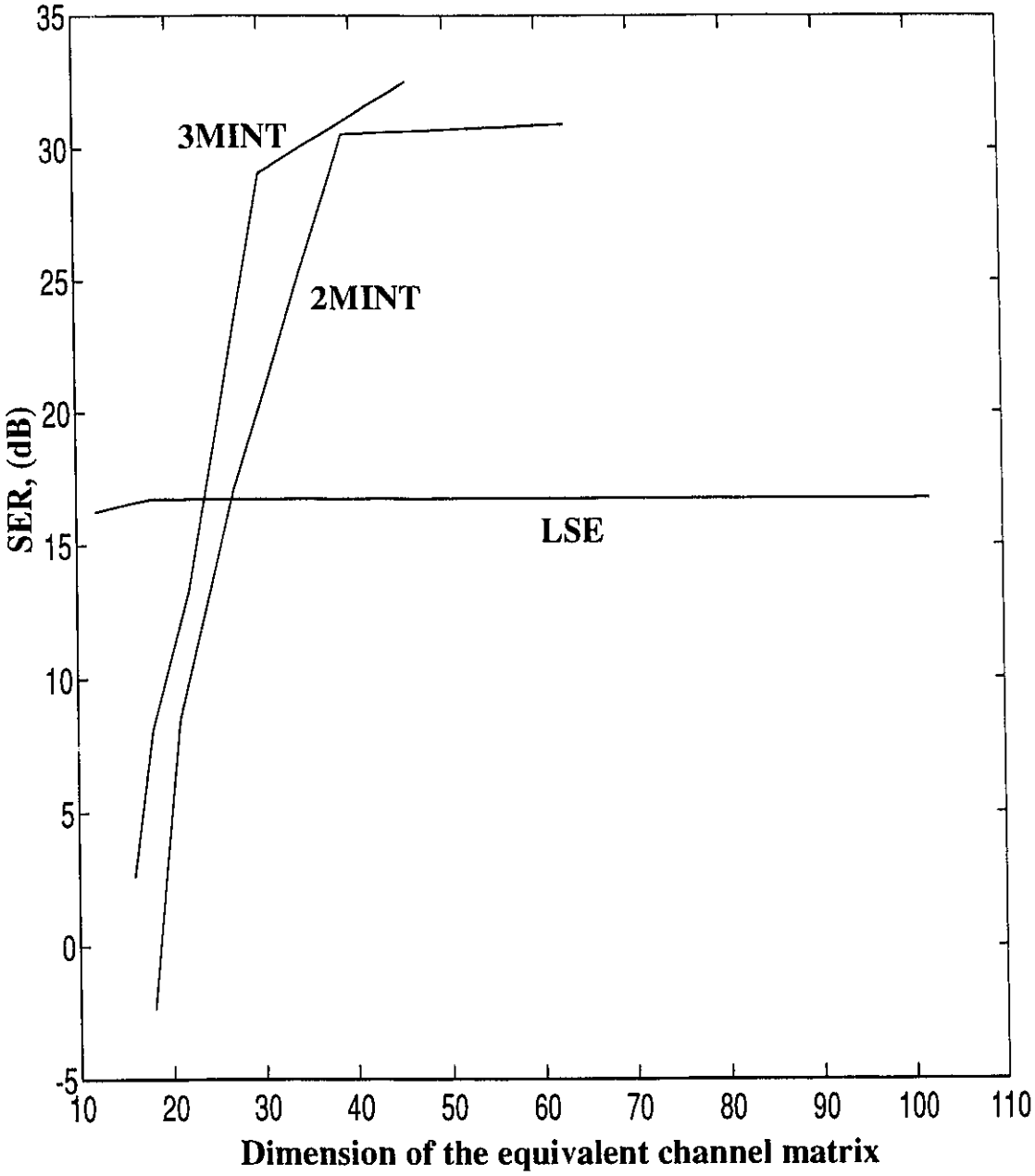

Figure 5.19: Comparison of Signal-to-Error Ratio against the dimension of the equivalent channel matrix to be inverted.

5.5.3 Aliasing of the derived channels

A simulation is conducted to study the aliasing of the derived channels described in Section 5.5.3. The performance of a 3MINT equalizer is studied. Four scenario are formed with two types of input signal under two aliasing conditions.

The input signals are low-pass signals and their bandwidths f_l (3 dB cut-off frequencies) are 0.6 and 0.9 relative to the Nyquist sampling frequency f_s which is 2. The bandwidth of the low-pass channels are 0.8 and 1.2. The following table depicts the performance of the 3MINT equalizers under these four scenario.

	Bandwidth of low-pass channel $f_l = 0.8$		Bandwidth of low-pass channel $f_l = 1.2$	
Scenario	1	2	3	4
Bandwidth of input signal f_x	0.6	0.9	0.6	0.9
Signal to Error Ratio, **SER**(dB)	41.01	32.18	66.03	22.46
Filter Norm, **FN**	17100		2	
Noise Enhancement Ratio **NER**(dB)	-1.262	2.022	-1.263	-2.386

The Filter Norm (FN) is about 17100 and 2 when the bandwidth of the channel is set to 0.8 and 1.2 respectively. This is because more aliasing on the derived channels occurs in latter case. This leads to more differences among the three virtual channels, thus the impact of close zeros is reduced; therefore, the filters have smaller coefficient values.

Aliasing brings about the difference in the 3 virtual channels and this leads to a smaller FN. However more aliasing also brings about more residue errors because of the larger difference between the actual analog channel and its digital model on which the determination of filter coefficients is based. These two factors have counter effect on the inverse filtering capacity of the equalizer.(refer to Section 5.3.2 for the discussion)

Figure 5.20 depicts the power spectrum of the error signals under these four scenario. The additional aliasing of the 3 virtual channels in scenario 3 and 4, in which the bandwidth f_l of the low-pass channel is 1.2, leads to a much lower FN; hence the equalizer has a better performance over the pass-band, from 0 to 0.8.

In scenario 4, the bandwidth of the input signal is 0.9, larger than 0.8. Frequency components of the input signal outside the usable pass-band of the equalizer is not restored properly. It is because of the significant aliasing error of channels at this region. Hence scenario 4 has a poorer performance (SER) than scenario 3.

The residue error due to the aliasing of the 3 virtual channels found in scenario 4 is so great that its SER is even lower than those of scenario 1 and 2. Nonetheless, any input signal with bandwidth smaller than 0.8 should be better restored by the equalizer with f_l = 1.2 than the one with f_l = 0.8. This also confirms that the usable pass-band of the equalizer is from 0 to f_s - f_l(when the FN is small).

The residue error is more significant at the high end of the frequency spectrum of the channels. Therefore the SER in scenario 2 is lower than the SER in scenario 1. Note also in scenario 2 that the signal (from 0.8 to 0.9), which is cut off by the channel, is restored by the equalizer.

Another aspect is the enhancement of input noise. The noise is assumed to be inputted at a single point to the system. It is added to $\mathbf{y}(t)$ just before the sampling device (Figure 5.10). Figure 5.21 depicts the amplification of the low-pass noises for the four scenario.

In general, the graph indicates that the overall response of the equalizer leads to the attenuation of input noise although the FN is bigger then unity. It is because the amplified noise of each filter branches compensated with each others. The responses are similar in the usable pass-band (0 to 0.8) and this leads to similar NER for scenario 1 and 3. The bigger noise enhancement outside 0.8 in scenario 2 indicates that each filter branches compliment, instead of compensate, each others to overcome the attenuation of the channel outside 0.8.

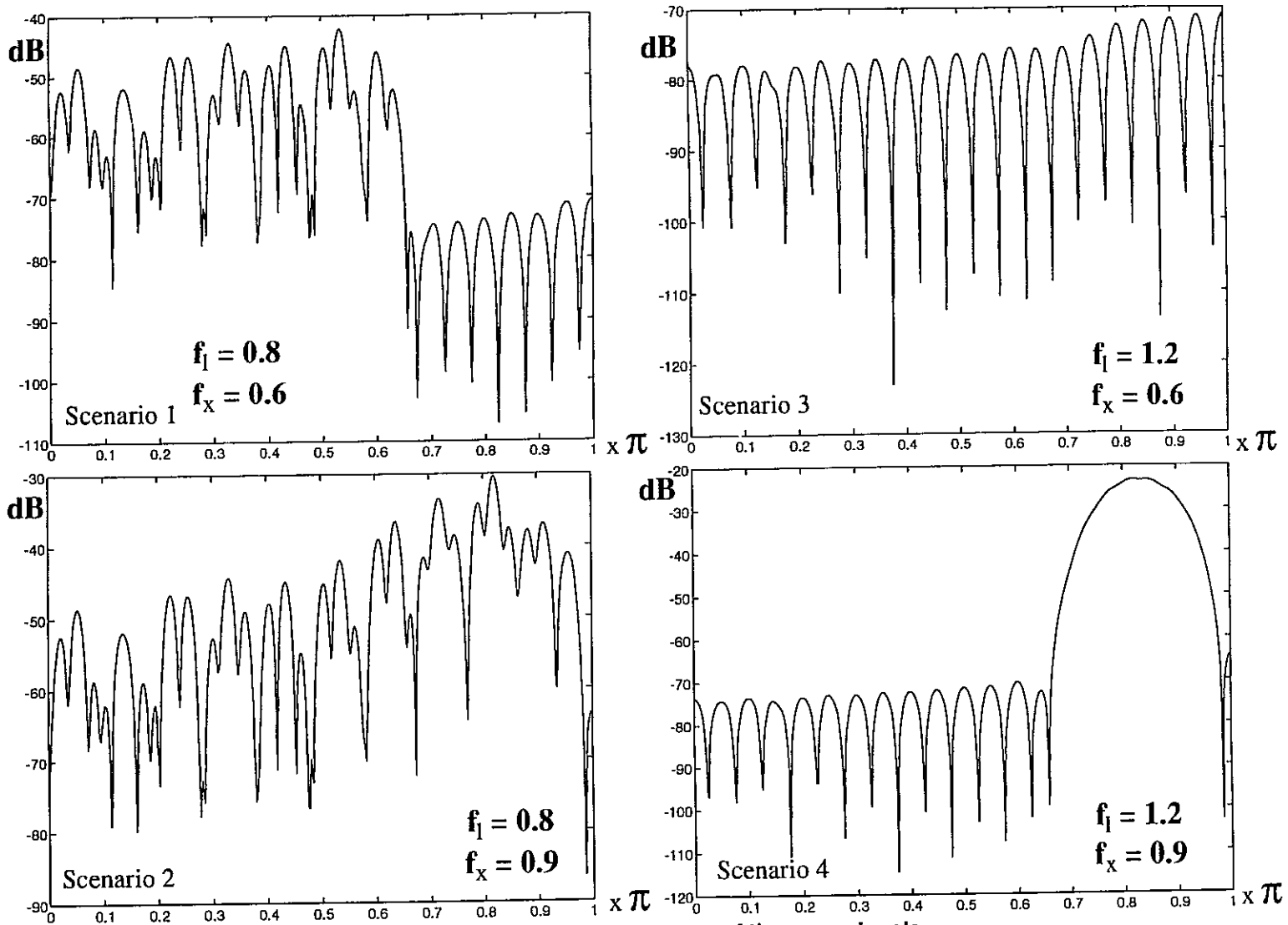

Figure 5.20: Frequency (power) spectrum of the error signals

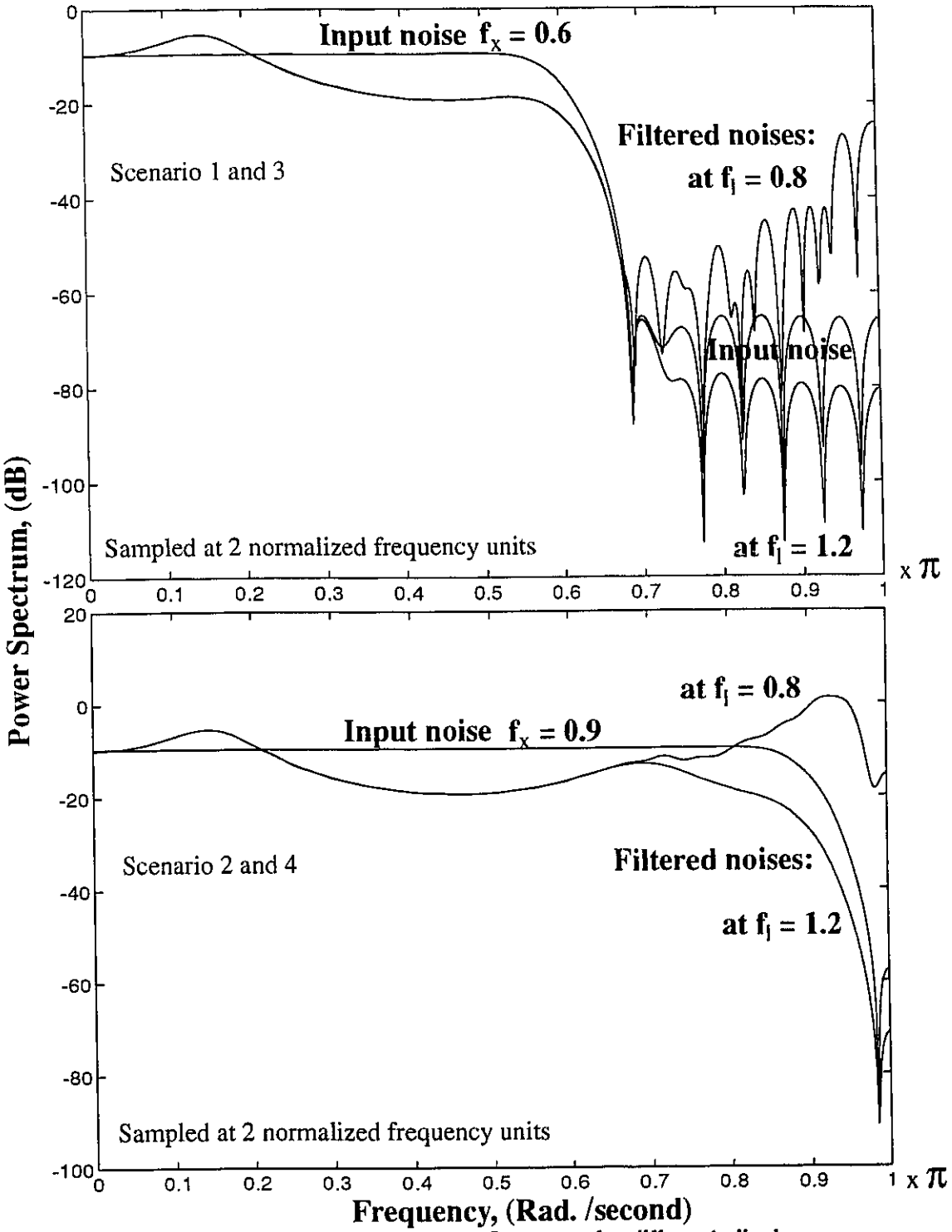

Figure 5.21: Enhanced Noise Power Spectrum for different aliasing.

5.6 Application: Cancellation of reverberation

In this section, a simulation is run to study the cancelation of the reverberation in an acoustic chamber. This leads to a comparison of the performances among the three equalizer structures, discussed in Section 5.5, with a channel that consists of a few hundreds coefficients. The channel of a sample acoustic chamber is simulated [19]. Refer to Section B.3 (page 119) of the appendix for the detail of the setup.

The performance of the three equalizers is compared at the same computational effort in determining the filter coefficients. Figure 5.22 shows the frequency spectrum of the input signal **x**(t) and the effective low-pass channel **GL**(w). Figure 5.23 shows the error signals of each equalizers. The following table depicts the results of this simulation.

	LSE	2MINT	3MINT
Total length of filters, **TFL**	764	1360	2040
Dimension of channel matrix	848 by 764	764 by 1360	764 by 2040
Dimension of the matrix to be inverted†, **DECM**	764 by 764		
Signal to Error Ratio **SER** (dB)	41.42	46.49	48.78
Filter Norm **FN** (dB)	23.18	21.63	19.73
Noise Enhancement Ratio **NER** (dB)	18.46	12.44	8.927
System delay introduced	30	24	25

†. The formulae for the dimension of the equivalent channel matrix to be inverted is described in Section B.2 (page 117)

The 3MINT equalizer has the best inverse filtering capability and the largest TFL of the others.

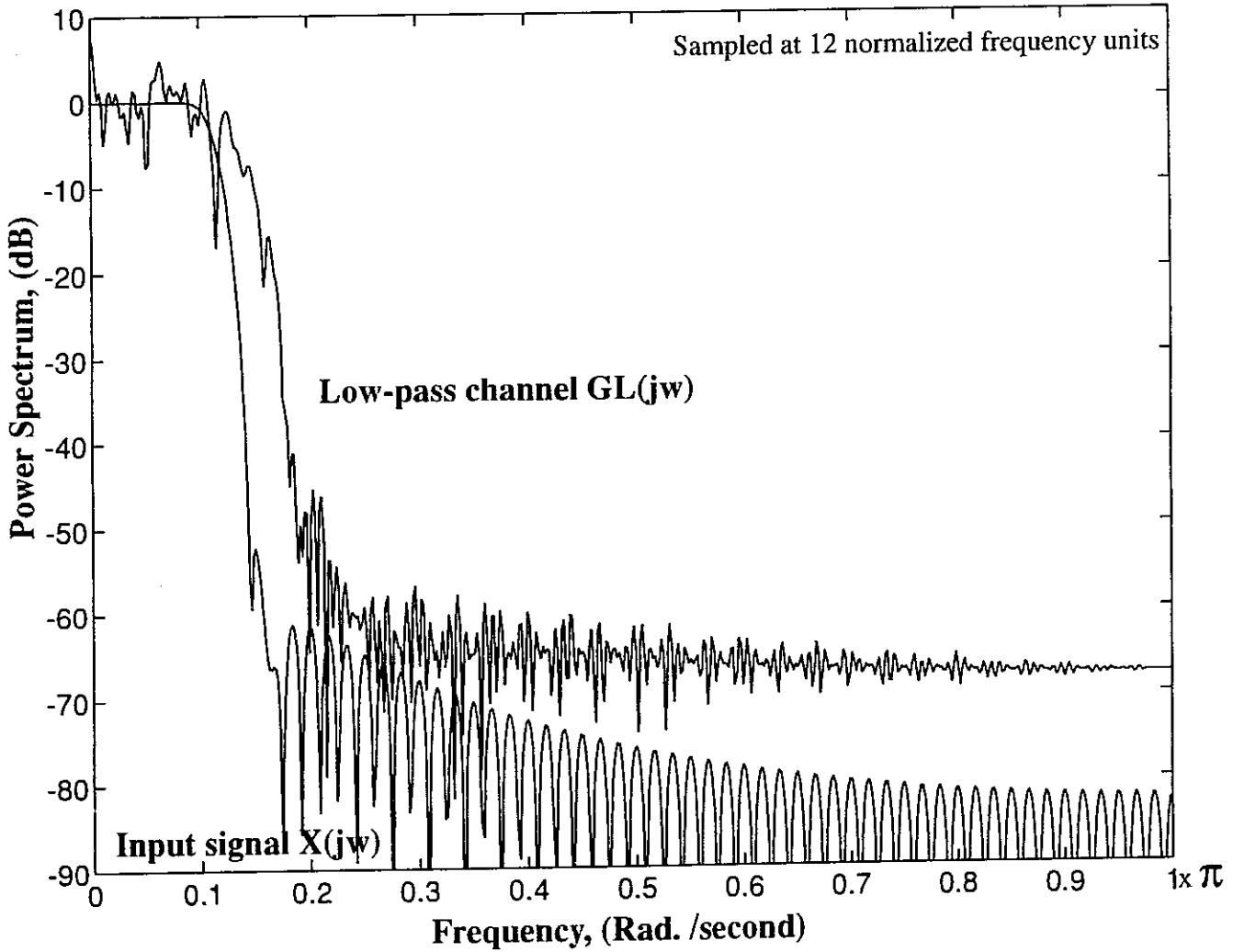

Figure 5.22: Frequency spectrum of the low-pass channel and input signal.

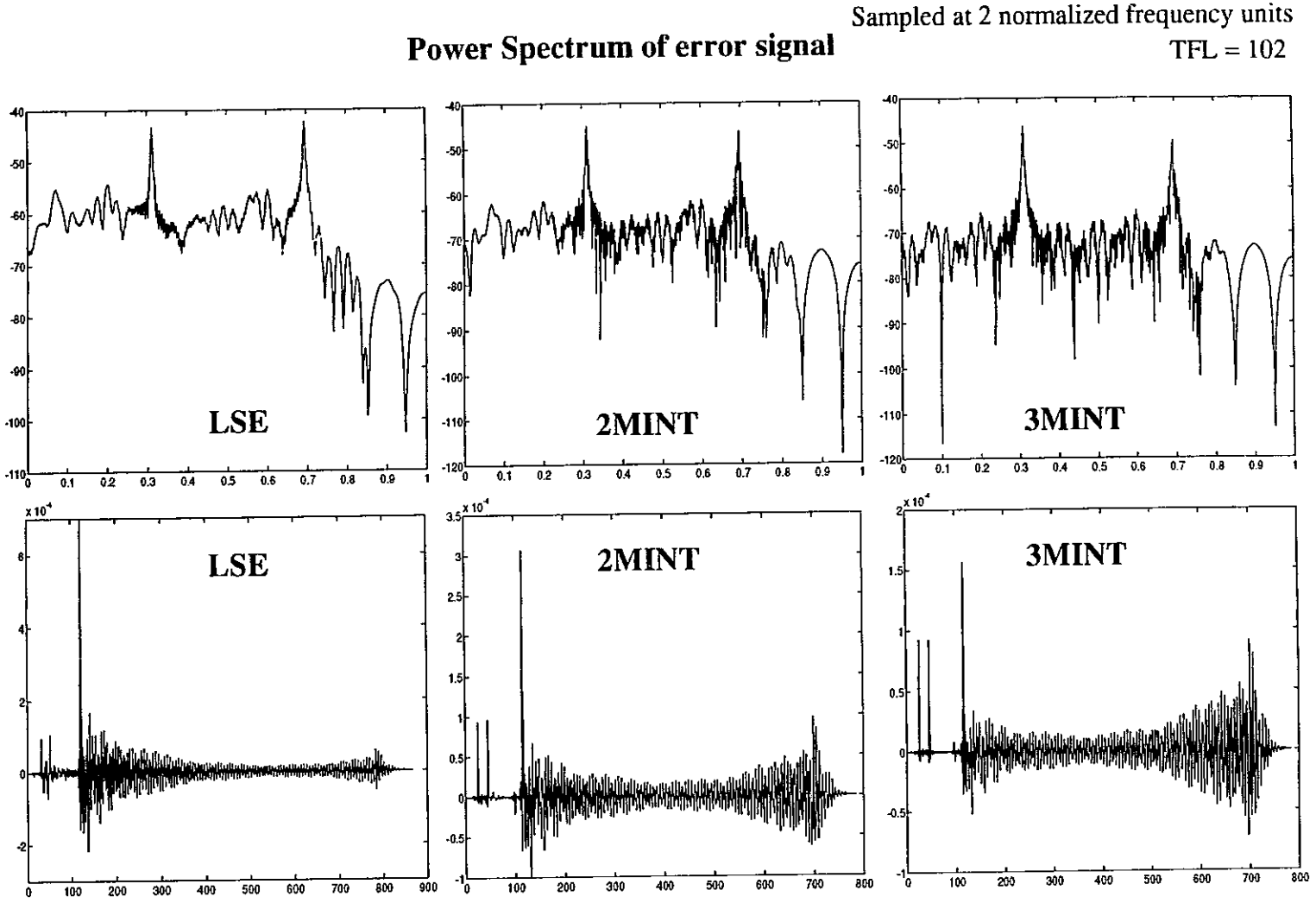

Figure 5.23: Characteristic of the error signals of the three equalizers.

5.7 Conclusion

The concept of the equalization of a single channel was described. The conventional equalizers based on the Least-Square Error (LSE) criterion cannot realize exact inverse to a channel that has non-minimum phase zeros. MINT can yield an exact inverse filter system for both the minimum phase and non-minimum phase channel; however, it requires the existence of multiple channels which do not contain common zeros. Additional physical channels are required.

New digital equalizer structures based on the MINT were proposed and their performances were studied.

As an alternative to the LSE equalizer, the MINT equalizer can be applied in the inverse filtering of a linearly distorted analog signal. In general the performance of the MINT equalizer improves as the total filter length (TFL) increases and surpasses the performance of the LSE equalizer when TFL is large enough.

The simulations show that the performance of the 3MINT equalizer is superior than those of the 2MINT equalizer and yet the 3MINT equalizer requires less computational effort in determining the filter coefficients. However, a higher system clock rate is required by the 3MINT equalizer.

Chapter 6

Conclusions

6.1 Summary

In this thesis, the principle of multiple-input/output inverse theorem(MINT) was studied. Its potential implications and applications were explored.

The major conclusions are summarized below:

- Four general properties of MINT for a dual-channel system are given: 1) the length requirement of the filters, 2) the filtering capability, 3) the uniqueness of the solution, 4) the existence of exact solutions.
- In addition to the Square Matrix solution shown in [2], the Minimum Norm solution is proposed. Both of these solutions are a subset of the Rectangular Matrix Solution which embodies the total solution set for MINT.
- MINT on a multiple channels system is studied. The equation (3.5) on page 30 for a M-input-1-output system with square channel matrix indicates that the total number of the filter coefficients and the computational effort for determining the filter coefficients reduce to a lower bound as M, the number of channels, increases to an upper bound L.

- Filtering capabilities of MINT are not restricted to inverse filtering. One of them is the selective reception, filtering and distribution of signals in a linear, shift-invariant, deterministic, noiseless, finite-impulse-response system and is demonstrated in the design of a speakerphone system.

- Common zeros or, more likely, close zeros may occur in the channels. The common zeros leads to the non-existence of the solution. The problem of having common zeros can be solved by introducing a third channel so that the three channels do not have the same zero in common. Another approach is the use of an IIR filter to remove one or two minimum phase common zeros.

- Filter coefficients of large value, which render the filter impractical, are also found to be a problem in the equalizer based on the LSE criterion. They are associated with close zeros for MINT. In addition to the two solutions for common zeros, the minimum norm solution with system delay can resolve the problem.

- New equalizer structures based on MINT are viable on a single analog channel from which virtual channels can be derived. They have better performance, in terms of more accurate restoration of the distorted signal, less noise enhancement and less sensitive to error, than the conventional equalizer based on the LSE criterion. However the improved performance came at the expense of more filter coefficients.

- The 3MINT equalizer has better performance than the 2MINT equalizer and yet requires less computational effort in determining the filter coefficients. However the 3MINT equalizer is required to oversample the analog signal by a factor of 3; whereas the oversample factor of the 2MINT equalizer is only 2.

6.2 Suggestions for Future Research

This final section suggests two areas for future research:

1)***Random model of MINT: adaptive MINT.***

- The current study was based on the deterministic system. A study of MINT in a stochastic model may lead to the development of an adaptive MINT equalizer. The research on the fast computation of the filter coefficients is also required so that responsive adaptive algorithm is possible.

2) ***Performance of multiple channel-filter system.***

- A comparison between the 2MINT equalizer and the 3MINT equalizer is done in this thesis. However, the performance of a MINT equalizer (filter) with more than 3 channels is not studied. The suggested research will lead to the optimal design of MINT filters since the concept of multi-channel filters can range from the structure which has all filter coefficients in one branch, to the structure which has multiple filters each with one coefficient.

References

[1] M. Miyoshi and Y. Kaneda, "Inverse Control of Room Acoustics using Multiple Loudspeakers and/or Microphones," in Proc. *ICASSP86*, Tokyo, Japan, Apr. 1986, pp. 18.4.1-4.

[2] M. Miyoshi and Y. Kaneda, "Inverse Filtering of Room Acoustics," *IEEE Transaction on Acoustics, Speech and Signal Processing*, Vol. 36, No. 2, pp. 145-152, Feb. 1988.

[3] S. T. Neely and J. B. Allen, "Invertibility of a Room Impulse Response," *J. Acoust. Soc. Amer.*, Vol. 66, pp. 165-169, July 1979.

[4] B. Widrow and E. Walach, "Adaptive Signal Processing for Adaptive Control," in Proc. *ICASSP84*, San Diego, CA, Mar. 1984, pp. 21.1.1-4.

[5] L. A. Poole, G. E. Warnaka and R. C. Cutter, "The Implementation of Digital Filters Using a Modified Widrow-Hoff Algorithm for the Adaptive Cancellation of Acoustic Noise," in Proc. *ICASSP84*, San Diego, CA, Mar. 1984, pp. 21.7.1-4.

[6] W. L. Brogan, *Modern Control Theory*. Englewood Cliffs, NJ: Prentice-Hall, 1982.

[7] R. Kuc, *Introduction to Signal Processing*. Englewood Cliffs, NJ: Prentice-Hall, 1988, pp. 426-432.

[8] A. J. Berkhout, "On the Minimum Phase Criterion of Sampled Signals," *IEEE Trans. Geosci. Elect.*, Vol. GE-11, No. 4, pp. 186-198, Oct. 1973.

[9] A. J. E. M. Janssen, "Short Communication note on a Linear System occurring in Perfect Reconstructions," *Signal Process*, Vol. 17, pp. 109-114, 1989.

[10] S. Barnett, *Matrices in Control Theory*. Van Nostrand, New York, 1971, pp. 29-53.

[11] J. W. Archbold, *Algebra*. London: Sir Isaac Pitman Sons Ltd., 1961.

[12] F. G. Florey, *Elementary Linear Algebra with Applications*. Englewood Cliffs, NJ: Prentice-Hall, 1979.

[13] S. Barnett, "Matrices, Polynomials, and Linear Time-Invariant Systems," *IEEE Trans. on Automatic Control*, Vol. AC-18, No. 1, pp. 1-10, Feb. 1973

[14] E. Masgrau and J. A. RodrÍguez-Fonollosa, "Acoustic Cancellation of Engine Noise by Fast Adaptive IIR Filtering," in Proc. *EUSIPCO-90: Fifth European Signal Processing Conference*, Barcelona, Spain, 18-21 Sept. 1990, pp.1999-2002.

[15] H. Yamada, H. W. Wang and F. Itakura, "Recovering of Broad Band Reverberant Speech Signal by Sub-band MINT method," in Proc. *ICASSP*91, Toronto, Canada, 14-15 May 1991, Vol. 2, pp. 969-72.

[16] M. J. T. Smith and T. P. Barnwell, "A Procedure for designing Exact Reconstruction Filter Banks for Tree-structured Subband Coders," in Pro. *IEEE Int. Conf. Acoust. Speech Signal Process*, San Diego, March 1984, pp. 27.1.1-4.

[17] M. Vetterli, "Filter Banks allowing Perfect Reconstructions," *Signal Process*, Vol. 10, pp. 219-244, 1986.

[18] R. E. Crochiere and L. R. Rabiner, *Multirate Digital Signal Processing*. Englewood Cliffs, NJ: Prentice-Hall, 1983.

[19] J. B. Allen and D. A. Berkley, "Image Method for Efficiently Simulating Small-Room Acoustics," *J. Acout. Soc. Amer.*, Vol. 65, pp. 943-950, April 1979.

[20] B. Widrow and S. D. Stearns, *Adaptive Digital Signal Processing*. Englewood Cliffs, NJ: Prentice-Hall, 1985, pp. 231-249.

[21] A.V. Oppenheim and R.W. Schafer, *Digital Signal Processing*. Englewood Cliffs, NJ: Prentice-Hall, 1979, pp. 345-353.

[22] E. A. Lee and D. G. Messerschmitt, *Digital Communication*. Boston: Kluwer Academic Publishers, 1988.

[23] B.P. Lathi, *Modern Digital and Analog Communication Systems*. New York: Holt, Rinehart and Winston, 1983.

[24] J.G. Proakis, *Digital Communications 2nd Ed.*, McGraw-Hill Book Company, New York, New York, 1989.

[25] T. W. Parks, J. H. McClellan and L. R. Rabiner, "A Computer Program for designing Optimum FIR Linear Phase Digital Filters," *IEEE Trans. Audio Electroacoust.*, Vol. AU-21, pp. 506-562, Dec. 1973.

[26] R. D. Gitlin and S. B. Weinstein, "Fractionally-spaced Equalization: An improved digital transversal equalizer," *BSTJ*, Vol. 60, No. 2, pp. 275-297, Feb. 1981.

[27] W.Steenaart and C.Y. Cheung, "Exact Solution to the Inverse Filter Problem and Applications," in Proc. *Canadian Conf. on Electrical and Computer Engineering*, Montreal, Canada, 17-20 Sept., 1989, pp. 181-183.

Appendix A
LSE Equalizer

In this appendix, the conventional inverse filtering method based on the Least Square Error (LSE) criterion [6] is described. Its properties and performance are illustrated.

A.1 Inverse filtering system

Section 5.2 describes the system of inverse filtering with one channel. Similar to Figure 5.2 (page 62), the following diagram depicts the digital model of the inverse filtering system.

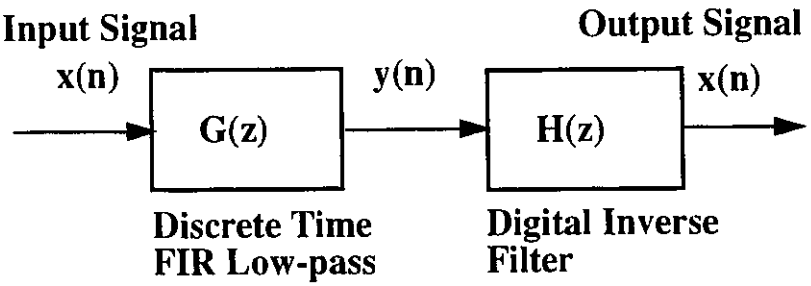

Figure A.1: Discrete model on inverse filtering with one channel.

The input signal **x**(n) is distorted by the channel, which is modelled as a Finite Impulse Response (FIR) digital channel **G**(z), to form **y**(n). The objective is to design the digital FIR filter (equalizer) **H**(z) to compensate the distortion and regenerate **x**(n) from **y**(n).

The design of LSE equalizer attempts to satisfy the following convolution equation:

$$\mathbf{h}(n) * \mathbf{g}(n) = \mathbf{d}(n)$$

$$\mathbf{d}(n) = \begin{cases} 1, & n = k \\ 0, & n \neq k \end{cases} \qquad \text{(A.1)}$$

where k is the allowable delay; k=0,1,2,...K-1 and K is the length of the desired overall response **d**(n). Note that a delay is allowed in this design. This leads to better equalizer performance which is demonstrated in later section. Given the length (number of coefficient) of the channel **G**(z) is M and those of the filter **H**(z) is I, K is equal to M+I-1. There is no restriction on the filter length; i.e. $I \geq 1$.

The convolution equation can be expressed in the matrix form:

$$\begin{bmatrix} g(0) & 0 & \cdots & 0 & 0 \\ g(1) & g(0) & \cdots & \cdots & 0 \\ \vdots & \vdots & \cdots & \cdots & \vdots \\ \vdots & \vdots & \cdots & \cdots & \vdots \\ g(M-1) & \vdots & \cdots & \cdots & g(0) \\ 0 & g(M-1) & \cdots & \cdots & g(1) \\ \vdots & 0 & \cdots & \cdots & \vdots \\ \vdots & \vdots & \cdots & \cdots & \vdots \\ 0 & 0 & \cdots & \cdots & g(M-1) \end{bmatrix} \begin{bmatrix} h(0) \\ h(1) \\ \vdots \\ \vdots \\ h(I-1) \end{bmatrix} = \begin{bmatrix} d(0) \\ d(1) \\ \vdots \\ \vdots \\ \vdots \\ \vdots \\ d(k-1) \end{bmatrix}$$

or

$$\mathbf{GH} = \mathbf{D}$$

G, **H** and **D** are the channel matrix, filter vector and desired response vector respectively. The dimension of **G** is I by M+I-1. There is no solution in determining filter vector **H** because the number of rows (M+I-1) is always bigger than the number of columns (I) of the channel matrix **G**.

Approximate solution can be obtained using the conventional LSE method [2] [6] as:

$$\mathbf{H} = (\mathbf{G}^T\mathbf{G})^{-1}\mathbf{G}^T\mathbf{D} \qquad \text{(A.2)}$$

A.2 Properties of LSE equalizer

In this section, we look at the performance of the LSE equalizer, in terms of Signal-to-Error Ratio (SER) and Filter Norm (FN) (defined in Section 5.5.1 (page 78)), with respect to:

1) different system delay,

2) increasing filter length.

A sample simulation is conducted with the system depicted in Figure A.1. Channel **G**(z), which has 13 coefficients, is the same channel used in the simulation on Section 5.5.2 (page 80). Aliasing of the subchannels is introduced to demonstrate the performance of the LSE equalizer under this environment.

A.2.1 LSE equalizer with different system delay

The length of the filter is set to 36. System delay k may be applied such that the impulse response d(n), depicted in equation A.1, is 1 when n is equal to k. Different sets of filter coefficients are computed for different system delays. For each set of filter coefficients the FN and the SERU of the filter are computed. SERU is defined as the SER of an equalizer when the input signal is a unit impulse;i.e. x(n) = 1.

A maximum SERU is shown in Figure A.2 which depicts the change of SERU and FN of the LSE equalizer with increasing system delay (from 0 to 35). This demonstrates that the inverse filtering capacity of the LSE equalizer can be greatly improved by introducing some delay to the system.

The Filter Norm (FN) is at the lowest with no delay. It rises to about 16.7dB when delay is 7 and remains fairly constant until the delay is 30. It drops back to 2.33dB when delay is 35. Furthermore, the FN of the LSE equalizer is high and fairly constant when it has the best inverse filtering capacity. And it is small when delay is either close to zero or more than 30 where the SER is also small.

A.2.2 LSE equalizer with increasing filter length

The channel G(z) in Section A.2.1 is used. Filter performance with different length are computed. The filter length used is: 3, 6, 9, 12, 15, 18, 21, 24, 27, 30. For each filter length, the followings are computed:

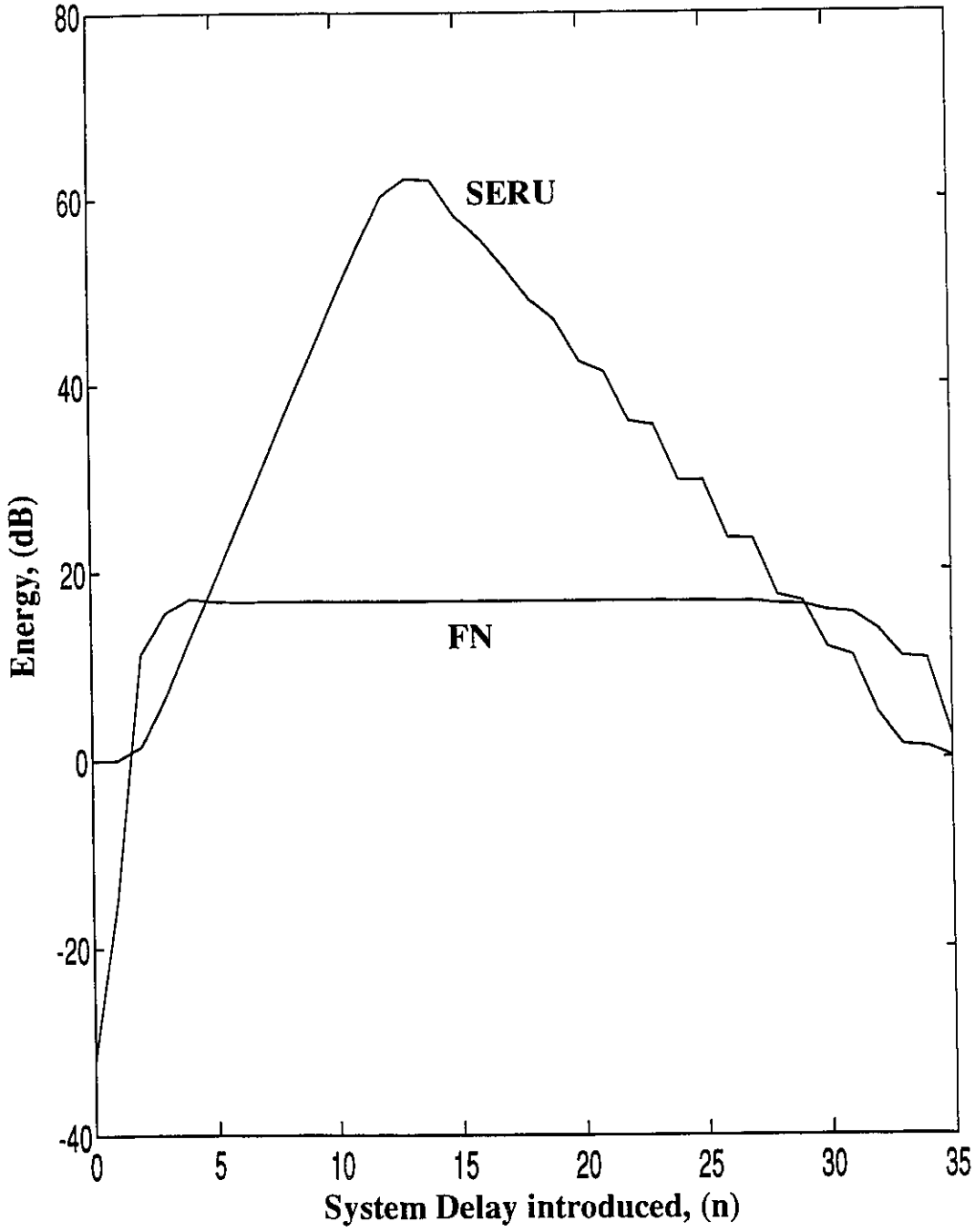

Figure A.2: The FN and SERU of a LSE equalizer with different system delay.

1) For filter with no system delay:

- the SERU (SER when the input signal is a unit impulse;i.e. x(n) = 1).

2) For filter with system delay such that it has maximum SERU:

- the SERU,
- the SER when the low-pass signal depicted in Section 5.5.2 is inputted,
- the FN.

For a non-minimum phase channel, the difference (error) between the restored signal of a LSE equalizer and the input signal remains of finite value [2] and do not convert to zero with increasing filter length. This is illustrated in Figure A.3 that the SERU for a filter without delay converts to a upper bound with increasing filter length. However with the introduction of system delay, the SERU (inverse filtering capacity for unit impulse input) improves with increasing filter length.

With low-pass input signal, however, the SER converts to a upper bound (about 16.8dB) and can no longer be improved with additional filter coefficients. This can be explained by referring to Figure A.4. It depicts the change of FN of the filter, that has system delays and is inputted with a low-pass input signal, with increasing filter length. The FN of the LSE equalizers is fairly constant and is around 16.7dB. Any error due the different of the analog channel† and the aliased digital channel is amplified by the filter **H**(z). Hence the upper bound in SER is set by the amplification of these error.

This simulation indicates that the FN of this LSE equalizer is quite insensitive to the change of the filter length. On the other hand, the FN of MINT equalizer could be reduced to a small value if sufficient filter coefficients are used; thereby, the upper bound of the SER is extended. This makes it possible for MINT equalizer to improve the SER by increasing filter length.

---

†. The distortion of the input signal by the channel is simulated at an oversampling factor of 6 (refer to Section 5.5.2 for detail)

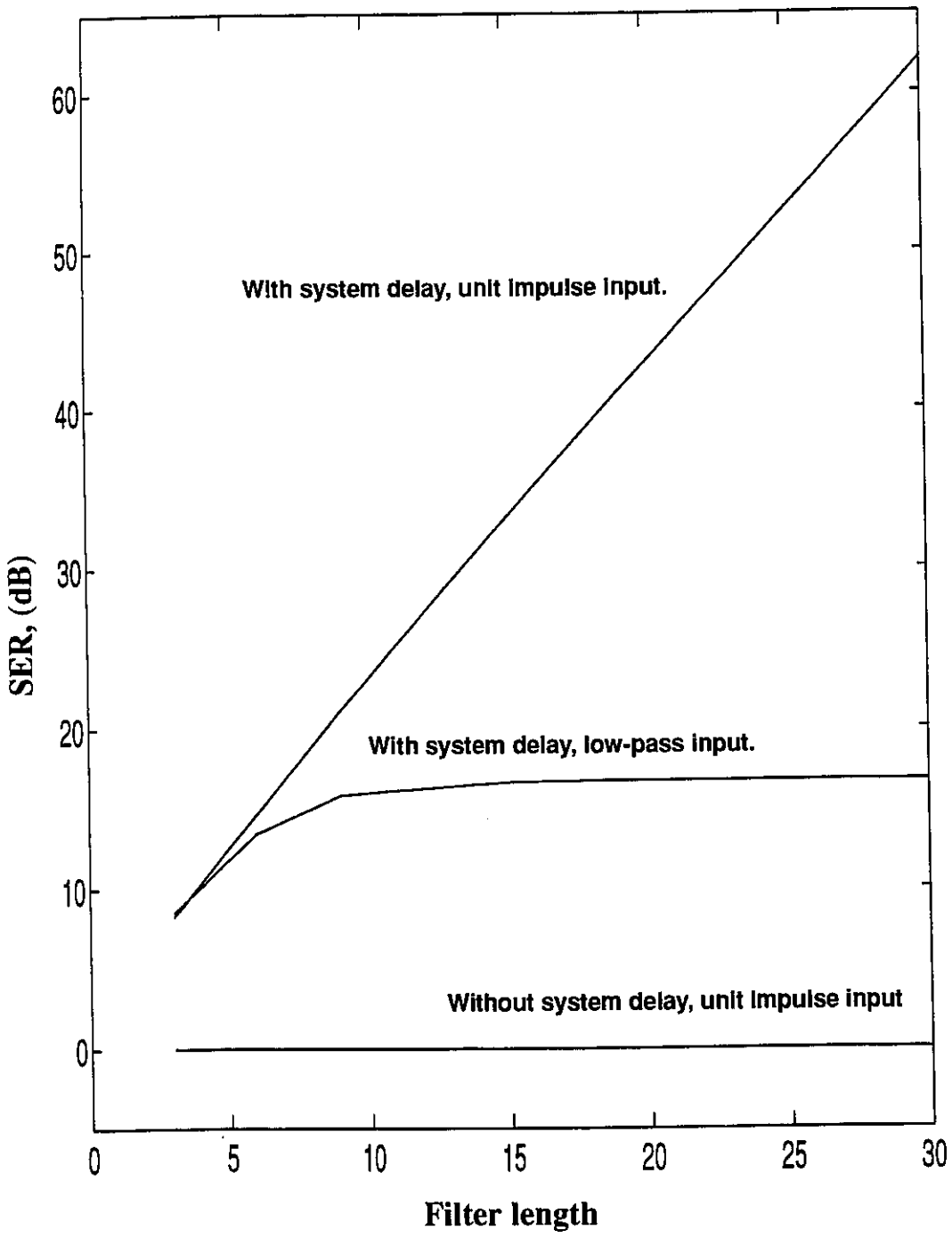

Figure A.3: Change of SER with increasing filter length.

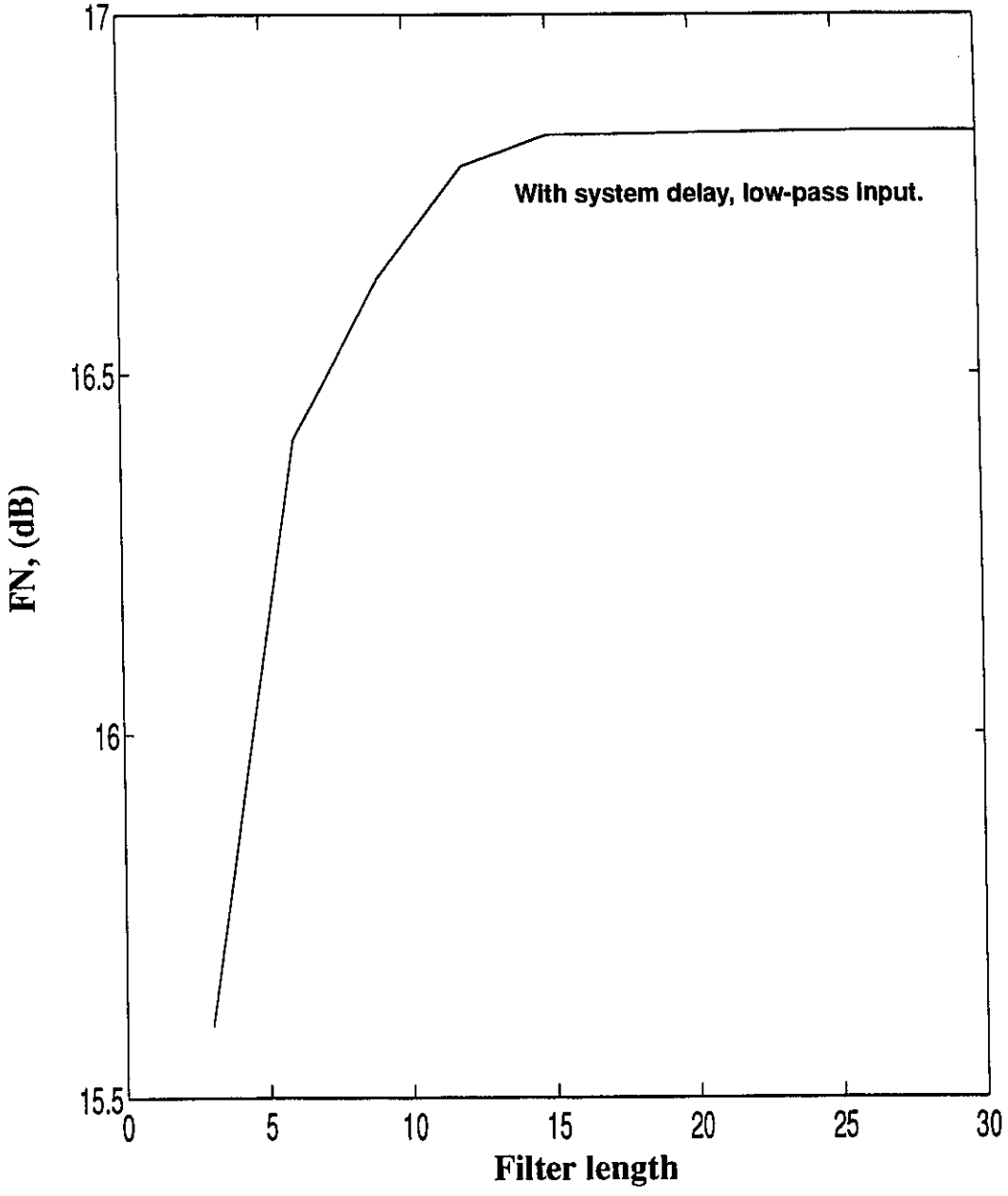

Figure A.4: Change of FN with increasing filter length.

Appendix B
Simulation Data

In this appendix, data of the simulations done in previous chapters are captured.

B.1 Simulation data of Section 4.3.1

The change of the filter norm (FN in dB) with increasing filter length for the ten channel sets is summarized in table below:

Table B.1:

Channel sets	Length of $\mathbf{H}_1(n)$												
	4	10	20	30	40	50	60	70	80	90	100	110	120
	Filter Norm (FN) in dB												
1	1.91	-0.40	-1.05	-1.10	-1.10	-1.10	-1.10	-1.10	-1.10	-1.10	-1.10	-1.10	-1.10
2	0.57	-1.25	-1.61	-1.61	-1.61	-1.61	-1.61	-1.61	-1.61	-1.61	-1.61	-1.61	-1.61
3	1.92	-1.21	-1.63	-1.63	-1.63	-1.63	-1.63	-1.63	-1.63	-1.63	-1.63	-1.63	-1.63
4	71.58	63.42	53.57	44.34	35.18	26.06	17.15	9.47	3.62	1.22	0.59	0.46	0.44
5	64.99	56.83	46.98	37.75	28.60	19.56	11.24	4.65	1.48	0.52	0.36	0.33	0.33

Table B.1:

Channel sets	Length of $\mathbf{H}_1(n)$												
	4	10	20	30	40	50	60	70	80	90	100	110	120
	Filter Norm (FN) in dB												
6	72.10	63.74	54.57	46.18	37.89	29.61	21.39	13.44	6.90	3.39	2.27	2.06	2.02
7	60.81	24.89	-0.63	-0.66	-0.66	-0.66	-0.66	-0.66	-0.66	-0.66	-0.66	-0.66	-0.66
8	65.70	57.00	47.10	38.00	29.77	21.45	12.87	6.67	2.92	1.90	1.69	1.66	1.66
9	72.94	65.13	56.03	47.64	39.36	31.16	23.35	15.55	8.37	3.77	1.59	0.92	0.78
10	62.60	57.07	51.96	47.57	43.22	38.88	34.56	30.25	25.94	21.64	17.40	13.30	9.55

B.2 Simulation data of Section 5.5.2

The following table summaries the setup of this simulation. All frequencies are normalized. The data rate of the filter elements is 2 normalized frequency units (the system clock rate). The reference sampling frequency in this simulation is 12 since an oversampling factor of 6 is applied. Due to the requirement of the simulation tool, the bandwidth of the input signal and the receiving low-pass filter is specified in terms of the 3-dB cutoff frequency. In order to avoid significant aliasing error when sampled at 2, their 3-dB cutoff frequency is chosen to be smaller than 1. They should also have a sharp roll-off at the transition band as well.

Reference sampling frequency	f_S	12
Relative 3-db cut-off frequency of the input low-pass signal $\mathbf{x}(t)$	f_X	0.7
Length of the input low-pass signal $\mathbf{x}(n)$ sampled at 12	l_X	121
Relative 3-db cut-off frequency of the low-pass filter $\mathbf{L}(w)$	f_l	0.8

Length of the low-pass filter **L**(jw) sampled at 12	l_l	60
Length of the channel **g**(n) sampled at 12	l_g	19
Effective length of the low-pass channel **GL**(z) sampled at 2	l_{gl}	13

There are 1, 2, 3 subchannels in the LSE, 2MINT, 3MINT equalizer respectively. Each subchannel has 13 coefficients.

Matrix inversion, which demands the most computational effort, is performed in this simulation to determine the filter coefficients of each equalizers. The dimensions of the matrix to be inverted(DECM) for each equalizers with same TFL are depicted in the following table. For example, if l_{TFL} and l_{gl} are 102 and 13 respectively, the size of the matrix to be inverted are:

- 102 by 102 for LSE,
- 63 by 63 for 2MINT,
- 46 by 46 for 3MINT.

	LSE	2MINT	3MINT
Decimation factor on the distorted signal	6	3	2
Effective sampling frequency	2	4	6
Oversampling factor	1	2	3
Effective clock rate at the output	2	2	2
Total filter length (TFL)	l_{TFL}	l_{TFL}	l_{TFL}
Dimension of channel matrix	$(l_{gl}$ -1 + $l_{TFL})$ by l_{TFL}	$[l_{gl}$ -1 +$(l_{TFL}/2)]$ by l_{TFL}	$[l_{gl}$ -1 + $(l_{TFL}/3)]$ by l_{TFL}
Dimension of matrix to be inverted	l_{TFL} by l_{TFL}	$[l_{gl}$ -1 +$(l_{TFL}/2)]$ by $[l_{gl}$ -1 +$(l_{TFL}/2)]$	$[l_{gl}$ -1 + $(l_{TFL}/3)]$ by $[l_{gl}$ -1 + $(l_{TFL}/3)]$

Refer to point 2 of Section 3.3.3 (page 29) for the computational requirement of MINT

equalizers.

The following table captures the data of the simulation.

Total filters length, TFL		12	18	30	54	102
Signal to Error Ratio,	LSE	16.250	16.716	16.726	16.727	16.727
SER (dB)	2MINT	-2.382	8.475	17.073	30.527	30.894
	3MINT	2.591	8.104	13.228	29.052	32.499
Noise Enhancement Ratio,	LSE	17.435	17.503	17.509	17.509	17.509
NER (dB)	2MINT	12.163	8.560	10.803	10.816	10.816
	3MINT	6.435	5.727	7.166	7.272	7.302
Filter Norm,	LSE	16.787	16.832	16.836	16.836	16.836
FN (dB)	2MINT	33.521	27.380	17.650	12.820	12.780
	3MINT	28.643	24.645	18.077	11.452	11.027
Delay introduced	LSE	7	9	13	21	38
	2MINT	8	9	11	15	24
	3MINT	6	6	8	10	16

B.3 Simulation data of Section 5.6

The following table depicts the condition of the simulation.

Dimension of the acoustics chamber (meter)	0.7 by 1.1 by 1.3
Wall reflection coefficient	0.3
Sampling rate (samples per second)	68500
3-db cut off frequency of input signal **x**(t) (Hz)	3996
3-db cut off frequency of **L**(z) (Hz)	4567

Length of receiving low-pass filter $\mathbf{L}(z)$	60
Number of channel coefficients	451
Total length of the low-pass channel $\mathbf{GL}(z)$	510
Effective length of the low-pass channel $\mathbf{GL}(z)$ sampled at f_S = 11417 samples/second	85

Note that the outputs of the three equalizers have same data rate. This is because the input low-pass signal $\mathbf{X}(w)$, the channel $\mathbf{G}(w)$ and the receiving low-pass filter $\mathbf{L}(w)$ are all oversampled by a factor of 6 and different decimations are applied by the three equalizers accordingly before the sampled signals are processed.